2014

Design, Synthesis, and Antibacterial Properties of Dual-Ligand Inhibitors of Acetyl-CoA Carboxylase and Mechanism of Action for the Antibacterial Agent Moiramide B

Molly Anne Silvers
Louisiana State University and Agricultural and Mechanical College

DESIGN, SYNTHESIS, AND ANTIBACTERIAL PROPERTIES OF DUAL-LIGAND INHIBITORS OF ACETYL-COA CARBOXYLASE AND MECHANISM OF ACTION FOR THE ANTIBACTERIAL AGENT MOIRAMIDE B

A Dissertation

Submitted to the Graduate Faculty of the
Louisiana State University and
Agricultural and Mechanical College
in partial fulfillment of the
requirements for the degree of
Doctor of Philosophy

in

The Department of Biological Sciences

by
Molly Anne Silvers
B.S., Louisiana State University, 2009
December 2014

This dissertation is dedicated to my family:

My Dad, David P. Hughes

My Mom, Diane C. Hughes

My Sister, Amy L. Woods

My Brother, Andrew J. Hughes

And to

My Husband, William C. Silvers

ACKNOWLEDGEMENTS

First and foremost, I would like to express my deepest gratitude for my advisor, Dr. Grover Waldrop. His insight, guidance, advice, and support throughout the years have been nothing but beneficial and advantageous to my growth as a scientist. I would also like to thank Dr. Carol Taylor for her understanding, assistance, and help in molding a biologist into an organic chemist. I would also like to thank my other committee members, Dr. Aaron Smith and Dr. David Donze for your guidance and encouragement with my research. I would also like to thank Dr. Thomas Weldeghiorghis and the late Dr. Dale Treleaven for help with numerous NMR studies as well as Connie David for assistance and training in the Mass Spectrometry facility.

I would like to thank the Waldrop research group: Tyler, Amanda, Susan, Alexandra, and Eric for their friendship and support, for the entertaining conversations, and for help in the maintaining of my sanity. I would also like to thank the Taylor research group: Benson, Doug, Ning, Saroj, and Chamini for all their invaluable advice and friendship over the grueling years of wishing for reactions to work the first time, and especially Chyree Batton for all the laughter, adventures of sharing hood space, jamming to lab music, and overall good times I'll never forget.

To my friends, I'm thankful for knowing all of you. Each and every one of you has made life before and during graduate school an unforgettable experience. I am truly grateful for every memory we've shared together and am eager for the continuation of our friendship for years to come.

To my family, your love and support through the years have been appreciated in more ways than I can express. You've been at many sporting events, graduations, concerts,

and competitions and your sacrifices do not go unnoticed. I am eternally grateful to be surrounded by the people that love and care for me and just hope I do something with my life to make you all proud.

Lastly, I would like to thank my amazing husband, William. I can't even begin to express my thanks and gratitude for everything you have done for me. You pushed me to do my best and help support me during the demanding years of graduate school. This journey would never have been possible without you. I often wonder how I was ever so lucky to find someone like you and convince them to marry me. You are my rock, my heart, and my soulmate.

TABLE OF CONTENTS

LIST OF ABBREVIATIONS AND SYMBOLS

Å	Angstrom
ACC	Acetyl-CoA carboxylase
ACP	Acyl carrier protein
ADP	Adenosine diphosphate
$ADPCF_2P$	Phosphodifluoromethylphosphonic acid-adenylate ester
AG	Aminoglycosides
AMPCP	Adenosine 5'-[(α,β)-methyleno]diphosphate
AMPPNP	Adenylyl-imidodiphosphate
ATP	Adenosine triphosphate
BC	Biotin carboxylase
BCCP	Biotin carboxyl carrier protein
Bn	Benzyl
Boc	*tert*-butoxycarbonyl
BPL	Biotin protein ligase
br s	Broad singlet
CDC	Centers for Disease Control and Prevention
CER	Cerulenin
CLSI	Clinical and Laboratory Standards Institute
CoA	Coenzyme A
CT	Carboxyltransferase
$^{i}Pr_2NEt$	*N,N*-Diisopropylethylamine

d	Doublet
dd	Doublet of doublets
ddt	Doublet of doublets of triplets
DMF	Dimethylformamide
DMSO	Dimethyl sulfoxide
*Ec*BC	*Escherichia coli* biotin carboxylase
EDC	1-Ethyl-3-(3-dimethylaminopropyl)carbodiimide
ESI-TOF	Electrospray ionization-time-of-flight
fab	Fatty acid biosynthesis (gene)
FAS	Fatty acid synthesis
FASI	Type 1 fatty acid synthase
FASII	Type 2 fatty acid synthase
FDA	Food and Drug Administration
HATU	*O*-(7-azabenzotriazol-1-yl)-1,1,3,3-tetramethyluronium hexafluorophosphate
HOBt	1-hydroxybenzotriazole
HPLC	High performance liquid chromatography
HRMS	High resolution mass spectrometry
HTS	High-throughput screening
Hz	Hertz
J	Coupling constant
K_i	Inhibition constant
K_{ii}	Intercept inhibition constant

K_{is}	Slope inhibition constant
K_m	Michaelis constant; substrate affinity
LB	Luria broth
LPS	Lipopolysaccharide
m	Multiplet
MFP	Membrane fusion protein
MHII	Cation-adjusted Mueller Hinton media
MIC	Minimum inhibitory concentration
MPC	Mutant prevention concentration
MRSA	Methicillin-resistant *Staphylococcus aureus*
MSW	Mutant selection window
NAD^+	Nicotinamide adenine dinucleotide
NADH	Reduced nicotinamide adenine dinucleotide
NMR	Nuclear magnetic resonance
p	Pentet
*Pa*BC	*Pseudomonas aeruginosa* biotin carboxylase
PBP	Penicillin-binding protein
PG	Peptidoglycan
pK_a	Acid dissociation constant
PMB	Polymyxin B
PMBN	Polymyxin B nonapeptide
ppm	Parts per million
RND	Resistance nodulation division

R_f	Retention factor
rt	Room temperature
s	Singlet
*Sa*BC	*Staphylococcus aureus* biotin carboxylase
SAR	Structure-activity relationship
SBDD	Structure-based drug design
S_N2	Bimolecular nucleophilic substitution
t	Triplet
TFA	Trifluoroacetic acid
THF	Tetrahydrofuran
TLC	Thin layer chromatography
TLM	Thiolactomycin
TMS	Tetramethylsilane
UV	Ultraviolet
V_{max}	Maximum theoretical turnover rate
VS	Virtual screening

Standard 3 letter codes are utilized throughout the document for amino acids.

ABSTRACT

An urgent demand for the development of new antibiotics has been created by the increase in clinical cases involving drug-resistant pathogenic bacteria. A novel target for antibacterial development is acetyl-CoA carboxylase, a multifunctional enzyme that catalyzes the first committed step in fatty acid synthesis. The bacterial form of the enzyme consists of three proteins: biotin carboxylase, biotin carboxyl carrier protein, and carboxyltransferase. The research presented in this dissertation describes dual-ligand inhibitors incorporating selective inhibitors against biotin carboxylase and carboxyltransferase that were synthesized by covalently attaching them with saturated hydrocarbon linkers containing 7 and 15 carbon atoms. The ability to inhibit two different enzymes with the same compound expounds on the theory of increasing overall potency and impeding the ability for the development of resistance.

Kinetic results revealed both dual-ligands displayed inhibition constants in the nanomolar range. However, microbiology assays showed the dual-ligand with the longer linker did not exhibit antibacterial activity. The dual-ligand with the shorter linker showed antibacterial activity against both Gram-positive and Gram-negative organisms as well as decreased susceptibility to the development of bacterial resistance. These results suggest that the length and chemical properties of the covalent linker is critically important for maintaining the antibacterial activities of the two incorporated pharmacophores. Based on biochemical activities, likely reflects alteration in cell permeability or avoidance of intrinsic efflux of the tested dual-ligand molecules.

The natural product moiramide B is a broad spectrum antibiotic that inhibits the carboxyltransferase component of acetyl-CoA carboxylase. A crystal structure of moiramide B was solved in complex with carboxyltransferase. The structure shows that only the (*S*)-methyl pyrrolidinedione head group of moiramide B is used to inhibit the enzyme by taking advantage of the two oxyanion holes that the enzyme normally uses to stabilize enolate anions that form in the substrates during catalysis. The fatty acid tail of moiramide B appears to be only needed for entry into the bacterial cell. Structure-activity relationship studies validated the necessary structural features that contribute to the inhibitory and antibacterial properties of moiramide B. These findings can lead to further design and development of a potent carboxyltransferase antibacterial agent.

CHAPTER 1: INTRODUCTION

1.1 ANTIBIOTICS

Antibiotics can be divided into two methods of action: inhibition of microorganism replication (bacteriostatic) or cytotoxic (bactericidal), Figure 1.1.[1-2] The term 'antibiotic' was first defined by Selman Waksman in 1942 as "inhibiting the growth or the metabolic activities of bacteria and other microorganisms by a chemical substance of microbial origin."[3] Typical antibiotics are either natural products, semisynthetic derivatives of natural products, or completely synthetic in origin.[1]

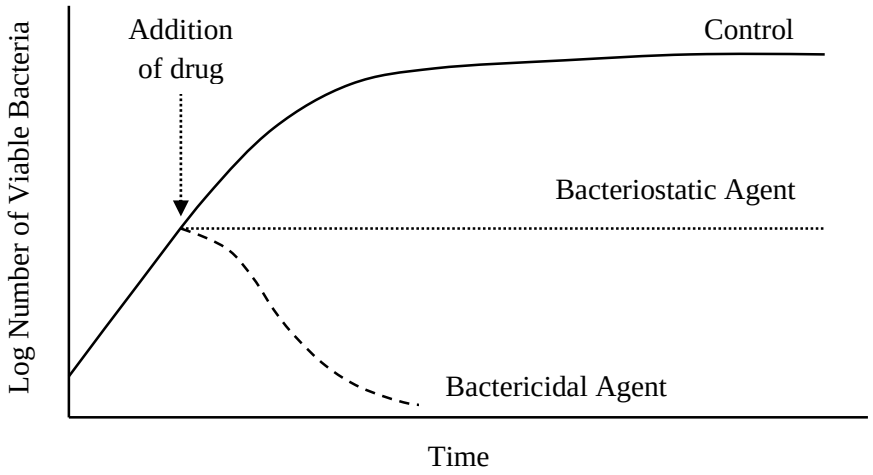

Figure 1.1. The biological effects of bacteriostatic versus bactericidal antibiotics on growing cells; adapted from Walsh (2003).[1]

1.1.1 History of Antibiotics

The idea for creating drugs that would selectively target and kill bacteria was introduced by Paul Ehrlich who developed the concept of synthetic antibiotic chemotherapy.[4] The first reported antibiotic used to treat an infectious disease was in 1910 when Ehrlich discovered Salvarsan, an arsenic-based compound used to cure syphilis.[5] This paved the way for the identification of sulfonamides, or sulfa drugs, in the 1930s which were designated as the first class of antibiotics that were produced solely by

chemical synthesis.[6] The first commercially available sulfa drug, Prontosil, was developed by Gerhard Domagk and coworkers at Bayer in 1932.[4] The most notable antibacterial agent was discovered by Sir Alexander Fleming in 1929 when he isolated penicillin from *Penicillium rubens* and found it displayed antibiotic properties.[7] Penicillin is classified as a β-lactam antibiotic and with the help of Ernest Chain and Howard Florey, penicillin G was introduced clinically in 1942.[6, 8]

After the introduction of β-lactams, there was a dramatic increase in the number of antibiotic classes being discovered and introduced to the market from the 1940s to the 1960s. These new classes included: polyketides, aminoglycosides, macrolides, glycopeptides, and quinolones. Since the introduction of quinolones in 1962, no novel antibiotic classes were identified until linezolid was introduced to the market in 2000, Figure 1.2.[9] The most recently discovered class is lipopeptides, which includes the antibiotic daptomycin. Daptomycin was introduced in 2003 as a treatment for drug-resistant Gram-positive pathogens.[10]

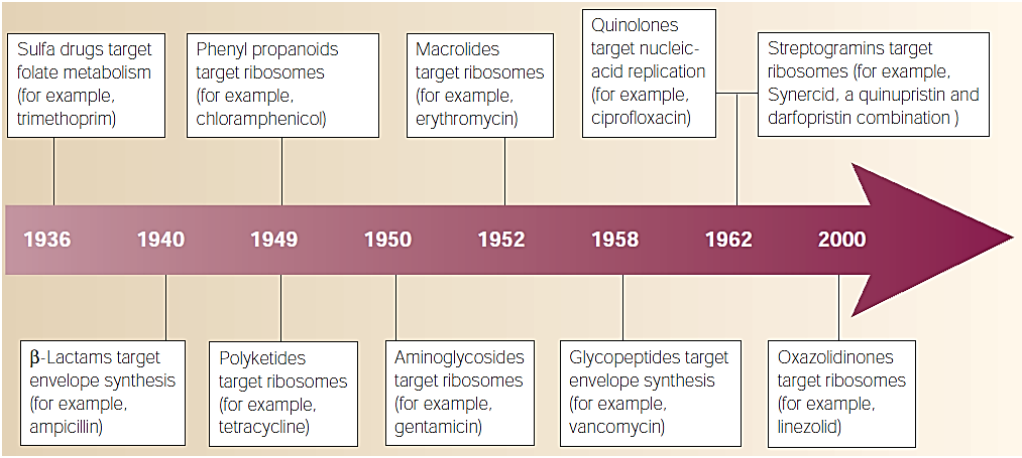

Figure 1.2. Timeline showing introduction of new classes of antibiotics into clinical practice; from Walsh (2003).[11]

1.1.2 Modes of Action

The classes of antibiotics are grouped together based on their targets in the bacterial cell. The four major targets are: cell wall synthesis, protein synthesis, DNA or RNA synthesis, and folate coenzyme synthesis, Figure 1.3.[1, 12]

Class	Target	Bacterial Activity	Notable Examples
Sulfa drugs	Folate Coenzyme Synthesis	Gram-positive	Prontosil
β-Lactams	Cell Wall Biosynthesis	Broad-spectrum	Penicillin, Ampicillin
Aminoglycosides	Protein Biosynthesis	Broad-spectrum	Streptomycin, Kanamycin
Phenylpropanoids	Protein Biosynthesis	Broad-spectrum	Chloramphenicol
Macrolides	Protein Biosynthesis	Broad-spectrum	Erythromycin
Polyketides	Protein Biosynthesis	Broad-spectrum	Tetracycline, Oxytetracycline
Rifamycin	RNA Synthesis	Broad-spectrum	Rifampin
Glycopeptides	Cell Wall Biosynthesis	Gram-positive	Vancomycin
Quinolones	DNA Synthesis	Broad-spectrum	Ciprofloxacin, Fluoroquinolones
Lantibiotics	Cell Wall Biosynthesis	Gram-positive	Nisin
Streptogramins	Protein Biosynthesis	Gram-positive	Pristinamycin
Oxazolidinones	Protein Biosynthesis	Gram-positive	Linezolid
Lipopeptides	Bacterial Membrane	Gram-positive	Daptomycin

Figure 1.3. List of drug classes, their targets, bacterial activity, and notable examples in order by date of introduction to the market; adapted from Lewis (2013).[12]

The antibiotic classes that target cell wall biosynthesis include the β-lactams and glycopeptides. The composition of the cell wall of both Gram-negative and Gram-positive bacteria contains a peptidoglycan (PG) layer, though the PG layer is considerably thicker in Gram-positive bacteria. Antibiotics containing a β-lactam (Figure 1.4) bind irreversibly to penicillin-binding proteins (PBPs), which are involved in transpeptidase activity to cross-link peptidoglycan units. This binding results in cell wall instability and increases permeability.[1-2, 13] Glycopeptides, such as vancomycin, bind to the amino acid precursors used to assemble the cell wall, which prevents the bound amino acids from binding to the PBPs. Glycopeptides are only potent against Gram-positive bacteria due to their inability to penetrate the Gram-negative outer membrane.[1, 14]

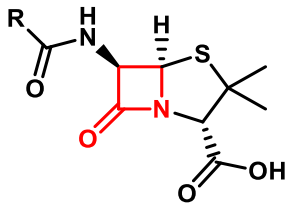

Figure 1.4. The core structure of penicillin with variation occurring at the R group. The β-lactam ring is in red.

The antibiotic classes that inhibit protein biosynthesis, bind to the 50S subunit or 30S subunit of the bacterial ribosome and include: aminoglycosides, macrolides, polyketides, and oxazolidinones, to name a few.[12] Erythromycin, a macrolide, binds to the 50S ribosomal subunit and prevents aminoacyl-tRNA translocation from the A site to the P site. This action causes a premature release of peptidyl-tRNA intermediates that are required for polypeptide elongation.[1, 15] A second group of antibiotics that bind to the 50S subunit are the oxazolidinones, which inhibit the formation of the ribosome complex needed for the initiation of protein synthesis.[16] The broad-spectrum tetracycline (a polyketide antibiotic) inhibits protein synthesis by blocking the attachment of aminoacyl-tRNA from binding to the A site of the 30S subunit of the ribosome, preventing the incorporation of new amino acids to the polypeptide chain.[17]

The antibiotic classes that target DNA or RNA synthesis include the quinolones and rifamycin. The quinolones inhibit DNA synthesis by interacting with either topoisomerase IV or DNA gyrase (topoisomerase II). These topoisomerases are critical in maintaining the conformations required for DNA replication.[18] The quinolones inhibit the topoisomerase reactions resulting in the RNA polymerase and helicase being blocked at the replication fork leading to cell death.[19] The antibiotic rifampin is used to inhibit RNA synthesis by binding in an allosteric site and sterically blocking the elongation of RNA.[20]

Sulfa drugs are synthetic compounds responsible for inhibiting folate coenzyme synthesis and are considered bacteriostatic. The most recent generation of the sulfa drug, sulfamethoxazole, inhibits dihydropteroate synthase and is used in combination with trimethoprim, which inhibits dihydrofolate reductase. By using these two drugs in combination, folic acid metabolism is halted. Inhibition of the folate coenzyme synthesis pathway ultimately leads to the lack of production of thymine, which is an essential nucleotide for DNA biosynthesis.[1, 21]

1.1.3 Resistance Mechanisms

Over the years, pathogenic bacteria have formed resistance mechanisms to current treatments due to the large number of bacterial cells in populations and their short generation times. While this resistance develops naturally over time, the inappropriate use and distribution of antibiotics in a clinical setting plays a fundamental role in the formation of resistant bacteria.[22-23] Bacteria utilize a variety of mechanisms to ensure their survival that include active efflux, inactivation, or modification of the antibiotic, Figure 1.5.[1-2]

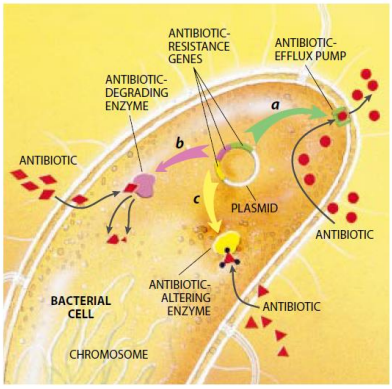

Figure 1.5. Antibiotic-resistant bacteria owe their drug insensitivity to resistance genes. These genes might code for a variety of mechanisms: (A) efflux pumps that eject antibiotics from cells, (B) genes that give rise to enzymes that degrade the antibiotics, or (C) genes that chemically alter the antibiotic; from Levy (1998).[2]

Efflux pump systems play an integral role in the multidrug resistance of clinically important Gram-negative pathogens and have been identified and characterized in strains of *Escherichia coli* and *Pseudomonas aeruginosa*.[24-28] Efflux pumps are transmembrane systems that transport substances from within the cell into the external environment and can be specific for one substrate or a range of compounds. These systems are energy dependent and consist of three components: a resistance nodulation division (RND) exporter protein found in the cytoplasmic membrane, a gated outer membrane protein, and a membrane fusion protein (MFP) that links the two membrane proteins, Figure 1.6.[27]

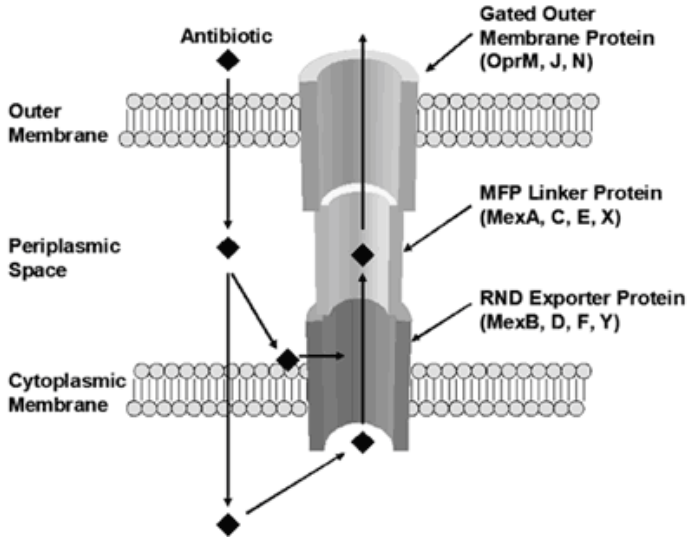

Figure 1.6. Proposed structure and function of the MexAB-OprM and related efflux pumps of *P. aeruginosa*. Antibiotics can be captured from the periplasmic space, cytoplasmic membrane, and/or cytoplasmic space by MexB, D, F, or Y (RND exporter proteins). MexA, C, E, or X (MFP proteins) serve as conduits between the cytoplasmic and outer membranes. OprM, J, or N (gated outer membrane porin proteins) serve as the final step in removal of the antibiotic from the cell; from Aeschlimann (2003).[27]

Different combinations of proteins create efflux pump systems that allow for selectivity of specific antibiotics. The MexA-MexB-OprM pump in *P. aeruginosa* has the broadest-spectrum of activity by recognizing and ejecting tetracycline, quinolones, and most β-lactams.[1] Genetic deletion of this pump results in a significant decrease in the

minimum inhibitory concentration (MIC) values for many antipseudomonal drugs.[27] The MexX-MexY-OprM pump system is also involved in multidrug resistance, though it has a narrower spectrum of selectivity than MexA-MexB-OprM. The MexX-MexY-OprM pump system removes aminoglycosides, fluoroquinolones, marcolides, and tetracycline.[27] The most common pump system in *E. coli* is the AcrA-AcrB-TolC efflux pump, with TolC being the outer membrane protein. Deletion of the *acrAB* genes results in hypersensitivity of *E. coli* to various antibacterial agents.[29] The Acr efflux system selectively expels chloramphenicol, fluoroquinolones, rifampin, tetracycline, and some β-lactams.[30]

Another common resistance mechanism is the inactivation of the antibiotic. This method is more often observed with natural products than with synthetic compounds, with the most prevalent example being the inactivation of β-lactams. β-lactam antibiotics are the most common class of antibiotics used over the past 50 years and due to its prolonged exposure to bacteria, resistance against the β-lactams has resulted from the production of hydrolytic enzymes called β-lactamases. These enzymes hydrolyze the amide bond in the four-membered β-lactam ring needed for binding to PBPs, thus rendering the antibiotic ineffective.[31]

Another resistance mechanism is the modification of the drug by an antibiotic-altering enzyme. A notable example is the modification of aminoglycosides (AG). There are three types of aminoglycoside-modifying enzymes found in bacteria: an AG acetyltransferase, an AG phosphotransferase, and an AG nucleotidyltransferase. These modifications result in reduced binding of the aminoglycoside to the 30S ribosomal subunit.[32] The antibiotic-altering enzymes are known to work in different combinations

and these various distributions are specific to either Gram-positive or Gram-negative bacteria.[16, 32]

1.1.4 Current Antibiotic Crisis

Bacterial resistance to the current arsenal of antibiotics is an emerging threat to society.[1, 11] In recent years, the development of new antibiotics has dramatically decreased and the pharmaceutical industry has shifted its focus towards drugs for chronic, persistent illnesses. In addition, the cost of modifying current antibiotics to improve their overall efficacy has a low monetary return when compared to developing the drugs for chronic diseases. It is undeniable that antibiotic development has dramatically decreased within the past 25 years, as illustrated in Figure 1.7.[33] In fact, since 2008, only six antibiotics have been approved by the FDA compared to the sixteen that were approved from 1983-1987.[33-34] There is a dire need to discover novel targets and design innovative antibiotics to combat resistant pathogens against these targets.[1, 35]

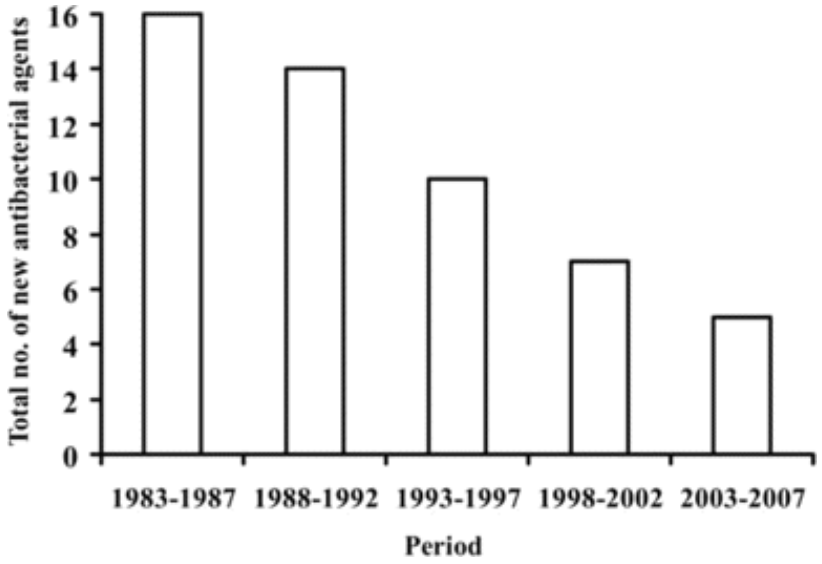

Figure 1.7. Antibacterial entities approved by the Food and Drug Administration per 5-year period; from Spellberg (2008).[33]

1.1.5 Antibiotic Drug Design

There are several approaches to design and develop novel antibiotics. These approaches include natural product screening, target identification and validation, high-throughput screening, structure-based drug design, virtual screening, and multitargeted strategies.

1.1.5.1 Natural Product Screening

Natural product screening is the most successful method in the discovery of novel antibiotics. Antibacterial agents derived from naturally occurring compounds have proven to be effective, as unmodified natural products or natural product derivatives, account for 75% of current antibiotics[36] and an estimated 40% of all medicines.[37] Natural products can be obtained from microbes and plant extracts, although many microbial and plant sources remain unexplored.[38] Natural products inherently possess more structural diversity than purely synthetic compounds.[39] Due to this diversity, the total synthesis, elaboration, and modification of many natural products present synthetic challenges. Although antibacterial potency can be high, the isolation of these antibiotics from their natural source runs the high risk of rediscovering known antibiotics and requires a significant amount of effort for a low yield of compound.[37]

1.1.5.2 Target Identification and Validation

There is a crucial need to identify and expand the list of potential targets for antibacterial action. Any resistance mechanisms against any new antibacterial agents for novel targets are unlikely to exist due to the lack of exposure to current antibiotics.[40] One way to identify targets is classic bacterial genetics which uses random mutagenesis of the genome to observe any lethal phenotypes, and then sequencing of the genome identifies

the mutated gene.[41] Another way to identify potential targets is a comparison of a sequence alignment between conserved bacterial genes and the human genome and looking for a bacterial gene that lacks a human homologue.[41]

Once a target is identified, validation of the target will determine if it is essential for the growth and viability of that organism. The typical approach is to construct a gene knockout using homologous recombination.[42] If the organism can survive without the gene product, then it is not considered essential and thus is not a valid target for antibiotic development. Once a target is validated, the next step is finding small molecules to act as antibacterial agents against those targets.

1.1.5.3 High-throughput Screening

High-throughput screening (HTS) involves screening millions of small molecules to determine inhibitory activity against a target.[43] HTS has not been particularly successful at identifying antibacterial agents due to the lack of whole-cell activity. In fact, Payne *et al.* reported 34 pharmaceutical companies have screened 60 different targets using HTS and failed to acquire any likely antibacterial agents. A suggested reason for the lack of viable antibiotic candidates is the absence of chemical diversity amongst the compounds in the screening libraries.[44] It also can take many years and the synthesis of multiple derivatives before a lead compound possesses all the necessary antibacterial and pharmaceutical properties to become a clinically useful antibiotic.[44]

1.1.5.4 Structure-based Drug Design

Structure-based drug design (SBDD) is a technique that utilizes a three-dimensional structure of the target to observe protein-ligand interactions. An analysis of how the ligand binds to a target can reveal whether or not modifications can be made to improve the

inhibitor.[45] For example, SBDD was pivotal in the modifications to new oxazolidinones that displayed increased potency and a better safety profile.[46] As of September 16th, 2014, there are 103,354 three-dimensional structures in the Protein Data Bank. The number of structures will continue to increase exponentially and the vast amount of structures available provides the tools needed for developing new antibacterial compounds.[47-48]

1.1.5.5 Virtual Screening

Virtual screening (VS) is a method that takes advantage of SBDD for discovering novel antibacterial agents. VS is a computer-based method that can utilize a structure with either an empty binding site or with a ligand bound in the active site.[39] Without a ligand, structure-based virtual screening utilizes docking algorithms to generate different positions of a ligand as well as score those positions to estimate binding affinity.[49] The ligand-based method uses a co-structure of an inhibitor which provides for a more rapid determination of steric and electronic features.[50] The combination of virtual screening approaches can result in the identification of a significant number of potential inhibitors without expending the time and resources for HTS.

1.1.5.6 Multitargeted Strategies

While all the aforementioned approaches utilize single small molecules for antibiotic development, resistance to these compounds is inevitable. Therefore, alternative approaches to combat antibacterial resistance involving multitarget strategies are preferred. Multitargeted chemotherapy is defined as either a combination therapy with two or more compounds (drug cocktail), two or more chemical agents within a single tablet (multicomponent drugs), or a single compound that targets two or more biological targets (multitarget ligands), Figure 1.8.[51] While the traditional drug cocktail is the most

frequently used form of treatment, it is often compromised due to low patient compliance for taking multiple medications.[51] There is currently a rise in the implementation of multicomponent drugs to simplify dosing and improve patient compliance. However, clinicians still prefer to prescribe a combination of monotherapies because it offers greater dose flexibility and overall lower cost for treatment. The advantage of a multi-ligand agent is a reduced amount of protein-ligand interactions taking place throughout the cell when compared to drug cocktails.[52] The downside to the multiple ligand approach is the difficulty in altering the ratio of activity for the different targets when using a single compound. However, the risks and costs of development for multiple ligand drugs are no different than that of single agent therapeutics.[51]

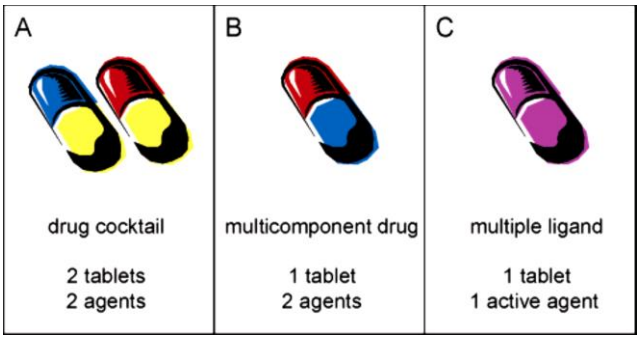

Figure 1.8. Three main clinical approaches for developing multitarget therapeutics; from Morphy (2005).[51]

The design and use of hybrid, or dual-ligand, molecules is more ideal than developing the perfect drug cocktail or multicomponent drug.[53-54] The majority of successful dual-ligand molecules consist of two protein-binding moieties joined via a linker of an appropriate length, Figure 1.9.[55] Covalently linking active biomolecules can use the cell membrane penetration of one antibiotic to boost the penetration of the other, as well as improve overall efficacy of both targets simultaneously.[56] Dual-ligand compounds that bind to sites whose structure is determined by more than one gene should not be susceptible

to single-step resistant mutations, leading to a reduced probability of forming antibiotic resistant bacteria.[35]

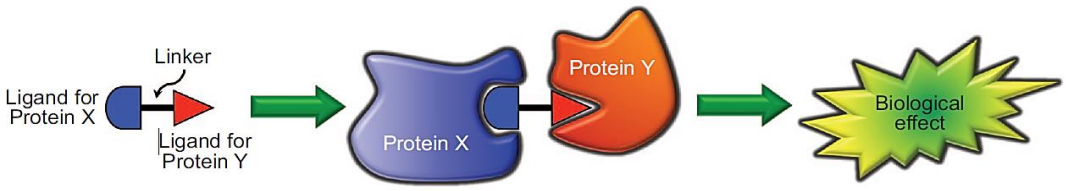

Figure 1.9. A dual-ligand compound interacting with two proteins can induce a biological effect; from Corson (2008).[55]

1.2 FATTY ACID BIOSYNTHESIS AS A TARGET FOR ANTIBIOTICS

1.2.1 Fatty Acid Synthesis

Fatty acid biosynthesis (FAS) is one of the most important and fundamental metabolic pathways in nature and is critical to bacterial viability.[57] The enzymes of the FAS pathway are divided into two distinct arrangements: type I or type II. The proteins of type I fatty acid synthase (FASI) in eukaryotes are expressed on a single large, multifunctional polypeptide containing domains for each enzyme.[58] Type I FAS enzymes are found most commonly in mammals, fungi, and some mycobacteria.[57, 59] In contrast, type II fatty acid synthase (FASII), found in the plastids of plants[60] and most bacteria, contains individual proteins that are encoded by discrete genes with the reaction intermediates being carried through the cytosol via a thioester on the acyl carrier protein (ACP).[57, 61-62] The steps in the FAS pathway are identical in mammals and bacteria, so the reactions catalyzed by the enzymes in the FAS pathway are the same. However, inhibitors can be produced to selectively target the bacterial system enzymes, as the protein sequences and active site arrangements are different in the enzymes compared to the human forms.[59, 63]

The enzymes of fatty acid biosynthesis are targets for the development of novel antibacterial agents, as fatty acids are crucial for membrane biogenesis and cell proliferation.[62] The enzymes and proteins involved with FASII consist of highly conserved protein sequences and are often encoded in clusters.[58] The ability to isolate the enzymatic activity of each protein in this pathway also makes this an ideal system for studying potential antibacterial agents.[59] The *acc* genes initiate the entire pathway of saturated fatty acid synthesis and encode the four-subunit, biotin-dependent enzyme acetyl-CoA carboxylase (ACC), which catalyzes the first committed step in this pathway. The *fab* (fatty acid biosynthesis) genes are responsible for encoding the majority of the proteins of this pathway.[59] The enzymes encoded by these genes are desirable targets for therapeutic developments, Figure 1.10.[63]

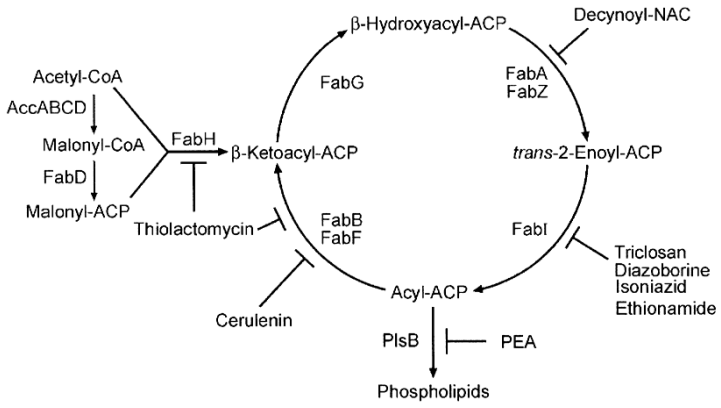

Figure 1.10. Pathway of fatty acid biosynthesis (FAS). Known inhibitors of the respective steps are shown; from Heath (2001).[58]

1.2.2 Fatty Acid Synthesis Inhibitors

Multiple FAS inhibitors have been developed as antibacterial agents, with the most well-known example being triclosan. Triclosan acts as a slow-binding inhibitor against enoyl-ACP reductase, encoded by the *fabI* gene.[58,63] Triclosan was originally patented as a herbicide, but was revealed to possess broad-spectrum antibacterial properties.[64] The

antibacterial power and safety of triclosan has led to its inclusion in many consumer products including antibacterial soaps, plastics, toothpaste, and detergents. Many structurally related analogues of triclosan, including hexachlorophene (Figure 1.11), also possess antimicrobial activities.[58] Early studies showed that triclosan and hexachlorophene displayed a mode of action causing *E. coli* to release cytoplasmic material following a drug treatment.[64] This indicated a non-specific disruption and led to the initial assumption that bacteria cannot become resistant to non-specific biocides.[58] Despite a non-specific mode of action, the widespread use of triclosan is now presenting a potential health risk as resistance is developing against clinically important pathogens.[65] For example, the pathogen *P. aeruginosa* is resistant to triclosan as a result of its multidrug efflux pumps.[66-67]

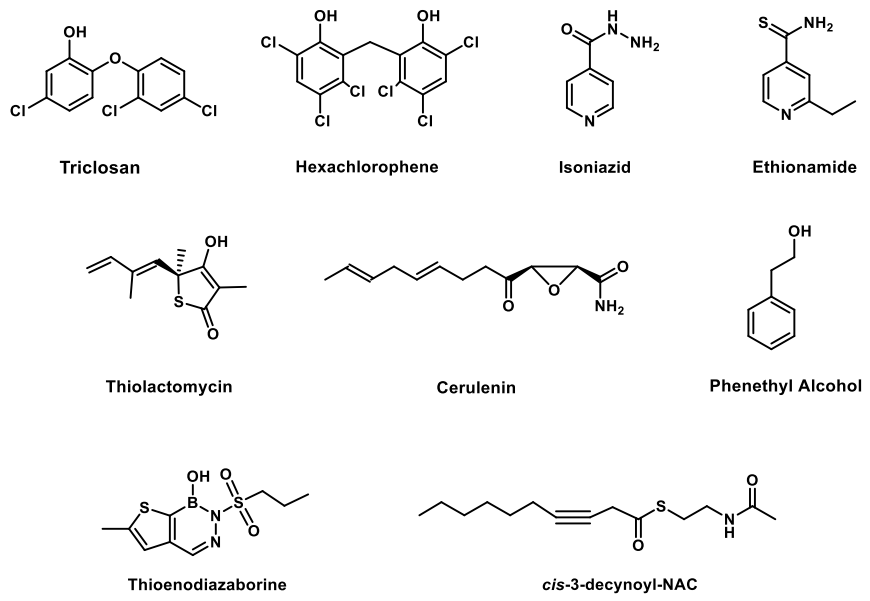

Figure 1.11. Structures of triclosan and hexachlorophene, as well as other compounds known to inhibit fatty acid biosynthesis.

Two other antibacterial compounds which inhibit FAS enzymes are cerulenin and thiolactomycin.[59] Cerulenin (CER) was the first compound identified to inhibit the

elongation condensing enzymes β-ketoacyl-ACP synthase I and II, encoded by the genes *fabB* and *fabF*, respectively.[63] CER occupies the hydrophobic channel in the enzyme where the growing chain of acyl-ACP would bind. However, CER is unlikely to ever become clinically useful due to its instability, poor pharmacological properties, and weak inhibition of mammalian fatty acid synthesis.[59] Thiolactomycin (TLM) was isolated from soil samples and was shown to have potent antibiotic activity against different bacterial species both *in vitro* and in animal studies, while lacking activity against FASI enzymes.[59] In contrast to CER, TLM binds to the malonyl-ACP binding site of β-ketoacyl-ACP synthase, which is found on the other side of the active site from the acyl-ACP channel.[63] Even though TLM only has modest antibacterial activity, it exhibits broad-spectrum activity against important pathogens, such as *Mycobacterium tuberculosis* and malaria.[68]

With a majority of the enzymes found in FASII being essential for bacterial viability, they are ideal targets for antibacterial drugs. However, there are currently no inhibitors being utilized clinically as antibacterial agents against the enzymes of bacterial acetyl-CoA carboxylase. Plants utilize the FASII system and plant ACC is a widely used target for herbicides, which confirms this step in the FAS pathway as a viable target for the development of novel antibacterial agents.[63, 69]

1.3 ACETYL-COA CARBOXYLASE

Acetyl-CoA carboxylase (ACC) is a multicomponent enzyme that catalyzes the first committed step in fatty acid synthesis and is found in animals, plants, and bacteria.[70] Acetyl-CoA carboxylase is made up of three subunits by four separately expressed proteins. They include a homodimeric biotin carboxylase (BC), a biotinylated biotin carboxyl carrier protein (BCCP), and an $\alpha_2\beta_2$ heterotetrameric carboxyltransferase (CT).

The genes for BC (*accC*) and BCCP (*accB)* are cotranscribed from an *accBC* mini-operon, while the genes for the α- and β-subunits of CT are encoded by *accA* and *accD*, respectively.[71-73] ACC was the first in a new class of enzymes to be recognized that use biotin as a prosthetic group.[74] The biotin is covalently attached to a lysine residue (Lys122; *E. coli* numbering) found on the biotin carboxyl carrier protein.[75] Isolated biotin carboxylase and carboxyltransferase can both utilize free biotin, i.e. not attached to BCCP, as a substrate making this enzyme an ideal system for studying biotin-dependent reactions.[76-77]

Acetyl-CoA carboxylase catalyzes the conversion of acetyl-CoA to malonyl-CoA via two half-reactions. In the first half-reaction, BC catalyzes the ATP-dependent carboxylation of the BCCP via a carboxyphosphate intermediate. In the second half-reaction, CT transfers the CO_2 group from carboxybiotin onto the acceptor molecule, acetyl-CoA, to generate malonyl-CoA, Figure 1.12.[78]

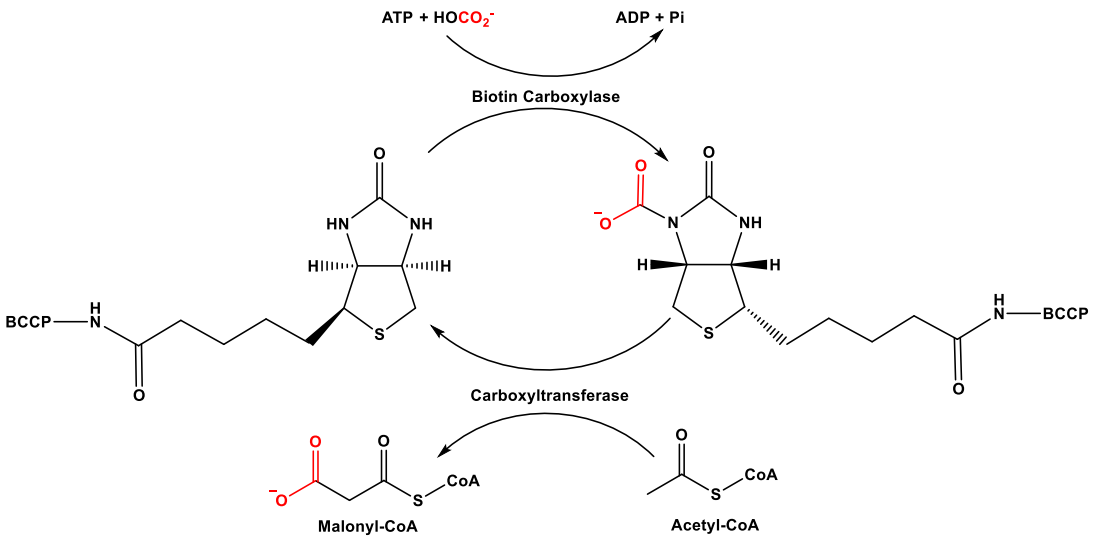

Figure 1.12. Acetyl-CoA (ACC) mechanism showing the two half-reactions catalyzed by biotin carboxylase (BC) and carboxyltransferase (CT).

1.3.1 Biotin Carboxylase

The structure of biotin carboxylase (BC) from *E. coli* was solved by Waldrop *et al.* in 1994 and was the first structure of a biotin-dependent carboxylase. BC is a homodimer and each monomer consists of 449 amino acid residues that are divided into three domains: an N-terminal domain, a B-domain or ATP-grasp domain, and a C-terminal domain.[79] Each monomer contains a complete active site as opposed to the active site being shared between residues or interfaces of the monomers.[79] The biotin carboxylase from *E. coli* is also similar in structure to the BC of *P. aeruginosa*, as well as other BC domains of biotin-dependent carboxylases.[80-82]

The three substrates of the BC reaction: ATP, biotin, and bicarbonate, follow a sequential kinetic mechanism, meaning that all substrates must bind to the enzyme before a product can be released.[83] Kinetic data also indicated that substrate addition was ordered with ATP binding first, followed by bicarbonate and then biotin, Figure 1.13.[84]

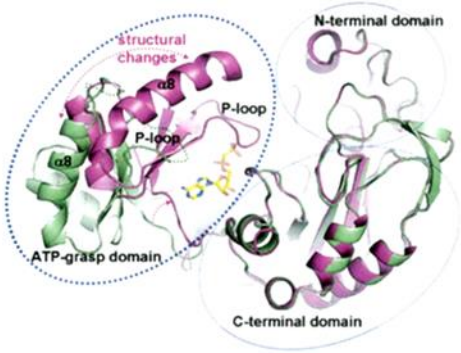

Figure 1.13. Structural changes at the ATP-binding site of *Pa*BC upon the binding of the ATP analog AMPCP. Ribbon representation of the protein coordinates of *Pa*BC in the apo form is colored in green. Ribbon representation of the *Pa*BC/AMPCP complex is colored in magenta; from Mochalkin (2008).[80]

When ATP, or an ATP analog binds to the active site, the ATP-grasp domain rotates 45° to close down on top of the substrate and hold it in the active site, Figure 1.13.[85-86] This is

considered the closed conformation and can be seen in crystal structures solved with ligands, including BC bound to all three substrates.[80, 87]

Biotin carboxylase has been shown to exhibit substrate-induced synergism, where the activity of BC is increased 1100-fold when biotin is bound.[88,70] Upon the binding of biotin, ATP will assume the more favorable extended conformation to allow for formation of the carboxyphosphate intermediate and subsequent carboxylation of biotin.[70] Evidence for the different binding modes of ATP can be seen in structures of AMPPNP, an ATP analog, bound to BC. The structure of AMPPNP bound to *E. coli* BC showed the γ-phosphate in a curled conformation, while the structure of *Staphylococcus aureus* BC bound with AMPPNP revealed an extended conformation, Figure 1.14.[80]

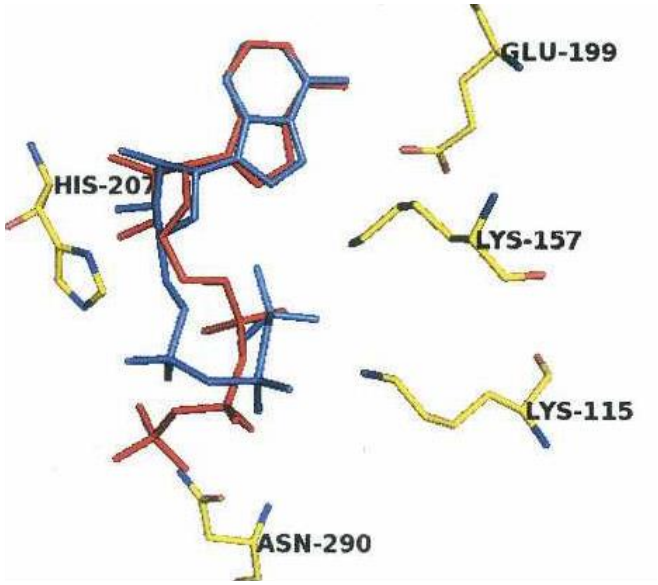

Figure 1.14. Superimposed AMPPNP in crystal structures of *Sa*BC and *Ec*BC. *Sa*BC/AMPPNP structure is colored in red and *Ec*BC/AMPPNP structure is colored in blue. *Sa*BC residues involved in interactions with the ligand are shown in sticks; from Mochalkin (2008).[80]

The active sites of BC have also been shown to display half-sites reactivity, or an extreme form of negative cooperativity, where the active sites alternate catalyzing the reaction.[89] In order to demonstrate this, hybrid dimers were created where one monomer

was wild-type BC and the other monomer was an inactive mutant. The mutant dimers were expected to display 50% of wild-type activity, but the overall activity ranged from 0.4-3.6%, revealing the mutant monomer was exerting a dominant-negative effect on the wild-type monomer.[89] This is indicative that the two active sites undergo oscillating cycles of catalysis whereby when one monomer of BC is releasing the product, the other monomer is binding substrates for catalysis. The structural evidence of the oscillating catalytic mechanism was observed in a crystal structure where one BC monomer was bound to $ADPCF_2P$ (an ATP analog) in the closed conformation and the other monomer was in the open conformation with no ligand in the active site, Figure 1.15.[80]

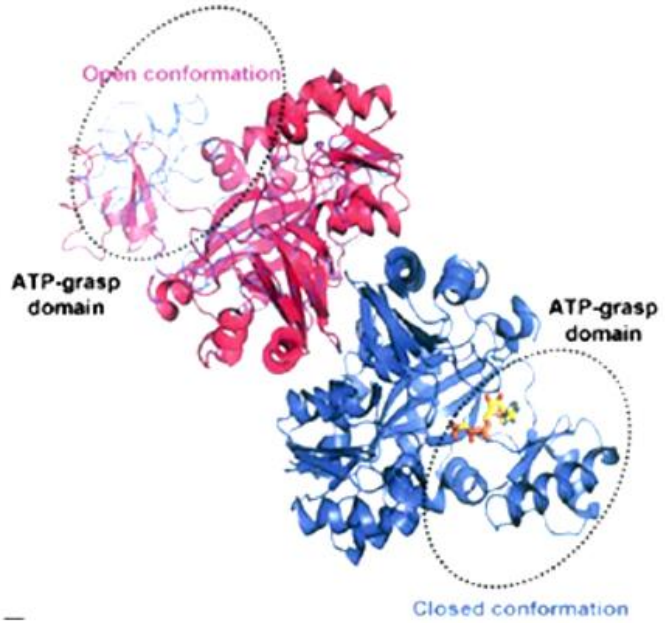

Figure 1.15. *Ec*BC dimer containing the $ADPCF_2P$ molecule bound to one subunit of the enzyme. The subunit with bound ATP analog is in closed conformation and colored in blue. Ribbon representation of the unliganded subunit of *Ec*BC is in open conformation and colored in pink. The backbone structure of the *Ec*BC subunit containing $ADPCF_2P$ is superimposed on the unliganded subunit for comparison and is shown in blue as a backbone representation; from Mochalkin (2008).[80]

1.3.2 Biotin Carboxyl Carrier Protein

1.3.2.1 Utilization of Biotin for Catalysis

The biotin carboxyl carrier protein (BCCP) uses the vitamin biotin for the ACC reaction. Biotin is a bicyclic compound composed of an ureido ring, a tetrahydrothiophene ring, and a valeric acid side chain.[85] There are eight stereoisomers of biotin, but D-(+)-biotin is the only active form found in nature and is only active when attached to certain metabolic enzymes (Figure 1.16).[75, 90-91] Biotin is the major cofactor found in metabolic processes involving carbon dioxide.

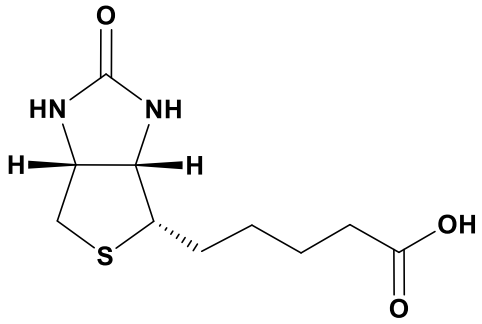

Figure 1.16. Active form of biotin, D-(+)-biotin.

The biotin cofactor is covalently attached to BCCP. Full length biotin carboxyl carrier protein has a molecular weight of 16.7 kDa, although early purification of BCCP yielded a range of molecular weights that were attributed to oligomerization or proteolytic cleavage of the full length protein.[92] A system was later developed to overexpress and purify the last 87 residues of BCCP (BCCP87).[93] BCCP87 can be biotinylated and has been shown to have an 8000-fold and 2000-fold greater catalytic efficiency than biotin in the BC and CT reactions, respectively.[94]

1.3.2.2 Structure of BCCP

The structure of *E. coli* BCCP is composed of two domains, an N-terminal domain and a C-terminal domain. The crystal structure of the C-terminal domain of *E. coli* BCCP

was first solved in 1995 by Athappilly *et al.* and contained two sets of four antiparallel β-strands.[95] In 1997, Yao *et al.* solved the NMR structure of apo-BCCP87 (i.e., without biotin attached) and the NMR structure of holo-BCCP87 was solved shortly thereafter and both NMR structures showed no difference compared to the crystal structure.[96] The C-terminal domain of BCCP is highly conserved and contains the lysine targeted for biotinylation in an AMKM motif that is highly conserved.[75] The AMKM motif is biotinylated at the Lys122 (*E. coli* numbering), and was found in a β-hairpin turn that extends out from the body of the C-terminal domain (Figure 1.17).[75, 97] The orientation of the residues in the C-terminal domain of BCCP affects efficient use of the protein as a substrate, as the C-terminal domain is thought to undergo a structural change upon biotinylation.[98]

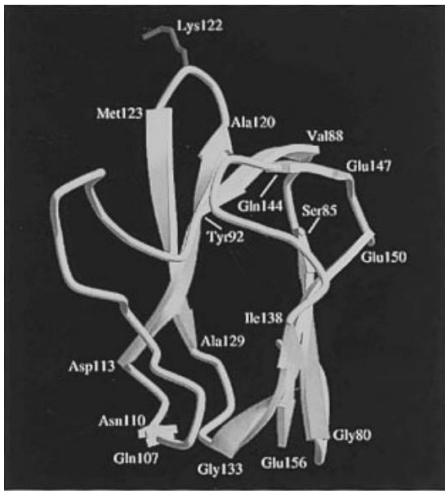

Figure 1.17. Ribbon drawing of the *E. coli* BCCP87 NMR structure with the biotin-binding Lys122 residue shown on the β-hairpin turn of the C-terminal domain; from Yao (1997).[97]

The structure of *E. coli* holo-BCCP still has not been crystallized, most likely due to a pro-ala rich linker region between the domains of BCCP that causes the N-terminal domain to be flexible.[99] Li *et al.* postulated the N-terminal domain of BCCP was involved

in the interaction of BCCP with the other subunits of ACC.[71] However, a recent crystal structure of the *E. coli* BC-BCCP complex showed the N-terminal domain was not involved in the interaction between these two subunits.[100]

A unique feature observed with *E. coli* BCCP is a "thumb" region that extends out from the body of the C-terminal domain, Figure 1.18. This thumb region was shown to be essential for bacterial viability of *E. coli* as deletion of the thumb region in BCCP mutants prevented growth.[101] The mechanism for this phenomenological result is not known. It is clearly not needed for catalysis because BCCP from other species lack a thumb, Figure 1.18.[100-101] Additionally, this region does not appear to be involved with the biotinylation reaction as proteins that lack a thumb region can still be biotinylated by biotin protein ligase.[102]

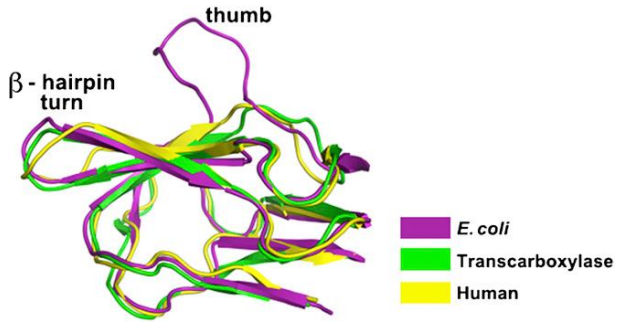

Figure 1.18. Overlay of *E. coli* BCCP (purple) with the BCCP domain from human acetyl-CoA carboxylase (yellow) and the 1.3S subunit of transcarboxylase (green). The β-hairpin turn is labeled and the unique thumb region of the *E. coli* BCCP is shown pointing upwards; from Broussard (2013).[100]

1.3.2.3 Biotin Protein Ligase

Biotin protein ligase (BPL), or holocarboxylase synthetase, is a highly conserved enzyme and is responsible for attaching the biotin onto the appropriate lysine residue via two half-reactions, Figure 1.19.[75] In the first half-reaction, BPL catalyzes the formation of biotinoyl-5′-AMP from the substrates, biotin and ATP. During the second half-reaction,

biotin is transferred from biotinoyl-5′-AMP to form an amide bond between the ε-amino group of lysine and the carboxylic acid on the valeric acid side chain of biotin.[75] BPL is able to selectively biotinylate biotin-dependent enzymes from many bacterial species, although in *E. coli*, acetyl-CoA carboxylase is the only carboxylase that undergoes this biotinylation reaction since ACC is the only biotin-dependent enzyme found in *E. coli*.[103-104]

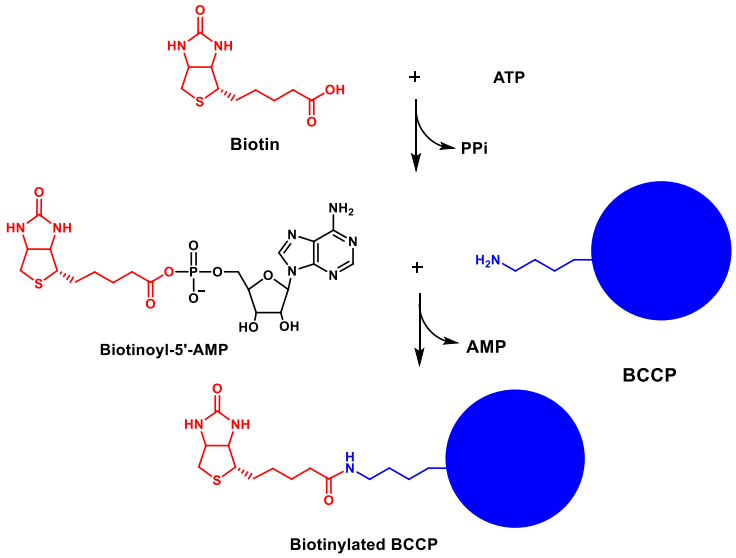

Figure 1.19. The biotin protein ligase (BPL) reaction; adapted from Chapman-Smith (1999).[75]

1.3.3 Carboxyltransferase

Carboxyltransferase was the last of the ACC subunits to be crystallized. The carboxyltransferase domain of yeast ACC was first crystallized in 2003 by Zhang and coworkers.[105] The crystal structures of *S. aureus* and *E. coli* CT were crystallized by Bilder *et al.* in 2006. The structure confirmed the bacterial form of CT exists as an $\alpha_2\beta_2$ heterotetramer, Figure 1.20, which was first suggested by Guchhait *et al.* in 1974.[106-107] This observation was in contrast to the yeast CT structure which existed as a dimer, with each monomer containing two domains. These two domains appeared to mimic the

individual α- and β-subunits found in bacterial CT.[85, 105] The active sites of bacterial CT are formed at the interface of the α- and β-subunits, where the α-subunit binds biotin and the β-subunit binds acetyl-CoA.

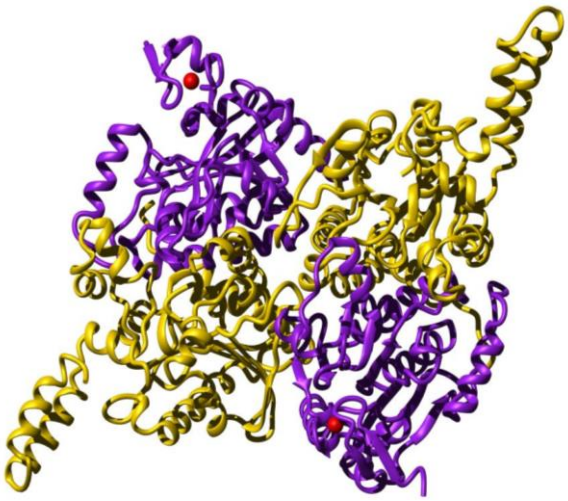

Figure 1.20. The $\alpha_2\beta_2$ heterotetrameric structure of carboxyltransferase with the α-subunit in yellow and the β-subunit in purple; from Bilder (2006).[106]

An interesting feature of this active site is that both the α- and β-subunits contain a symmetrical core fold where the binding of these substrates occurs, placing carboxyltransferase in the crotonase superfamily of enzymes, Figure 1.21, (A).[106, 108] The members of this superfamily of enzymes all catalyze reactions that involve enolate anions.[109] In order to stabilize these oxyanions, two peptidic -NH groups form an oxyanion hole allowing hydrogen bonding from the peptidic protons to the enolate anions. The peptidic -NH groups responsible for hydrogen bonding are found at the N-terminus of an α-helix, where the helix dipole helps provide an overall positive charge for anion stabilization.[85] In *E. coli*, the putative active site residues involved in the formation of these oxyanion holes are Gly204 and Gly205 in the β-subunit and Gly206 and Gly207 in

the α-subunit and are used to stabilize the enolate and imidate anions in acetyl-CoA and biotin generated during catalysis, respectively, Figure 1.21, (B). [106]

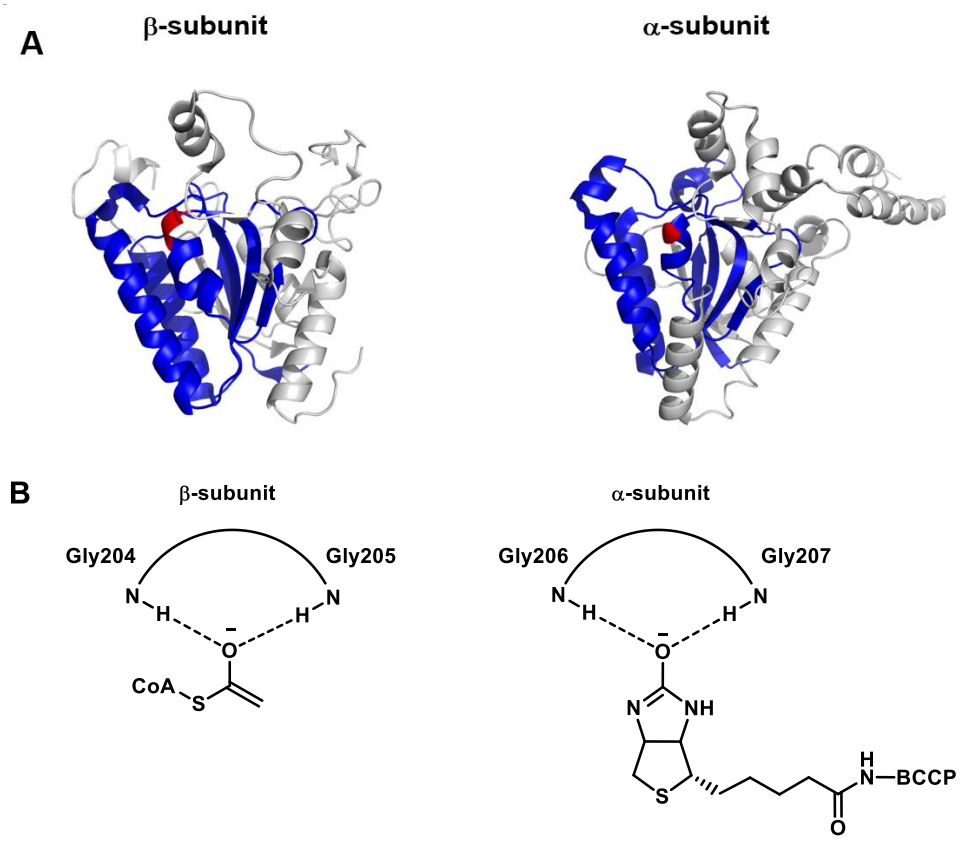

Figure 1.21. (A) The structure of the α- and β-subunits of carboxyltransferase with the crotonase-fold motif highlighted in blue and the adjacent glycine residues that form the oxyanion holes highlighted in red; from Waldrop (2011).[108] (B) The oxyanion holes generated from peptidic amine groups in the α- and β-subunits of carboxyltransferase.

The crystal structures of *E. coli* and *S. aureus* also revealed a four-cysteine zinc finger domain on the N-terminus of the β-subunit, which had never been observed before with the eukaryotic carboxyltransferases, Figure 1.22.[85, 106] The amino acids that constitute and surround this domain have a positive electrostatic surface potential, while the rest of the protein has an overall negative electrostatic surface potential.[106, 110] A common feature associated with zinc finger domains is their ability to bind nucleic acids. Benson *et al.* showed that *E. coli* CT was indeed able to bind DNA in a non-specific manner.[110] The

study also revealed that not only does DNA inhibit CT activity, but the binding of the CT substrates (malonyl-CoA and biocytin) inhibit the binding of DNA.[110] Mutational analysis of the zinc finger domain displayed a substantial decrease in activity when only one cysteine was mutated, while more than one mutation resulted in complete loss of activity.[111]

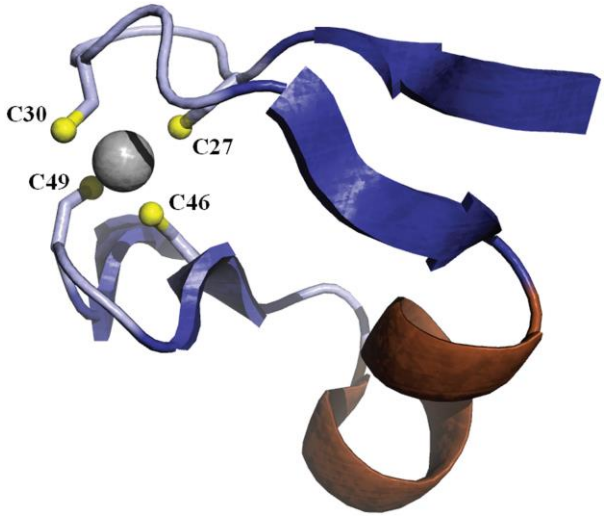

Figure 1.22. The four-cysteine zinc finger found on the N-terminus of the β-subunit of carboxyltransferase; from Meades (2010).[111]

1.3.4 Regulation of Bacterial ACC

The reaction catalyzed by acetyl-CoA carboxylase is the rate-limiting and committed step in fatty acid biosynthesis.[112] Fatty acid synthesis accounts for 94% of ATP consumption for membrane biogenesis and inefficient regulation of this pathway would result in an unnecessary use of cellular energy.[113]

The BC-BCCP genes may be transcriptionally regulated. The overexpression of BCCP down-regulated expression of the chromosomal *accBC* operon and more specifically, the overexpression of the first 44 residues of the N-terminal of BCCP decreased transcript levels.[73] In addition, James and Cronan replaced the promoter of the *accBC* mini-operon with the promoter from the lactose operon and found expression of the

accBC gene increased by 5-fold in comparison to transcription levels in the presence of the wild-type promoter. This result led to the conclusion that BCCP, and more specifically the N-terminal domain of BCCP, is involved in autoregulating the transcription of the *accBC* operon and is likely the method of regulation in many bacterial species due to the cotranscription of these two genes being highly conserved.[73] In contrast, the *accA* and *accD* genes encoding the α- and β-subunits of CT, respectively, are expressed in gene clusters on opposite sides of the *E. coli* chromosome.[113] Both genes are transcribed in a clockwise rotation and could be co-regulated, although there is no data to support this.[71, 113]

There are different ways that acetyl-CoA carboxylase is regulated. For example, Meades *et al.* has recently shown that CT can regulate its own translation by specifically binding to the mRNA that codes for the α- and β-subunits of CT.[111] Acetyl-CoA competes with its own mRNA for binding to the active site of CT. This allows for CT to work as a "dimmer switch" for its own translation by detecting the cellular levels of acetyl-CoA.[111] For instance, when there is an increase in cellular growth rates and the intracellular levels of acetyl-CoA are high, CT is displaced from its mRNA allowing for the translation of CT and subsequent production of malonyl-CoA.[111] Additionally, a recent study by Broussard *et al*. has shown that the BC reaction displays substrate synergism with acetyl-CoA; in other words, the three components of ACC do not undergo catalysis unless acetyl-CoA is also present in order to avoid wasteful hydrolysis of ATP.[114] The ACC complex is also subject to negative feedback inhibition by the end products of fatty acid synthesis, the long chain acyl-ACPs.[58]

1.4 BACTERIAL ACETYL-COA CARBOXYLASE AS A NOVEL TARGET FOR ANTIBIOTICS

ACC catalyzes the first committed step in fatty acid synthesis and is essential for bacterial viability, making ACC a promising target for the development of antibiotics with novel modes of action.[115-116] Acetyl-CoA carboxylase is highly conserved among bacteria therefore novel antibiotics have the potential to behave as broad-spectrum agents. There are currently no examples of ACC inhibitors being clinically used as antibacterial agents. The recent discovery of small molecule inhibitors of ACC present potential clinical antibiotics.[117]

1.4.1 Antibacterial Agents of Biotin Carboxylase

Biotin carboxylase is the target for three different types of antibacterial compounds: pyridopyrimidines[118], aminooxazoles[119] and benzimidazole-carboxamides[115].

1.4.1.1 Pyridopyrimidines

The pyridopyrimidines were the first class of antibacterial agents found to inhibit BC. Miller *et al.* utilized bacterial whole-cell screening on a library of 1.6 million compounds originally designed to target eukaryotic tyrosine kinases.[118] While screening these compounds, they discovered a class of pyridopyrimidines that exhibited antibacterial activity.[118] The target of the pyridopyrimidines was determined by generating spontaneous-resistant mutations in bacteria. The strains responsible for exhibiting resistance were sequenced and the resistance-conferring gene was mapped back to *accC*, which encodes the BC component of ACC. The resistance mutation resulted in the isoleucine at position 437 being replaced with a threonine and this mutation was found to reside in the ATP-binding site of BC.[80, 118]

The pyridopyrimidines were bactericidal *in vitro* as well as *in vivo* against Gram-negative pathogens, such as *E. coli* and *Haemophilus influenzae*, as well as the Gram-positive *S. aureus*. However, the MIC values were higher for Gram-positive pathogens indicating selectivity for Gram-negative BC. The selective action of the pyridopyrimidines for Gram-negative bacteria can be traced back to the I437T mutation that was used to identify the target. Biotin carboxylase in Gram-positive bacteria naturally contain a threonine at that position. Structural analysis of pyridopyrimidine **1** bound to the I437T mutant in *E. coli* revealed the threonine caused a decrease in antibacterial activity due to loss of hydrophobic contacts as well as reduced shape complementarity with the inhibitor.[118-120] The pyridopyrimidines were also revealed to be selective for bacterial BC over eukaryotic BC.[118]

1.4.1.2 Aminooxazoles

To expand on the findings of the pyridopyrimidines, Mochalkin *et al.* utilized virtual screening and fragment-based drug discovery to identify novel inhibitors for biotin carboxylase. First, they used ligand-based virtual screening using pyridopyrimidine **1** (Figure 1.23A) as a starting point for screening a library of 2.2 million compounds to identify structures with similar shapes and surface electrostatics as the lead inhibitor.[117, 119] After *in vitro* testing of 525 compounds identified in the screen, a total of 48 compounds displayed 50% inhibitory concentration (IC_{50}) values of less than 10 μM.

In addition, Mochalkin *et al.* used fragment-based screening on a library of 5,200 fragments to yield 142 compounds that exhibited significant inhibition of BC. Superimposition of the structures revealed the pharmacophore features that were important for binding in the ATP-binding site of BC.[117] For example, fragment **2**, Figure 1.23, (A),

was found to be an inhibitor of BC and shared similar binding features with pyridopyrimidine **1**.[119] A comparison of structures shows that fragment **2** contains an exo-cyclic amine group on the oxazole ring, analogous to the exo-cyclic amine in the pyrimidine ring of compound **1**. Structural analysis confirmed the aminooxazole fragment interacts in the same manner and with the same active site residues in BC as the pyridopyrimidines, Figure 1.23, (B).[119-120]

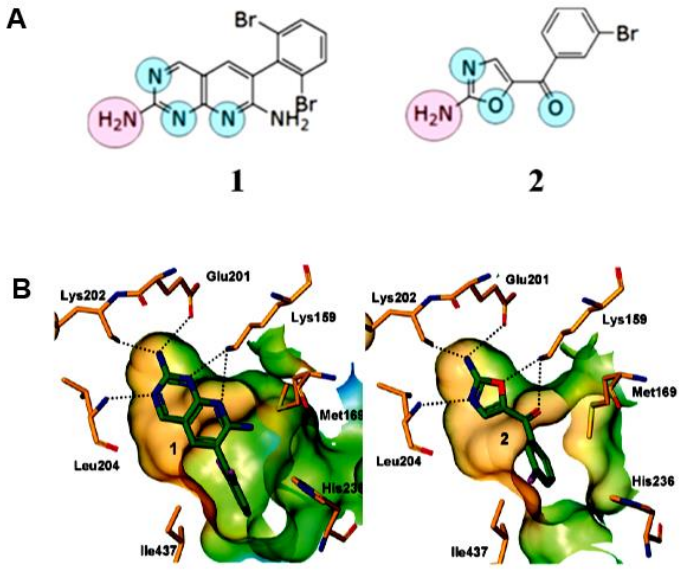

Figure 1.23. (A) Pyridopyrimidine BC inhibitor **1** and fragment hit **2**. Selected pharmacophore features essential for binding interactions shown in following colors: cyan (hydrogen bond acceptors) and pink (hydrogen bond donors). (B) Binding modes of compound **1** and fragment **2** to the ATP-binding site of *Ec*BC determined by X-ray crystallography; from Mochalkin (2009).[119]

While fragment-based screening allows for testing of large libraries of compounds, these compounds usually display low binding affinity to the target; therefore, fragment-to-lead optimization was utilized to discover more potent inhibitors. The use of fragment growing, merging, and morphing was used to identify compounds with a much higher affinity for BC. Even though pyridopyrimidine **1** is a potent inhibitor (K_i = 5 nM), the aminooxazoles were more amenable to synthetic elaboration and thus were used in these

studies. The aminooxazole moiety from fragment **2** provided an "anchor" for binding to the ATP site while extending fragment **2** out into the active site allowed for increased interaction with hydrophobic residues that led to increased potency without compromising binding efficiency.[119]

This fragment-based approach led to different aminooxazole analogs (compounds **3-5**, Figure 1.24) that were synthesized and analyzed for inhibitory and antibacterial activity.[119] Fragment **3** showed a 20-fold increase in potency over starting fragment **2** while fragment **4** containing the dibenzylamide side chain had a net 200-fold increase in potency over fragment **2**. The selection of a more electron-rich side chain led to the generation of fragment **5** with an impressive 3000-fold increase in potency over fragment **2**. The more potent inhibitors of BC, fragments **4** and **5**, displayed antibacterial activity against efflux-pump-deficient *H. influenzae* and *E. coli*.[119-120] However, fragment **5** overall displayed whole-cell activity that was markedly lower than fragment **4**. This highlights a major challenge when developing new antibacterial agents in that target potency does not necessarily correlate to whole-cell antibacterial activity.[119] Fragments **4** and **5** also displayed a reduction in antibacterial activity against bacteria with the I437T mutation, similar to pyridopyrimidine **1**.[119]

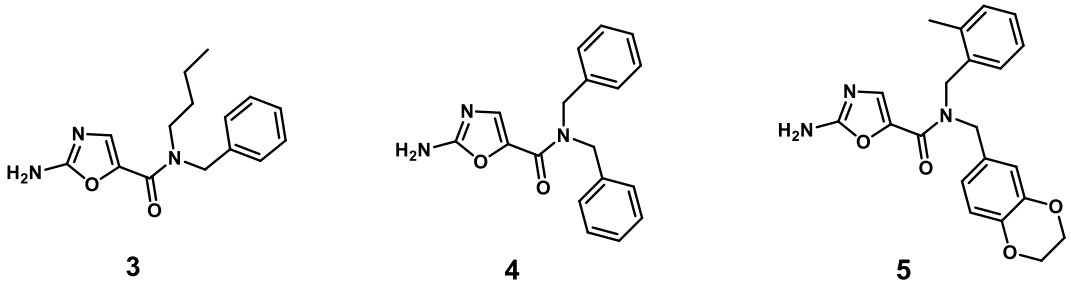

3 **4** **5**

Figure 1.24. BC inhibitor fragments **3-5**.

1.4.1.3 Benzimidazole-carboxamides

Around the same time the pyridopyrimidines and aminooxazoles were being discovered, a group at Schering-Plough was developing their own class of BC inhibitors, the benzimidazole-carboxamides.[115] Cheng *et al.* utilized HTS to identify a group of compounds that displayed inhibitory activity against BC. Additional SBDD and computer-guided modeling of the initial hits generated a series of benzimidazole-carboxamide derivatives, for example benzimidazole **6**, Figure 1.25, (A). X-ray crystallography confirmed benzimidazole **6** bound in the ATP-binding site of BC, Figure 1.25, (B). The $-NH_2$ of benzimidazole **6** was found to interact with both Glu201 and Lys202, which are the same residues that interact with the exo-cyclic amines found in both the pyridopyrimidines and the aminooxazoles. This indicates the primary $-NH_2$ groups are an essential structural moiety for enzyme recognition and binding. The benzimidazoles also inhibited a broad-spectrum of pathogenic bacteria and were shown not to inhibit eukaryotic ACC.[115]

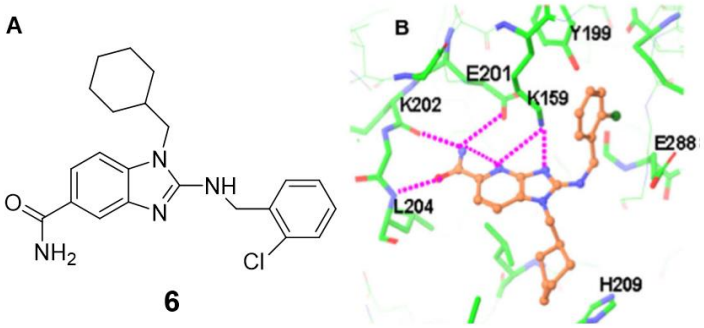

Figure 1.25. (A) Structure of benzimidazole **6**. (B) Structure of benzimidazole **6** bound in the BC active site; from Cheng (2009).[115]

1.4.2 Antibacterial Agents of Carboxyltransferase

In contrast to the biotin carboxylase, there is only one known class of antibacterial agents known to inhibit carboxyltransferase, the natural products andrimid and moiramide B, Figure 1.26. Andrimid was isolated and characterized from an *Enterobacter* sp. in an

intracellular symbiont found in the brown planthopper, *Nilaparvata lugens*.[121] A few years later, Needham *et al.* isolated marine microorganisms from their habitats and screened them for antibiotics with antibacterial activity.[122] Through screening of these marine organisms, an isolate of the bacterium *Pseudomonas fluorescens* was acquired and an extract from this marine species displayed strong inhibition against methicillin-resistant *S. aureus* (MRSA). Fractionation of the extract resulted in the identification of four metabolites: andrimid and moiramides A-C (Figure 1.26) with only andrimid and moiramide B exhibiting any antibacterial activity.[122]

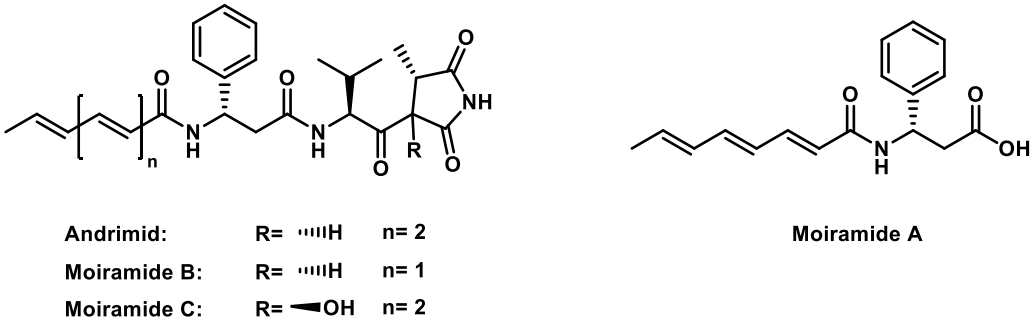

Figure 1.26. Structures of the natural products andrimid and moiramides A-C.

Biological studies revealed that andrimid and moiramide B both showed broad-spectrum *in vitro* antibacterial activity, with moiramide B being more potent.[122-123] Prior synthesis of andrimid revealed the pyrrolidinedione fragment containing the 4*S*-methyl substituent to be essential for activity, as removal of the methyl group abolished activity.[124-125] Moiramides A and C were both inactive in regards to MRSA and other species, which further reiterates the strict structural conformation of the pyrrolidinedione fragment; moiramide A lacks a pyrrolidinedione unit completely while moiramide C contains a 3*R*-hydroxyl substitution on the pyrrolidinedione ring.[122, 126]

The target for moiramide B was determined by Freiberg *et al.* to be the carboxyltransferase enzyme of acetyl-CoA carboxylase. Moiramide B displayed

competitive inhibition against malonyl-CoA (K_{is} = 5 nM) and noncompetitive inhibition against biocytin.[123] The generation of various resistant mutants of *S. aureus* revealed single amino acid mutations in not only the α–subunit of CT, but also the β-subunit which validated moiramide B targets the CT component of ACC.[116, 123] Studies also revealed a lack of inhibition against eukaryotic ACC, indicating selectivity for the prokaryotic form of the enzyme.[123] Structure-activity relationship (SAR) studies of moiramide B revealed that the fatty acid chain and the pyrrolidinedione moiety play two different roles in binding to the target. Variations to the fatty acid side chain showed it was not pivotal to binding while limited modifications to the pyrrolidinedione head group were tolerated. Analogs with either bulky, hydrophobic groups on the pyrrolidinedione nitrogen or modification of the (4*S*)-methyl group displayed a significant decrease or total loss in antibacterial activity.[125] A crystal structure of these potent natural products in complex with carboxyltransferase would further validate the mode of action.

1.5 PURPOSE OF DISSERTATION

The identification of inhibitors targeting each enzyme of ACC has the potential to generate a dual-ligand inhibitor for this multicomponent enzyme. Aminooxazole **4** is amenable to synthetic variations on the dibenzylamide side chain without affecting the crucial moieties necessary for binding in the ATP-binding site of biotin carboxylase. Likewise, the acyl side chain is not required for moiramide B to bind to carboxyltransferase, allowing for modifications to this portion of the molecule. This allows for appropriate functional groups to be placed on each known inhibitor to be chemically modified into a dual-ligand inhibitor connected via a linker segment. A designed dual-ligand inhibitor incorporating these known ACC inhibitors could ultimately generate an

inhibitor that behaves as a broad-spectrum antibacterial agent. A dual-ligand inhibitor can also possess an overall tighter affinity than individual agents which ultimately leads to using less antibiotics to generate the same effect; therefore, bacteria are less likely to develop resistance mechanisms. The design and synthesis of dual-ligand inhibitors for ACC and the biological testing of their potency will determine the overall best model for generating multitarget therapeutics to combat resistant pathogenic bacteria.[56]

The ability to synthesize the natural product moiramide B paves the way for further characterization and determination of the mode of action for this class of antibiotics. The construction of moiramide B proceeds in a head-to-tail fashion, starting with the pyrrolidinedione head group and ending with the attachment of the unsaturated acyl chain. By isolating moiramide B into molecular fragments, the function of those fragments with respect to the inhibition of carboxyltransferase and the antibacterial properties can be determined. The availability of moiramide B in milligram quantities also yields enough compound to determine the three-dimensional structure of moiramide B bound to carboxyltransferase and reveal the mechanism of action.

1.6 REFERENCES

(1) Walsh, C., *Antibiotics: Actions, Origins, Resistance*. ASM Press: USA, **2003**.

(2) Levy, S. B., The challenge of antibiotic resistance. *Sci. Am.* **1998,** *278*, 46-53.

(3) Waksman, S. A., What is an antibiotic or an antibiotic substance? *Mycologia* **1947,** *39*, 565-569.

(4) Bosch, F.; Rosich, L., The contributions of Paul Ehrlich to pharmacology: a tribute on the occasion of the centenary of his Nobel Prize. *Pharmacology* **2008,** *82*, 171-179.

(5) Lloyd, N. C.; Morgan, H. W.; Nicholson, B. K.; Ronimus, R. S., The composition of Ehrlich's salvarsan: resolution of a century-old debate. *Angew. Chem. Int. Ed. Engl.* **2005,** *44*, 941-944.

(6) von Nussbaum, F.; Brands, M.; Hinzen, B.; Weigand, S.; Häbich, D., Antibacterial natural products in medicinal chemistry - Exodus or Revival? *Angew. Chem. Int. Ed.* **2006,** *45*, 5072-5219.

(7) Katz, M. L.; Mueller, L. V.; Polyakov, M.; Weinstock, S. F., Where have all the antibiotic patents gone? *Nat. Biotechnol.* **2006,** *24*, 1529-1531.

(8) Florey, H. W., Use of micro-organisms for therapeutic purposes. *Brit. Med. J.* **1945,** *2*, 635-642.

(9) O'Shea, R.; Moser, H. E., Physicochemical properties of antibacterial compounds: implications for drug discovery. *J. Med. Chem.* **2008,** *51*, 2871-2878.

(10) Carpenter, C. F.; Chambers, H. F., Daptomycin: another novel agent for treating infections due to drug-resistant Gram-positive pathogens. *Clin. Infect. Dis.* **2004,** *38*, 994-1000.

(11) Walsh, C., Where will new antibiotics come from? *Nat. Rev. Microbiol.* **2003,** *1*, 65-70.

(12) Lewis, K., Platforms for antibiotic discovery. *Nat. Rev. Drug Discov.* **2013,** *12*, 371-387.

(13) Drawz, S. M.; Bonomo, R. A., Three decades of β-lactamase inhibitors. *Clin. Microbiol. Rev.* **2010,** *23*, 160-201.

(14) Van Bambeke, F., Glycopeptides and glycodepsipeptides in clinical development: A comparative review of their antibacterial spectrum, pharmacokinetics, and clinical efficacy. *Curr. Opin. Investig. Drugs* **2006,** *7*, 740-749.

(15) Weisblum, B., Erythromycin resistance by ribosome modification. *Antimicrob. Agents Chemother.* **1995,** *39*, 577-585.

(16) Lambert, T., Antibiotics that affect the ribosome. *Rev. Sci. Tech.* **2012,** *31*, 57-64.

(17) Connell, S. R.; Tracz, D. M.; Nierhaus, K. H.; Taylor, D. E., Ribosomal protection proteins and their mechanism of tetracycline resistance. *Antimicrob. Agents Chemother.* **2003,** *47*, 3675-3681.

(18) Suto, M. J.; Domagala, J. M.; Roland, G. E.; Mailloux, G. B.; Cohen, M. A., Fluoroquinolones: relationships between structural variations, mammalian cell cytotoxicity, and antimicrobial activity. *J. Med. Chem.* **1992,** *35*, 4745-4750.

(19) Hooper, D. C., Emerging mechanisms of fluoroquinolone resistance. *Emerg. Infect. Dis.* **2001,** *7*, 337-341.

(20) Campbell, E. A.; Korzheva, N.; Mustaev, A.; Murakami, K.; Nair, S.; Goldfarb, A.; Darst, S. A., Structural mechanism for rifampicin inhibition of bacterial RNA polymerase. *Cell* **2001,** *104*, 901-912.

(21) Slatore, C. G.; Tilles, S. A., Sulfonamide hypersensitivity. *Immunol. Allergy Clin. North Am.* **2004,** *24*, 477-490, vii.

(22) Palumbi, S. R., Humans as the world's greatest evolutionary force. *Science* **2001,** *293*, 1786-1790.

(23) Levy, S. B., The 2000 Garrod lecture. Factors impacting on the problem of antibiotic resistance. *J. Antimicrob. Chemother.* **2002,** *49*, 25-30.

(24) Braoudaki, M.; Hilton, A. C., Low level of cross-resistance between triclosan and antibiotics in *Escherichia coli* K-12 and *E. coli* O55 compared to *E. coli* O157. *FEMS Microbiol. Lett.* **2004,** *235*, 305-309.

(25) Levy, S. B., Active efflux, a common mechanism for biocide and antibiotic resistance. *J. Appl. Microbiol.* **2002,** *92 Suppl*, 65S-71S.

(26) Nikaido, H., Antibiotic resistance caused by Gram-negative multidrug efflux pumps. *Clin. Infect. Dis.* **1998,** *27 Suppl 1*, S32-41.

(27) Aeschlimann, J. R., The role of multidrug efflux pumps in the antibiotic resistance of *Pseudomonas aeruginosa* and other Gram-negative bacteria. *Pharmacotherapy* **2003,** *23*, 916-924.

(28) Poole, K., Multidrug efflux pumps and antimicrobial resistance in *Pseudomonas aeruginosa* and related organisms. *J. Mol. Microbiol. Biotechnol.* **2001,** *3*, 255-264.

(29) Ma, D.; Cook, D. N.; Alberti, M.; Pon, N. G.; Nikaido, H.; Hearst, J. E., Genes *acrA* and *acrB* encode a stress-induced efflux system of *Escherichia coli*. *Mol. Microbiol.* **1995,** *16*, 45-55.

(30) Piddock, L. J., Multidrug-resistance efflux pumps - not just for resistance. *Nat. Rev. Microbiol.* **2006,** *4*, 629-636.

(31) Kotra, L. P.; Mobashery, S., Mechanistic and clinical aspects of β-lactam antibiotics and β-lactamases. *Arch. Immunol. Ther. Exp.* **1999,** *47*, 211-216.

(32) Green, K. D.; Chen, W.; Garneau-Tsodikova, S., Effects of altering aminoglycoside structures on bacterial resistance enzyme activities. *Antimicrob. Agents Chemother.* **2011,** *55*, 3207-3213.

(33) Spellberg, B.; Guidos, R.; Gilbert, D.; Bradley, J.; Boucher, H. W.; Scheld, W. M.; Bartlett, J. G.; Edwards, J., Jr.; Infectious Diseases Society of, A., The epidemic of antibiotic-resistant infections: a call to action for the medical community from the Infectious Diseases Society of America. *Clin. Infect. Dis.* **2008,** *46*, 155-164.

(34) Butler, M. S.; Blaskovich, M. A.; Cooper, M. A., Antibiotics in the clinical pipeline in 2013. *J. Antibiot. (Tokyo)* **2013,** *66*, 571-591.

(35) Silver, L. L., Multi-targeting by monotherapeutic antibacterials. *Nat. Rev. Drug Discov.* **2007,** *6*, 41-55.

(36) Newman, D. J.; Cragg, G. M., Natural products as sources of new drugs over the last 25 years. *J. Nat. Prod.* **2007,** *70*, 461-477.

(37) Lahlou, M., The success of natural products in drug discovery. *Pharmacology & Pharmacy* **2013,** *4*, 17-31.

(38) Clardy, J.; Fischbach, M. A.; Walsh, C. T., New antibiotics from bacterial natural products. *Nat. Biotechnol.* **2006,** *24*, 1541-1550.

(39) Shen, J.; Xu, X.; Cheng, F.; Liu, H.; Luo, X.; Shen, J.; Chen, K.; Zhao, W.; Shen, X.; Jiang, H., Virtual screening on natural products for discovering active compounds and target information. *Curr. Med. Chem.* **2003,** *10*, 2327-2342.

(40) Brown, E. D.; Wright, G. D., New targets and screening approaches in antimicrobial drug discovery. *Chem. Rev.* **2005,** *105*, 759-774.

(41) Black, M. T.; Hodgson, J., Novel target sites in bacteria for overcoming antibiotic resistance. *Adv. Drug Deliv. Rev.* **2005,** *57*, 1528-1538.

(42) Pucci, M. J., Use of genomics to select antibacterial targets. *Biochem. Pharmacol.* **2006,** *71*, 1066-1072.

(43) Szymański, P.; Markowicz, M.; Mikiciuk-Olasik, E., Adaptation of high-throughput screening in drug discovery—toxicological screening tests. *Int. J. Mol. Sci.* **2012,** *13*, 427-452.

(44) Payne, D. J.; Gwynn, M. N.; Holmes, D. J.; Pompliano, D. L., Drugs for bad bugs: confronting the challenges of antibacterial discovery. *Nat. Rev. Drug Discov.* **2007,** *6*, 29-40.

(45) Klebe, G., Recent developments in structure-based drug design. *J. Mol. Med. (Berl)* **2000,** *78*, 269-281.

(46) Reck, F.; Zhou, F.; Girardot, M.; Kern, G.; Eyermann, C. J.; Hales, N. J.; Ramsay, R. R.; Gravestock, M. B., Identification of 4-substituted 1,2,3-triazoles as novel oxazolidinone antibacterial agents with reduced activity against monoamine oxidase A. *J. Med. Chem.* **2005,** *48*, 499-506.

(47) Bank, R. P. D. Drug and Drug Target Mapping. http://www.rcsb.org/pdb/home/home.do (accessed 18 September 2014).

(48) Barker, J. J., Antibacterial drug discovery and structure-based design. *Drug Discov. Today* **2006,** *11*, 391-404.

(49) McInnes, C., Virtual screening strategies in drug discovery. *Curr. Opin. Chem. Biol.* **2007,** *11*, 494-502.

(50) Miller, J. R.; Waldrop, G. L., Discovery of novel antibacterials. *Expert Opin. Drug Discov.* **2010,** *5*, 145-154.

(51) Morphy, R.; Rankovic, Z., Designed multiple ligands: An emerging drug discovery paradigm. *J. Med. Chem.* **2005,** *48*, 6523-6543.

(52) Edwards, I. R.; Aronson, J. K., Adverse drug reactions: definitions, diagnosis, and management. *Lancet* **2000,** *356*, 1255-1259.

(53) Keith, C. T.; Borisy, A. A.; Stockwell, B. R., Multicomponent therapeutics for networked systems. *Nat. Rev. Drug Discov.* **2005,** *4*, 71-78.

(54) East, S. P.; Silver, L. L., Multitarget ligands in antibacterial research: progress and opportunities. *Expert Opin. Drug Discov.* **2013,** *8*, 143-156.

(55) Corson, T. W.; Aberle, N.; Crews, C. M., Design and applications of bifunctional small molecules: Why two heads are better than one. *ACS Chem. Biol.* **2008,** *3*, 677-692.

(56) Pokrovskaya, V.; Baasov, T., Dual-acting hybrid antibiotics: a promising strategy to combat bacterial resistance. *Expert Opin. Drug Discov.* **2010,** *5*, 883-902.

(57) Rock, C. O.; Cronan, J. E., *Escherichia coli* as a model for the regulation of dissociable (type II) fatty acid biosynthesis. *Biochim. Biophys. Acta* **1996,** *1302*, 1-16.

(58) Heath, R. J.; White, S. W.; Rock, C. O., Lipid biosynthesis as a target for antibacterial agents. *Prog. Lipid Res.* **2001,** *40*, 467-497.

(59) Campbell, J. W.; Cronan, J. E., Jr., Bacterial fatty acid biosynthesis: targets for antibacterial drug discovery. *Annu. Rev. Microbiol.* **2001,** *55*, 305-332.

(60) Konishi, T.; Shinohara, K.; Yamada, K.; Sasaki, Y., Acetyl-CoA carboxylase in higher plants: most plants other than Gramineae have both the prokaryotic and the eukaryotic forms of this enzyme. *Plant Cell Physiol.* **1996,** *37*, 117-122.

(61) White, S. W.; Zheng, J.; Zhang, Y. M.; Rock, The structural biology of type II fatty acid biosynthesis. *Annu. Rev. Biochem.* **2005,** *74*, 791-831.

(62) Heath, R. J.; White, S. W.; Rock, C. O., Inhibitors of fatty acid synthesis as antimicrobial chemotherapeutics. *Appl. Microbiol. Biotechnol.* **2002,** *58*, 695-703.

(63) Zhang, Y. M.; White, S. W.; Rock, C. O., Inhibiting bacterial fatty acid synthesis. *J. Biol. Chem.* **2006,** *281*, 17541-17544.

(64) Bhargava, H. N.; Leonard, P. A., Triclosan: applications and safety. *Am. J. Infect. Control* **1996,** *24*, 209-218.

(65) Yazdankhah, S. P.; Scheie, A. A.; Hoiby, E. A.; Lunestad, B. T.; Heir, E.; Fotland, T. O.; Naterstad, K.; Kruse, H., Triclosan and antimicrobial resistance in bacteria: an overview. *Microb. Drug Resist.* **2006,** *12*, 83-90.

(66) Chuanchuen, R.; Beinlich, K.; Hoang, T. T.; Becher, A.; Karkhoff-Schweizer, R. R.; Schweizer, H. P., Cross-resistance between triclosan and antibiotics in *Pseudomonas aeruginosa* is mediated by multidrug efflux pumps: exposure of a susceptible mutant strain to triclosan selects nfxB mutants overexpressing MexCD-OprJ. *Antimicrob. Agents Chemother.* **2001,** *45*, 428-432.

(67) Schweizer, H. P., Efflux as a mechanism of resistance to antimicrobials in *Pseudomonas aeruginosa* and related bacteria: unanswered questions. *Genet. Mol. Res.* **2003,** *2*, 48-62.

(68) Slayden, R. A.; Lee, R. E.; Armour, J. W.; Cooper, A. M.; Orme, I. M.; Brennan, P. J.; Besra, G. S., Antimycobacterial action of thiolactomycin: an inhibitor of fatty acid and mycolic acid synthesis. *Antimicrob. Agents Chemother.* **1996,** *40*, 2813-2819.

(69) Podkowiński, J.; Tworak, A., Acetyl-coenzyme A carboxylase – an attractive enzyme for biotechnology. *BioTechnologia* **2011,** *92*, 321-335.

(70) Cronan, J. E., Jr.; Waldrop, G. L., Multi-subunit acetyl-CoA carboxylases. *Prog. Lipid Res.* **2002,** *41*, 407-435.

(71) Li, S. J.; Cronan, J. E., Jr., The gene encoding the biotin carboxylase subunit of *Escherichia coli* acetyl-CoA carboxylase. *J. Biol. Chem.* **1992,** *267*, 855-863.

(72) Li, S. J.; Cronan, J. E., Jr., The genes encoding the two carboxyltransferase subunits of *Escherichia coli* acetyl-CoA carboxylase. *J. Biol. Chem.* **1992,** *267*, 16841-16847.

(73) James, E. S.; Cronan, J. E., Expression of two *Escherichia coli* acetyl-CoA carboxylase subunits is autoregulated. *J. Biol. Chem.* **2004,** *279*, 2520-2527.

(74) Wakil, S. J.; Titchener, E. B.; Gibson, D. M., Evidence for the participation of biotin in the enzymic synthesis of fatty acids. *Biochim. Biophys. Acta* **1958,** *29*, 225-226.

(75) Chapman-Smith, A.; Cronan, J. E., Jr., The enzymatic biotinylation of proteins: a post-translational modification of exceptional specificity. *Trends Biochem. Sci.* **1999,** *24*, 359-363.

(76) Guchhait, R. B.; Polakis, S. E.; Lane, M. D., Biotin carboxylase component of acetyl-CoA carboxylase from *Escherichia coli*. *Methods Enzymol.* **1975,** *35*, 25-31.

(77) Guchhait, R. B.; Polakis, S. E.; Lane, M. D., Carboxyltransferase component of acetyl-CoA carboxylase from *Escherichia coli*. *Methods Enzymol.* **1975,** *35*, 32-37.

(78) Polakis, S. E.; Guchhait, R. B.; Zwergel, E. E.; Lane, M. D.; Cooper, T. G., Acetyl coenzyme A carboxylase system of *Escherichia coli*. Studies on the mechanisms of the biotin carboxylase- and carboxyltransferase-catalyzed reactions. *J. Biol. Chem.* **1974,** *249*, 6657-6667.

(79) Waldrop, G. L.; Rayment, I.; Holden, H. M., Three-dimensional structure of the biotin carboxylase subunit of acetyl-CoA carboxylase. *Biochemistry* **1994,** *33*, 10249-10256.

(80) Mochalkin, I.; Miller, J. R.; Evdokimov, A.; Lightle, S.; Yan, C.; Stover, C. K.; Waldrop, G. L., Structural evidence for substrate-induced synergism and half-sites reactivity in biotin carboxylase. *Protein Sci.* **2008,** *17*, 1706-1718.

(81) St. Maurice, M. R., L.; Surinya, K.; Attwood, P.; Wallace, J.; Cleland, W.; Rayment I., Domain architecture of pyruvate carboxylase, a biotin-dependent multifunctional enzyme. *Science* **2007,** *317*, 1076-1079.

(82) Huang, C. S.; Sadre-Bazzaz, K.; Shen, Y.; Deng, B.; Zhou, Z. H.; Tong, L., Crystal structure of the $\alpha_6\beta_6$ holoenzyme of propionyl-coenzyme A carboxylase. *Nature* **2010,** *466*, 1001-1005.

(83) Tipton, P. A.; Cleland, W. W., Catalytic mechanism of biotin carboxylase: steady-state kinetic investigations. *Biochemistry* **1988,** *27*, 4317-4325.

(84) Blanchard, C. Z.; Amspacher, D.; Strongin, R.; Waldrop, G. L., Inhibition of biotin carboxylase by a reaction intermediate analog: implications for the kinetic mechanism. *Biochem. Biophys. Res. Commun.* **1999,** *266*, 466-471.

(85) Waldrop, G. L.; Holden, H. M.; St Maurice, M., The enzymes of biotin-dependent CO_2 metabolism: what structures reveal about their reaction mechanisms. *Protein Sci.* **2012,** *21*, 1597-1619.

(86) Thoden, J. B.; Blanchard, C. Z.; Holden, H. M.; Waldrop, G. L., Movement of the biotin carboxylase B-domain as a result of ATP binding. *J. Biol. Chem.* **2000,** *275*, 16183-16190.

(87) Chou, C. Y.; Yu, L. P.; Tong, L., Crystal structure of biotin carboxylase in complex with substrates and implications for its catalytic mechanism. *J. Biol. Chem.* **2009,** *284*, 11690-11697.

(88) Blanchard, C. Z.; Lee, Y. M.; Frantom, P. A.; Waldrop, G. L., Mutations at four active site residues of biotin carboxylase abolish substrate-induced synergism by biotin. *Biochemistry* **1999,** *38*, 3393-3400.

(89) Janiyani, K.; Bordelon, T.; Waldrop, G. L.; Cronan, J. E., Jr., Function of *Escherichia coli* biotin carboxylase requires catalytic activity of both subunits of the homodimer. *J. Biol. Chem.* **2001,** *276*, 29864-29870.

(90) Streit, W. R.; Entcheva, P., Biotin in microbes, the genes involved in its biosynthesis, its biochemical role and perspectives for biotechnological production. *Appl. Microbiol. Biotechnol.* **2003,** *61*, 21-31.

(91) Wolf, B.; Feldman, G. L., The biotin-dependent carboxylase deficiencies. *Am. J. Hum. Genet.* **1982,** *34*, 699-716.

(92) Fall, R. R.; Vagelos, P. R., Acetyl coenzyme A carboxylase. Molecular forms and subunit composition of biotin carboxyl carrier protein. *J. Biol. Chem.* **1972,** *247*, 8005-8015.

(93) Chapman-Smith, A.; Turner, D. L.; Cronan, J. E., Jr.; Morris, T. W.; Wallace, J. C., Expression, biotinylation and purification of a biotin-domain peptide from the biotin carboxy carrier protein of *Escherichia coli* acetyl-CoA carboxylase. *Biochem. J.* **1994,** *302 (Pt 3)*, 881-887.

(94) Blanchard, C. Z.; Chapman-Smith, A.; Wallace, J. C.; Waldrop, G. L., The biotin domain peptide from the biotin carboxyl carrier protein of *Escherichia coli* acetyl-CoA carboxylase causes a marked increase in the catalytic efficiency of biotin carboxylase and carboxyltransferase relative to free biotin. *J. Biol. Chem.* **1999,** *274*, 31767-31769.

(95) Athappilly, F. K.; Hendrickson, W. A., Structure of the biotinyl domain of acetyl-coenzyme A carboxylase determined by MAD phasing. *Structure* **1995,** *3*, 1407-1419.

(96) Roberts, E. L.; Shu, N.; Howard, M. J.; Broadhurst, R. W.; Chapman-Smith, A.; Wallace, J. C.; Morris, T.; Cronan, J. E., Jr.; Perham, R. N., Solution structures of apo- and holo-biotinyl domains from acetyl coenzyme A carboxylase of *Escherichia coli* determined by triple-resonance nuclear magnetic resonance spectroscopy. *Biochemistry* **1999,** *38*, 5045-5053.

(97) Yao, X.; Wei, D.; Soden, C., Jr.; Summers, M. F.; Beckett, D., Structure of the carboxy-terminal fragment of the apo-biotin carboxyl carrier subunit of *Escherichia coli* acetyl-CoA carboxylase. *Biochemistry* **1997,** *36*, 15089-15100.

(98) Chapman-Smith, A.; Forbes, B. E.; Wallace, J. C.; Cronan, J. E., Jr., Covalent modification of an exposed surface turn alters the global conformation of the biotin carrier domain of *Escherichia coli* acetyl-CoA carboxylase. *J. Biol. Chem.* **1997,** *272*, 26017-26022.

(99) Cronan, J. E., Jr., Interchangeable enzyme modules. Functional replacement of the essential linker of the biotinylated subunit of acetyl-CoA carboxylase with a linker from the lipoylated subunit of pyruvate dehydrogenase. *J. Biol. Chem.* **2002,** *277*, 22520-22527.

(100) Broussard, T. C.; Kobe, M. J.; Pakhomova, S.; Neau, D. B.; Price, A. E.; Champion, T. S.; Waldrop, G. L., The three-dimensional structure of the biotin carboxylase-biotin carboxyl carrier protein complex of *E. coli* acetyl-CoA carboxylase. *Structure* **2013,** *21*, 650-657.

(101) Cronan, J. E., Jr., The biotinyl domain of *Escherichia coli* acetyl-CoA carboxylase. Evidence that the "thumb" structure is essential and that the domain functions as a dimer. *J. Biol. Chem.* **2001,** *276*, 37355-37364.

(102) Chapman-Smith, A.; Cronan, J. E., Jr., Molecular biology of biotin attachment to proteins. *J. Nutr.* **1999,** *129*, 477S-484S.

(103) Cronan, J. E., Jr.; Wallace, J. C., The gene encoding the biotin-apoprotein ligase of *Saccharomyces cerevisiae*. *FEMS Microbiol. Lett.* **1995,** *130*, 221-229.

(104) Chapman-Smith, A.; Mulhern, T. D.; Whelan, F.; Cronan, J. E., Jr.; Wallace, J. C., The C-terminal domain of biotin protein ligase from *E. coli* is required for catalytic activity. *Protein Sci.* **2001,** *10*, 2608-2617.

(105) Zhang, H.; Yang, Z.; Shen, Y.; Tong, L., Crystal structure of the carboxyltransferase domain of acetyl-coenzyme A carboxylase. *Science* **2003,** *299*, 2064-2067.

(106) Bilder, P.; Lightle, S.; Bainbridge, G.; Ohren, J.; Finzel, B.; Sun, F.; Holley, S.; Al-Kassim, L.; Spessard, C.; Melnick, M.; Newcomer, M.; Waldrop, G. L., The structure of the carboxyltransferase component of acetyl-coA carboxylase reveals a zinc-binding motif unique to the bacterial enzyme. *Biochemistry* **2006,** *45*, 1712-1722.

(107) Guchhait, R. B.; Polakis, S. E.; Dimroth, P.; Stoll, E.; Moss, J.; Lane, M. D., Acetyl coenzyme A carboxylase system of *Escherichia coli*. Purification and properties of the biotin carboxylase, carboxyltransferase, and carboxyl carrier protein components. *J. Biol. Chem.* **1974,** *249*, 6633-6645.

(108) Waldrop, G. L., The role of symmetry in the regulation of bacterial carboxyltransferase. *Biomol. Concepts* **2011,** *2*, 47-52.

(109) Hamed, R. B.; Batchelar, E. T.; Clifton, I. J.; Schofield, C. J., Mechanisms and structures of crotonase superfamily enzymes--how nature controls enolate and oxyanion reactivity. *Cell Mol. Life Sci.* **2008,** *65*, 2507-2527.

(110) Benson, B. K.; Meades, G., Jr.; Grove, A.; Waldrop, G. L., DNA inhibits catalysis by the carboxyltransferase subunit of acetyl-CoA carboxylase: implications for active site communication. *Protein Sci.* **2008,** *17*, 34-42.

(111) Meades, G., Jr.; Benson, B. K.; Grove, A.; Waldrop, G. L., A tale of two functions: enzymatic activity and translational repression by carboxyltransferase. *Nucleic Acids Res.* **2010,** *38*, 1217-1227.

(112) Davis, M. S.; Solbiati, J.; Cronan, J. E., Jr., Overproduction of acetyl-CoA carboxylase activity increases the rate of fatty acid biosynthesis in *Escherichia coli*. *J. Biol. Chem.* **2000,** *275*, 28593-28598.

(113) Li, S. J.; Cronan, J. E., Jr., Growth rate regulation of *Escherichia coli* acetyl coenzyme A carboxylase, which catalyzes the first committed step of lipid biosynthesis. *J. Bacteriol.* **1993,** *175*, 332-340.

(114) Broussard, T. C.; Price, A. E.; Laborde, S. M.; Waldrop, G. L., Complex formation and regulation of *Escherichia coli* acetyl-CoA carboxylase. *Biochemistry* **2013,** *52*, 3346-3357.

(115) Cheng, C. C.; Shipps, G. W., Jr.; Yang, Z.; Sun, B.; Kawahata, N.; Soucy, K. A.; Soriano, A.; Orth, P.; Xiao, L.; Mann, P.; Black, T., Discovery and optimization of antibacterial AccC inhibitors. *Bioorg. Med. Chem. Lett.* **2009,** *19*, 6507-6514.

(116) Freiberg, C.; Pohlmann, J.; Nell, P. G.; Endermann, R.; Schuhmacher, J.; Newton, B.; Otteneder, M.; Lampe, T.; Habich, D.; Ziegelbauer, K., Novel bacterial acetyl coenzyme A carboxylase inhibitors with antibiotic efficacy *in vivo*. *Antimicrob. Agents Chemother.* **2006,** *50*, 2707-2712.

(117) Polyak, S. W.; Abell, A. D.; Wilce, M. C.; Zhang, L.; Booker, G. W., Structure, function and selective inhibition of bacterial acetyl-CoA carboxylase. *Appl. Microbiol. Biotechnol.* **2012,** *93*, 983-992.

(118) Miller, J. R.; Dunham, S.; Mochalkin, I.; Banotai, C.; Bowman, M.; Buist, S.; Dunkle, B.; Hanna, D.; Harwood, H. J.; Huband, M. D.; Karnovsky, A.; Kuhn, M.; Limberakis, C.; Liu, J. Y.; Mehrens, S.; Mueller, W. T.; Narasimhan, L.; Ogden, A.; Ohren, J.; Prasad, J. V.; Shelly, J. A.; Skerlos, L.; Sulavik, M.; Thomas, V. H.; VanderRoest, S.; Wang, L.; Wang, Z.; Whitton, A.; Zhu, T.; Stover, C. K., A class of selective antibacterials derived from a protein kinase inhibitor pharmacophore. *Proc. Natl. Acad. Sci. USA* **2009,** *106*, 1737-1742.

(119) Mochalkin, I.; Miller, J. R.; Narasimhan, L.; Thanabal, V.; Erdman, P.; Cox, P. B.; Prasad, J. V.; Lightle, S.; Huband, M. D.; Stover, C. K., Discovery of antibacterial biotin carboxylase inhibitors by virtual screening and fragment-based approaches. *ACS Chem. Biol.* **2009,** *4*, 473-483.

(120) Waldrop, G. L., Smaller is better for antibiotic discovery. *ACS Chem. Biol.* **2009,** *4*, 397-399.

(121) Fredenhagen, A.; Tamura, S. Y.; Kenny, P. T. M.; Komura, H.; Naya, Y.; Nakanishi, K.; Niegyama, K.; Sugiura, M.; Kita, H., Andrimid, a new peptide antibiotic produced by an intracellular bacterial symbiont isolated from a brown planthopper. *J. Am. Chem. Soc.* **1987,** *109*, 4409-4411.

(122) Needham, J.; Kelly, M. T.; Ishige, M.; Andersen, R. J., Andrimid and moiramides A-C, metabolites produced in culture by a marine isolate of the bacterium *Pseudomonas fluorescens*: Structure elucidation and biosynthesis. *J. Org. Chem.* **1994,** *59*, 2058-2063.

(123) Freiberg, C.; Brunner, N. A.; Schiffer, G.; Lampe, T.; Pohlmann, J.; Brands, M.; Raabe, M.; Habich, D.; Ziegelbauer, K., Identification and characterization of the first class of potent bacterial acetyl-CoA carboxylase inhibitors with antibacterial activity. *J. Biol. Chem.* **2004,** *279*, 26066-26073.

(124) McWhorter, W.; Fredenhagen, A.; Nakanishi, K.; Komura, H., Stereocontrolled synthesis of andrimid and a structural requirement for the activity. *J. Chem. Soc., Chem. Commun.* **1989**, 299-301.

(125) Pohlmann, J.; Lampe, T.; Shimada, M.; Nell, P. G.; Pernerstorfer, J.; Svenstrup, N.; Brunner, N. A.; Schiffer, G.; Freiberg, C., Pyrrolidinedione derivatives as antibacterial agents with a novel mode of action. *Bioorg. Med. Chem. Lett.* **2005,** *15*, 1189-1192.

(126) Rahman, H.; Austin, B.; Mitchell, W. J.; Morris, P. C.; Jamieson, D. J.; Adams, D. R.; Spragg, A. M.; Schweizer, M., Novel anti-infective compounds from marine bacteria. *Marine Drugs* **2010,** *8*, 498-518.

CHAPTER 2: DESIGN, SYNTHESIS, AND ANTIBACTERIAL PROPERTIES OF DUAL-LIGAND INHIBITORS OF ACETYL-COA CARBOXYLASE[1]

2.1 INTRODUCTION

In 2013, the CDC issued an alarming report on the dramatic rise in antibiotic resistant bacteria.[1] The report noted that over 2 million people per year are afflicted with bacterial infections resistant to at least one antibiotic. In addition, there are 23,000 deaths per year directly attributable to antibiotic resistant infections. One of the core recommendations in the report for combating this public health crisis is the development of new antibiotics. The current arsenal of antibiotics is directed at only 30-40 molecular targets. Thus, there is a pressing need to develop antibiotics against novel targets. Fatty acid biosynthesis is an essential metabolic pathway in both eukaryotes and prokaryotes and since fatty acids are required for membrane biogenesis in bacteria, fatty acid synthesis is an attractive pathway to focus on for antibiotic development.[2-4]

The first committed and regulated reaction in fatty acid biosynthesis is catalyzed by the multifunctional enzyme acetyl-CoA carboxylase (ACC).[5] The overall reaction catalyzed by ACC is shown in Scheme 2.1. ACC requires the vitamin biotin, which is covalently attached to the biotin carboxyl carrier protein (BCCP). In the first half-reaction, catalyzed by biotin carboxylase (BC), BCCP-biotin is carboxylated in an ATP-dependent manner where bicarbonate is the source of CO_2. The second half-reaction, catalyzed by carboxyltransferase (CT), involves the transfer of the carboxyl group from BCCP-biotin to acetyl-CoA to form malonyl-CoA. In eukaryotes, the three proteins that comprise ACC form domains on a single polypeptide chain,[6] whereas in prokaryotes,

[1]Reproduced with permission from Journal of Medicinal Chemistry, submitted for publication. Unpublished work copyright 2014 American Chemical Society.

they are encoded as three separate proteins.[7] The bacterial forms of biotin carboxylase and carboxyltransferase retain their activity when isolated from the other components and only utilize free biotin as a substrate.[4-5] With respect to antibacterial development, the different arrangement of the three protein components of ACC between eukaryotes and prokaryotes provides potential for the design of inhibitors that selectively target the bacterial system.[3-4] Moreover, the three components of ACC are highly conserved among bacterial species, increasing the likelihood of developing broad spectrum antibacterial agents.[7-8]

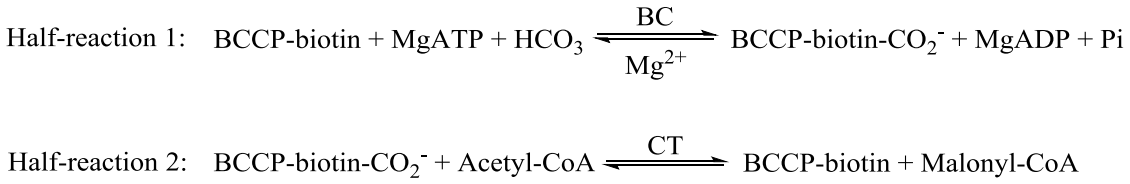

Scheme 2.1. Reactions catalyzed by acetyl-CoA carboxylase (ACC).

Both the biotin carboxylase and the carboxyltransferase components of acetyl-CoA carboxylase have served as targets for antibacterial agents. Miller *et al*. discovered that the antibacterial properties of the pyridopyrimidine class of molecules was due to the inhibition of biotin carboxylase.[9] The pyridopyrimidines (e.g. compound **1**, Figure 2.1) bound in the ATP binding site of bacterial biotin carboxylase but did not inhibit human biotin carboxylase. The pyridopyrimidines were not readily amenable to synthetic modifications, so Mochalkin *et al*. used fragment and virtual screening to identify a series of aminooxazole derivatives (e.g. compound **2** in Figure 2.1) that also inhibited biotin carboxylase by binding in the ATP binding site.[10] In common with the pyridopyrimidines, the aminooxazole derivatives were selective inhibitors of the

bacterial, but not human, biotin carboxylase, and were shown to exhibit potent antibacterial activity against efflux-compromised Gram-negative pathogens.[10]

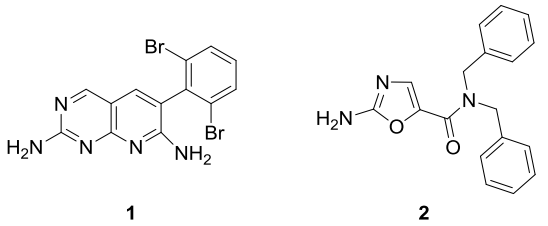

Figure 2.1. Pyridopyrimidine **1** and aminooxazole **2**, inhibitors of biotin carboxylase.

In contrast to biotin carboxylase, there is only one known class of molecules that inhibits the carboxyltransferase component of acetyl-CoA carboxylase and also possesses antibacterial activity. While the biotin carboxylase inhibitors are invariably of synthetic origin, the carboxyltransferase inhibitors are natural products. The antibacterial activity of andrimid (**3**) and moiramide B (**4**) (Figure 2.2) had been known for at least 10 years as broad spectrum antibacterial agents.[11] Freiberg *et al*. discovered that the molecular target for andrimid (**3**) and moiramide B (**4**) was the carboxyltransferase subunit of ACC.[11-12] Structure-activity relationship (SAR) studies revealed that the pyrrolidinedione head group was essential for enzyme inhibition and antibacterial activity, while the fatty acid chain is not required.[13] Moiramide B (**4**) was found to have an inhibition constant of 5 nM and exhibited competitive inhibition versus malonyl-CoA.[12, 14,2] Moiramide B (**4**) inhibited carboxyltransferase from both Gram-negative and Gram-positive organisms, which is consistent with its broad spectrum activity. In common with the biotin carboxylase inhibitors, moiramide B (**4**) did not inhibit human acetyl-CoA carboxylase.[12]

[2]The activity of carboxyltransferase is measured in the reverse or non-physiological direction where malonyl-CoA and biocytin (a biotin analog) are the substrates. The formation of the product acetyl-CoA is detected using the coupling enzymes, citrate synthase and malate dehydrogenase.

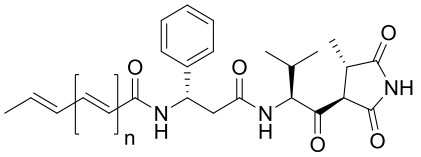

3 Andrimid n = 2
4 Moiramide B n = 1

Figure 2.2. Andrimid (**3**) and moiramide B (**4**), inhibitors of carboxyltransferase.

Despite the fact that both biotin carboxylase and carboxyltransferase have been validated as unique targets for antibacterial development through the discovery of selective antibacterial inhibitors, both targets suffer from high potential for spontaneous resistance through individual target-based mutations. One approach to decrease the likelihood of developing resistance is to make a single molecule that incorporates inhibitory motifs for both the biotin carboxylase and carboxyltransferase enzymatic activities. The potential lower frequency of resistance against such a dual-ligand inhibitor is explained by considering the genetic arrangement of ACC. Biotin carboxylase is a homodimer encoded by the *accB* gene, while carboxyltransferase is a heterotetramer with α- and β-subunits encoded by *accA* and *accD*, respectively. The *accA* and *accD* genes encoding the subunits of carboxyltransferase are not genetically linked.[15] This genetic arrangement is commonly found in both Gram-negative and Gram-positive bacteria. Thus, one would predict that nonessential missense mutations would have to arise in three different genes in order for the bacteria to become resistant to a molecule targeting both enzymes simultaneously.

While the use of dual-ligands for lowering the frequency of resistance is well documented,[16-19] most examples of dual-ligands as antibacterial agents involve inhibitors that target two enzymes that either do not interact and/or are not related metabolically.

Thus, a dual-ligand inhibitor of ACC would represent a departure from previous practice. In fact, a dual-ligand inhibitor of ACC is a particularly attractive strategy for inhibition of the enzyme in light of recent studies that have demonstrated that all three protein components (biotin carboxylase, BCCP and carboxyltransferase) must form a complex *in vivo* for activity.[20] On this background, we report the first step toward dual-ligand inhibition of ACC by linking the aminooxazole **2** inhibitor of biotin carboxylase to the carboxyltransferase inhibitor, moiramide B (**4**), and characterizing the inhibitory and antibacterial properties.

2.2 RESULTS AND DISCUSSION

2.2.1 Design Strategy

In order to generate dual-ligand inhibitors incorporating these known inhibitory motifs (compounds **5** and **6**, Figure 2.3), we needed to identify loci in each inhibitor where we could attach a metabolically stable linker without compromising binding and biological activity. A suitable, stable functional group needed to be placed on the dibenzylamide side chain of aminooxazole **2** (Figure 2.1). We decided to incorporate a hydroxyl group at the *para* position of one of the benzene rings (compound **13**, Scheme 2.2). This modification was not expected to affect binding to biotin carboxylase, since it is the aminooxazole moiety that is responsible for interaction with the ATP binding site.[10] In the case of moiramide B (**4**) (Figure 2.2), it has been shown that the fatty acid side chain can be significantly modified with retention of biological activity.[13] We thereby elected to replace this fatty acid chain with a lipophilic linker at the *N*-terminus of the β-phenylalanine residue in the naturally-occurring, biologically active pseudopeptide (Figure 2.3).

Finally, we needed to choose linkers to covalently connect the aminooxazole and moiramide components of the dual-ligand inhibitor. We chose a saturated aliphatic compound with a leaving group at one end, to form an ether with the phenol at the "aminooxazole end", and a carboxylic acid at the other end to forge an amide with the *N*-terminus of the moiramide fragment. We arbitrarily started with a 15-carbon linker since juniperic acid (compound **26**, Scheme 2.4) is commercially available. We later also synthesized a 7-carbon linker (compound **29**, Scheme 2.4) to more accurately mimic the fatty acid component of moiramide B. This design strategy generates dual-ligand inhibitors that incorporate the necessary pharmacophores for targeting both biotin carboxylase and carboxyltransferase while covalently attaching them using stable, saturated hydrocarbon linkers of various lengths (Figure 2.3).

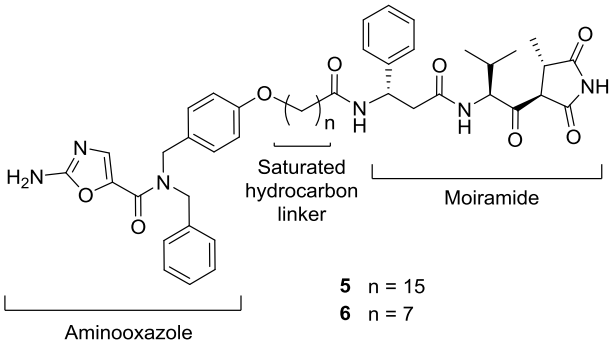

Figure 2.3. Dual-ligand inhibitors containing aminooxazole and moiramide pharmacophores with saturated hydrocarbon linkers with 15 carbons (**5**) and 7 carbons (**6**).

2.2.2 Chemistry

We generated the requisite unsymmetrical dibenzylamine via reductive amination of benzaldehyde with *p*-aminophenol to give compound **10** (Scheme 2.2).[21] Coupling of aminooxazole carboxylate **12** with secondary amine **10** afforded compound **13** (Scheme 2.2), the "aminooxazole" component of the dual-ligand inhibitor, with a handle for

attachment to other species.[10] However, compound **2** was also synthesized and used in biological studies as the "aminooxazole only" representative in order to eliminate any side reactions that might have been encountered with the phenol functionality of **13**.

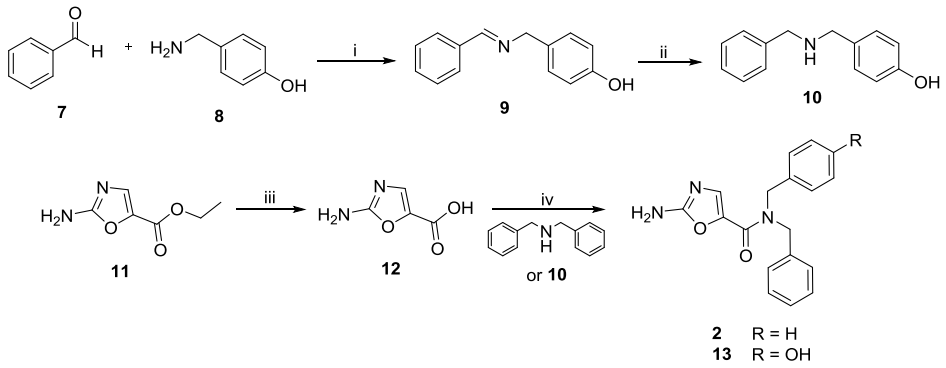

Scheme 2.2. Synthesis of aminooxazole **2** and aminooxazole **13** with *para*-hydroxyl group. Reagents and conditions: (i) triethylamine, dry methanol, 3Å molecular sieves, 65%; (ii) $NaBH_4$, dry methanol, 0 °C to rt, 84%; (iii) 1. 2M NaOH, 60 °C; 2. HCl, 98%; (iv) HATU, triethylamine, dry DMF, 31-35%.

Andrimid (**3**) and moiramide B (**4**) have been synthesized previously, although most reports are in communication format without experimental details.[13, 22-24] These accounts all alluded to the fragility of the β-ketoamide functionality; the pK_a for enolate formation of andrimid is 6.8.[25] We prepared (4*S*)-methyl-succinic anhydride **15** (Scheme 2.3) according to Midgley and Thomas[26] and converted this to the benzyl succinimide **17**.[27] Indeed, Pohlmann *et al*. had prepared a number of *N*-alkylated derivatives of moiramide for SAR studies but they did not prepare the benzyl derivative and it was not clear why they and others used benzyloxy protection for the succinimide nitrogen, which requires two steps for removal. We expected to cleave the benzylamine in a single hydrogenolytic step.

With **17** in hand, we faced the challenging acylation of the kinetic enolate of **17** with an acyl cation equivalent derived from *N*-*tert*-butoxycarbonyl-L-valine (Boc-Val-

OH). The discussion of Davies and Dixon informed us that the enolate was unstable and must be generated in the presence of an appropriate electrophile.[24] While they employed an *N*-carboxyanhydride, others invoked an acyl imidazole.[13, 23] We found the acyl imidazole was more convenient to generate and more stable than the *N*-carboxyanhydride. The acyl imidazole generated from Boc-Val-OH was added to a solution of succinimide **17**. The solution was added slowly to a solution of LiHMDS in THF at -78 °C. While TLC analysis of the reaction looked promising, poor yields of **18** were obtained by flash chromatography. Two-dimensional TLC confirmed that **18** was unstable to silica gel and was thus isolated by reversed-phase HPLC in low yield. Furthermore, the product was not particularly stable and standard hydrogenolysis procedures for removing the benzyl protecting group were unsuccessful.

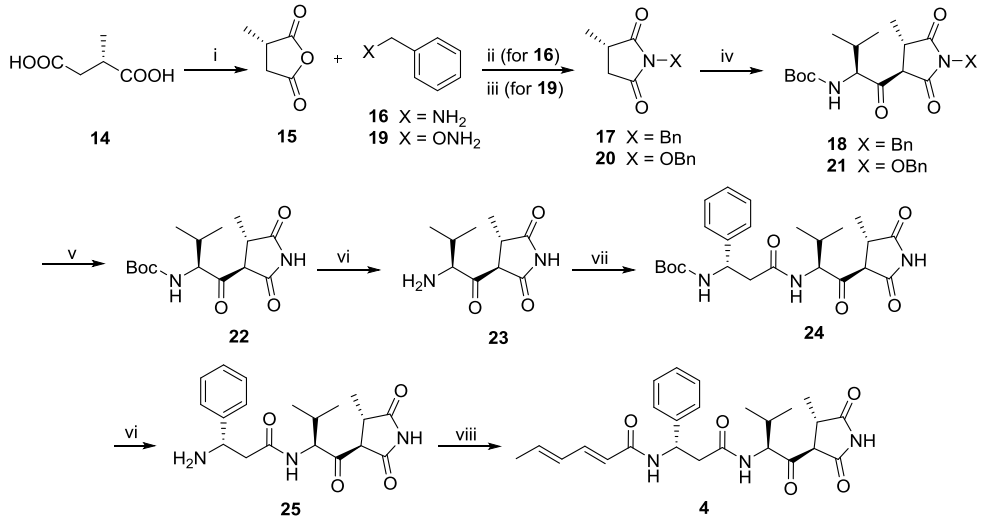

Scheme 2.3. Synthesis of moiramide **25** with free amine and moiramide B (**4**). Reagents and conditions: (i) AcCl, 60 °C, 97%; (ii) 1. Compound **16**, THF, Δ; 2. Ac_2O, Δ, 83%; (iii) Compound **19**, CDI, triethylamine, CH_2Cl_2, 89%; (iv) 1. *N*-Boc-L-valine, CDI, dry THF; 2. LiHMDS, -78 °C, dry THF, 42%; (v) 1. H_2, 5% Pd/C (20% w/w), dry methanol; 2. 2-bromoacetophenone, triethylamine, CH_3CN, 64%; (vi) TFA:CH_2Cl_2, 0 °C, 89-98%; (vii) (*S*)-*N*-Boc-3-amino-3-phenylpropanoic acid, HATU, $^{i}Pr_2NEt$, dry DMF, 0 °C to rt, 45%; (viii) Sorbic acid, TBTU, $^{i}Pr_2NEt$, dry DMF, 32%.

The *N*-benzyl group was replaced with the *N*-benzyloxy protecting group, ultimately leading to compound **21** (Scheme 2.3) that was remarkably stable to silica gel. An earlier paper by Robin *et al.*, outlining a synthesis of thalidomide, also utilized benzyloxy protection of the glutarimide ring, where the benzyl group had been problematic.[28] They suggested that resonance donation of electron density from the oxygen reduces the electrophilicity of the C=O groups and the acidity of the neighboring alpha protons. The acylation of **20** and purification of **21** was now realized in a better yield of 42% and the product was stable and generated an equilibrium mixture of predominantly the *trans* diastereomer and <10% of the diastereomer with *cis*-relative stereochemistry on the succinimide ring that arises via tautomerization to the enol form, evident in <6%. Earlier reports did not include NMR spectra as Supporting Information, although Davies and Dixon reported an 87:9:4 (*trans*:enol:*cis*) mixture for compound **21**. The benzylic C-O bond in **21** was cleaved by hydrogenolysis to afford the hydroxylamine that was treated with 2-bromoacetophenone to generate the phenacyl ester *in situ* which ultimately led to succinimide **22**.[24] The deprotected succinimide **22** existed as an 82:4:14 (*trans*:enol:*cis*) mixture; Davies and Dixon did not report a ratio of isomers for this compound. Removal of the Boc group at the *N*-terminus of compound **22** and elongation with commercially available Boc-β-Phe-OH gave compound **24**. The addition of the Boc-β-Phe moiety resulted in a single diastereomer, suggesting a stronger thermodynamic preference for the *trans* isomer with the larger acyl side chain. Compound **24** in turn underwent Boc deprotection to afford the free amine **25** that was coupled to sorbic acid to generate the natural product, moiramide B (compound **4**, Scheme 2.3).

Preparation of the 15 carbon linker followed a procedure that Overman and coworkers had previously reported for the conversion of juniperic acid **26** to allyl ester **27** (Scheme 2.4).[29] The primary alcohol was converted to an alkyl iodide (**28**) by analogy to a procedure of Jobron *et al*.[30] We also prepared a significantly shorter linker, **31**, from 8-hydroxyoctanoic acid (**29**) as shown in Scheme 2.4.

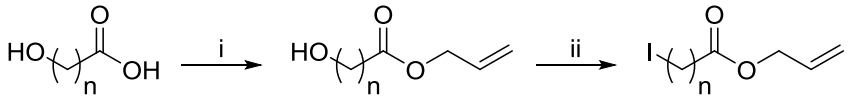

26 n = 15 **27** n = 15 **28** n = 15
29 n = 7 **30** n = 7 **31** n = 7

Scheme 2.4. Synthesis of modified saturated hydrocarbon linkers **28** and **31**. Reagents and conditions: (i) allyl alcohol, H_2SO_4, Δ, 59-61%; (ii) polymer-bound triphenylphosphine, I_2, imidazole, dry CH_2Cl_2, 78-83%.

The convergent assembly of the three fragments to generate the dual-ligand inhibitors is depicted in Scheme 2.5. The phenol of compound **13** was activated as the corresponding cesium salt using CsOH. This accentuated nucleophile then participated in an S_N2 reaction with the iodide of compounds **28** and **31** to generate an ether linkage viz. aminooxazole-linker derivatives **32** and **33**, respectively. The allyl protecting group of each derivative was removed by hydrolysis to generate the free carboxylic acids **34** and **35**, by a procedure analogous to Zhang *et al*.[31] The acids were each coupled to the amine in compound **25** using standard coupling reagents to generate the dual-ligands **5** and **6** with optimized conditions for each compound (Scheme 2.5).[13]

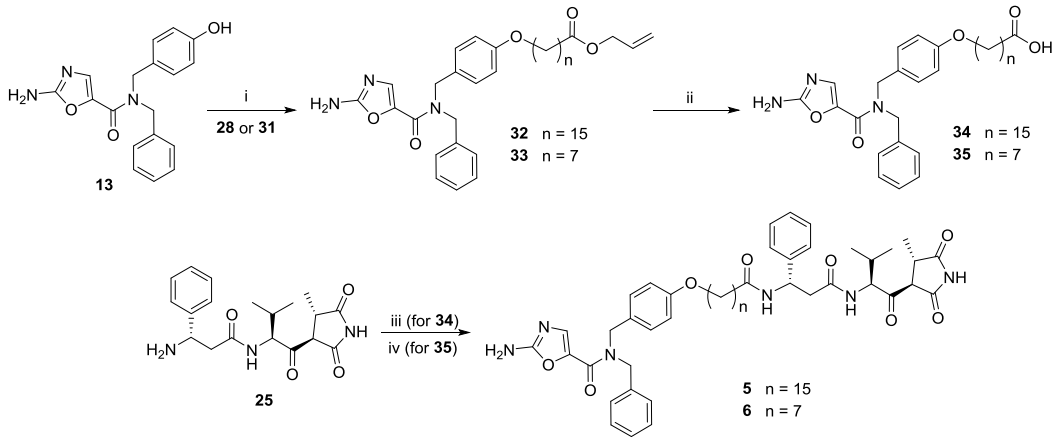

Scheme 2.5. Synthesis of dual-ligand inhibitors **5** and **6**. Reagents and conditions: (i) 1. CsOH, dry DMF; 2. Compounds **28** or **31**, dry THF, Δ, 20-21%; (ii) 2M NaOH, MeOH:THF, 71-89%; (iii) Compound **34**, HOBt, EDC, triethylamine, dry DMF, 19%; (iv) Compound **35**, HATU, $^{i}Pr_2EtN$, dry DMF, 0 °C to rt, 17%.

2.2.3 Inhibition of Acetyl-CoA Carboxylase by the Dual-Ligands

The targets of the antibacterial agents aminooxazole **2** and moiramide B (**4**) are biotin carboxylase and carboxyltransferase, respectively. The question now is: how would a molecule that incorporates the features of both aminooxazole **2** and moiramide B (**4**) inhibit the multiprotein complex comprising all three components of acetyl-CoA carboxylase (ACC)? Recent studies have shown that the three components of ACC: biotin carboxylase, BCCP and carboxyltransferase, form a multiprotein complex both *in vitro* and *in vivo*.[20] In order to compare the dual-ligand inhibitors to the two parent compounds, the inhibition of ACC by aminooxazole **2** and moiramide B (**4**) was also studied because the original characterization of these inhibitors utilized only the isolated subunits of biotin carboxylase or carboxyltransferase, not the ACC complex.

The inhibition of ACC by aminooxazole **2** was determined by varying ATP at increasing fixed concentrations of inhibitor, where acetyl-CoA was held constant at a subsaturating level. Aminooxazole **2** exhibited noncompetitive inhibition versus ATP

and this pattern was unexpected based on the competitive inhibition versus ATP that was observed with the isolated subunit of biotin carboxylase (Figure 2.4). However, the K_{is} of 0.8 ± 0.2 μM for isolated biotin carboxylase was close to the K_{is} value observed for ACC. Aminooxazole **2** exhibited a K_{is} of 0.4 ± 0.1 μM and a K_{ii} of 0.9 ± 0.2 μM, Figure 2.5, (A).

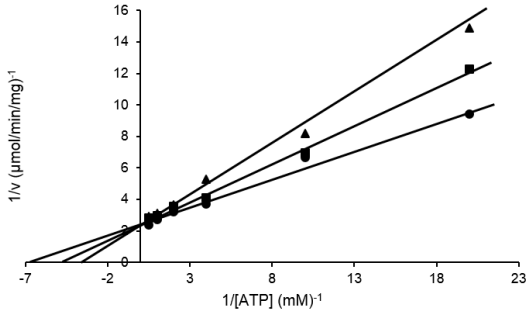

Figure 2.4. Inhibition of biotin carboxylase by 2-amino-*N*,*N*-dibenzyloxazole-5-carboxamide (**2**) at: 0 μM (●), 0.3 μM (■), and 0.7 μM (▲). The substrate ATP was varied while holding the other substrates, HCO_3^- and biotin, constant at 15 mM and 48 mM, respectively. The points represent the observed velocities and the lines represent the best fit of the data to Eq. 1.

The reason for the noncompetitive pattern in ACC is not clear at this time and awaits the determination of the three-dimensional structure of ACC bound to aminooxazole **2**. Nonetheless, the noncompetitive inhibition pattern observed for ACC has implications for targeting the biotin carboxylase subunit of the enzyme for pharmaceutical purposes. Namely, the noncompetitive inhibition pattern means that inhibitor binding is not precluded by saturating levels of ATP. Given that the K_m for ATP in ACC is about 1-2 μM[20] and the intracellular level of ATP in log phase *E. coli* is 9 mM[32], ACC is very likely saturated with the substrate ATP *in vivo*. Thus, at least for the biotin carboxylase inhibitor, aminooxazole **2**, saturation with ATP will not be problematic. These results show that it is imperative that any potential antibacterial

agents targeting either the biotin carboxylase or carboxyltransferase subunits of ACC must be characterized with ACC *in toto* and not just the isolated subunits because the multiprotein complex is the active form of the enzyme *in vivo*.

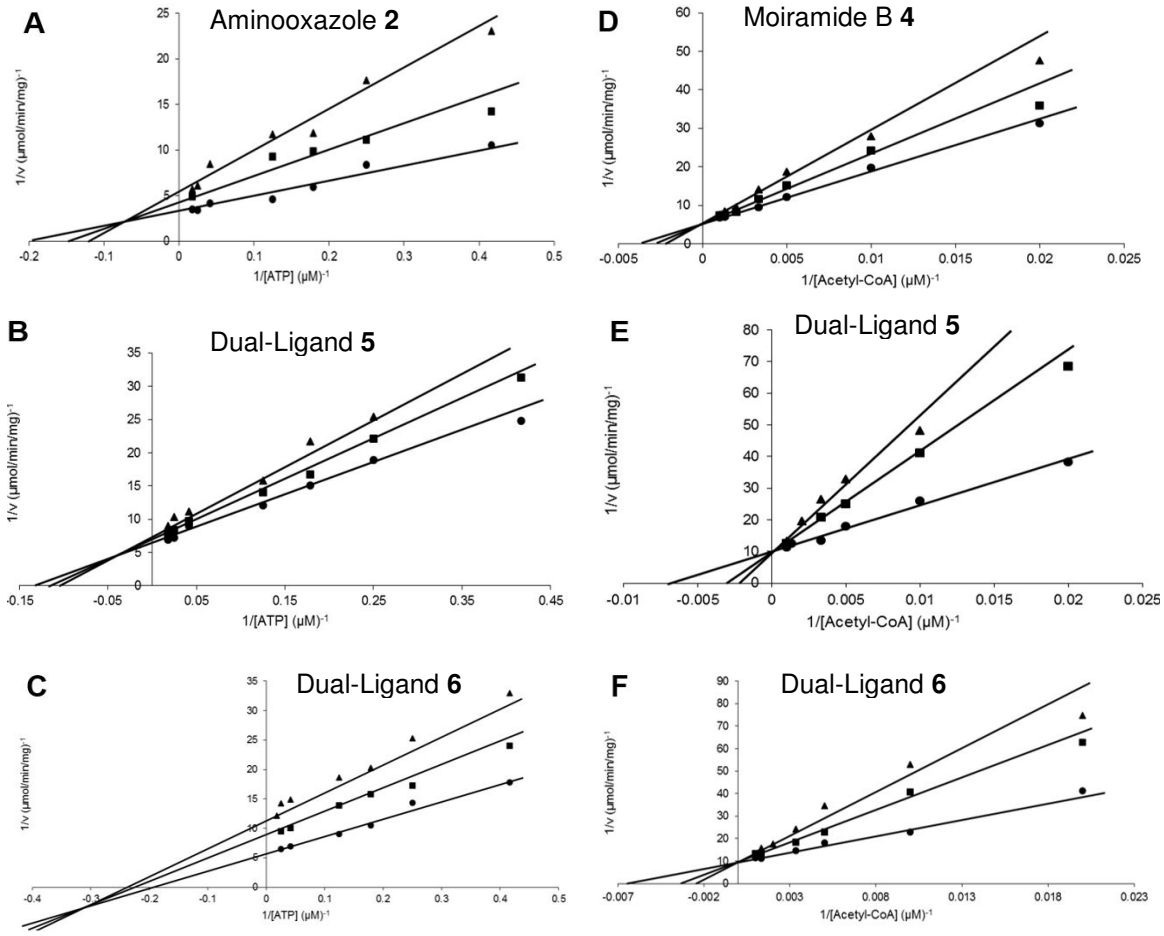

Figure 2.5. Inhibition of acetyl-CoA carboxylase. (A) Inhibition by 2-amino-*N*,*N*-dibenzyloxazole-5-carboxamide (**2**) at: 0 µM (●), 0.3 µM (■), and 0.7 µM (▲). (B) Inhibition by dual-ligand inhibitor **5** at: 0 nM (●), 6 nM (■), and 10 nM (▲). (C) Inhibition by dual-ligand inhibitor **6** at: 0 nM (●), 6 nM (■), and 10 nM (▲). For all three assays, the substrate ATP was varied while holding the other substrates, HCO_3^- and acetyl-CoA, constant at 15 mM and 200 µM, respectively. The points represent the observed velocities and the lines represent the best fit of the data to Eq. 2. (D) Inhibition by moiramide B (**4**) at: 0 nM (●), 3 nM (■), and 6 nM (▲). (E) Inhibition by dual-ligand inhibitor **5** at: 0 nM (●), 6 nM (■), and 10 nM (▲). (F) Inhibition by dual-ligand inhibitor **6** at: 0 nM (●), 6 nM (■), and 10 nM (▲). For all three assays, the substrate acetyl-CoA was varied while holding the other substrates, HCO_3^- and ATP, constant at 15 mM and 5 µM, respectively. The points represent the observed velocities and the lines represent the best fit of the data to Eq. 1.

The inhibition of ACC by moiramide B was determined by varying acetyl-CoA at increasing fixed concentrations of inhibitor, while ATP was held constant at a subsaturating level. Moiramide B exhibited competitive inhibition versus acetyl-CoA with a K_{is} of 7.9 ± 1.1 nM, Figure 2.5, (D). These results are similar to the competitive inhibition pattern of moiramide B (**4**) versus malonyl-CoA and K_{is} value of 5 nM for the isolated subunit of carboxyltransferase.[12]

For the dual-ligands, inhibition patterns using biochemical assays were determined versus both ATP and acetyl-CoA. The inhibition of ACC by dual-ligand **5** (15C linker) versus ATP at increasing fixed concentrations of inhibitor, with acetyl-CoA held constant at a subsaturating level, exhibited noncompetitive inhibition with a K_{is} of 28.7 ± 12.9 nM and a K_{ii} of 33.7 ± 7.2 nM, Figure 2.5, (B). The inhibition of ACC by dual-ligand **5** versus acetyl-CoA at increasing fixed concentrations of inhibitor, with ATP held constant at a subsaturating level, exhibited competitive inhibition with a K_{is} of 5.2 ± 0.7 nM, Figure 2.5, (E).

The inhibition of ACC by dual-ligand **6** (7C linker) versus ATP at increasing fixed concentrations of inhibitor, with acetyl-CoA held constant at a subsaturating level, exhibited noncompetitive inhibition with a K_{is} of 16.9 ± 6.8 nM and a K_{ii} of 9.6 ± 1.0 nM, Figure 2.5, (C). The inhibition of ACC by dual-ligand **6** versus acetyl-CoA at increasing fixed concentrations of inhibitor, with ATP held constant at a subsaturating level, exhibited competitive inhibition with a K_{is} of 5.5 ± 0.6 nM, Figure 2.5, (F).

The noncompetitive inhibition pattern versus ATP and the competitive pattern versus acetyl-CoA observed for both dual-ligands, **5** and **6**, could be due to the linker not being long enough to allow both parts of the dual-ligands to bind to the enzyme

simultaneously. As a consequence, the dual-ligands, **5** and **6**, only bind in the moiramide B binding site, by virtue of its higher affinity, compared to aminooxazole **2**. While this is a plausible explanation for the noncompetitive inhibition pattern versus ATP, it is inconsistent with the fact that the "parent" compound, aminooxazole **2**, also exhibited noncompetitive inhibition versus ATP in ACC. Thus, the inhibition patterns for the two dual-ligands, **5** and **6**, are perfectly consistent with the inhibition patterns observed for the two "parent" compounds, aminooxazole **2** and moiramide B (**4**). The molecular basis for the inhibition patterns will ultimately be revealed by the determination of the three-dimensional structure of ACC bound to either of the dual-ligands.

2.2.4 Antibacterial Activity of Dual-Ligands

Figure 2.6 lists the minimum inhibitory concentration (MIC) values for the "parent" compounds, aminooxazole **2** and moiramide B (**4**), as well as dual-ligands **5** and **6** against different bacterial strains. Aminooxazole **2** exhibited antibacterial activity against efflux-pump deficient *E. coli* and in fact, registered the same MIC value of 16 μg/mL as reported by Mochalkin *et al*.[10] Also consistent with the findings of Mochalkin *et al*., aminooxazole **2** was not active against any Gram-positive bacteria.[10] Moreover, aminooxazole **2** was effective against an *E. coli tolC* derivative that was selected for spontaneous resistance to moiramide B (**4**) suggesting that dual-ligands such as **6** would retain activity against strains bearing pre-existing moiramide-resistance.

Moiramide B (**4**) exhibited antibacterial activity against all strains tested except the wild-type strains of *P. aeruginosa* and *E. coli*. The lack of activity against these strains can be attributed to efflux-based intrinsic resistance, since efflux-pump-deficient strains of these organisms were susceptible to moiramide B (Figure 2.6). Moiramide B

also exhibited activity against spontaneous moiramide-resistant isolates of both *E. coli tolC* and *S. aureus*, with an observed 8-fold decrease in potency in each case. The elevated MICs against moiramide B suggest that some stable drug resistance was observed, most likely through a target-based spontaneous mutation. The results reported herein for moiramide B are consistent with previously reported antibacterial analyses.[12-13, 33]

Strain (genotype)[a]	MIC[b] (μg/mL)							
	Rifampin	Gentamicin	Chloramphenicol	Kanamycin	**2**	**4**	**5**	**6**
P. aeruginosa (wild-type)	31	2	>64	128	>64	>64	>64	>64
P. aeruginosa (ΔRND)[c]	31	0.5	2	64	>64	8	>64	>64
E. coli (wild-type)	31	0.1	8	2	>64	>64	>64	>64
E. coli (*lpxC101*)	0.06	0.12	4	1	>64	4	>64	>64
E. coli (*tolC*)	8	0.24	1	2	16	0.5	>64	8
E. coli (*tolC,* moir-R)[d]	ND	ND	ND	0.5	8	4	ND	16
E. coli (*lpxC101, tolC*)[d]	0.5	≤0.03	1	0.5	16	0.5	>64	4
S. aureus (wild-type)	≤0.03	0.5	8	4	>64	1	>64	4
S. aureus (moir-R)	ND	ND	ND	2	>64	8	ND	>64
S. aureus (*norA*^{up})	≤0.03	0.5	8	4	>64	4	>64	4
S. epidermidis (wild-type)	≤0.03	8	8	>128	>64	0.24	>64	1
E. faecalis (wild-type)	0.5	8	8	31	>64	8	>64	4

[a]The following designate targeted deletion mutants of efflux pumps or subunits of efflux pumps: *mexAB*, *mexCD*, *mexXY*, *mexHI*, *opmH*, *tolC*. The *lpxC101* allele enhances permeability of the *E. coli* outer membrane. The *norA*^{up} genotype results from a spontaneous mutation in *S. aureus* resulting in a gain of function of the *norA* efflux pump. The designation moir-R indicates a spontaneous moiramide resistance selected with moiramide B containing agar at 4-8x MIC. Wild-type *P. aeruginosa* is PA01; Wild-type *E. coli* is D21; Wild-type *S. aureus* is ATCC #29213; Wild-type *S. epidermidis* is ATCC #35984; Wild-type *E. faecalis* is ATCC #29212.
[b]Determined by the broth microdilution method.
[c](ΔRND) = mutation of *mexAB*, *mexCD*, *mexXY*, *mexHI*, *opmH*.
[d]These strains show a slight growth defect on agar medium.
ND = Not determined

Figure 2.6. Antibacterial activities of synthesized compounds against strains of bacteria.

Of the dual-ligands tested, compound **6** bearing the shorter 7C linker was found to exhibit the best overall antibacterial activity in MIC assays (Figure 2.6). Antibacterial activity was observed against an efflux compromised *E. coli* strain lacking the *tolC* outer membrane channel and wild-type *S. aureus*. In fact, dual-ligand **6** was effective against all of the Gram-positive strains investigated. Of particular note and, in contrast to moiramide B (**4**), dual-ligand **6** no longer seems to be subject to *norA*-based efflux in *S.*

aureus as the MIC remain unchanged at 4 μg/mL when tested against wild-type *S. aureus* and an otherwise isogenic strain bearing a gain-of-function mutation[34] effecting *norA*-based efflux activity. Dual-ligand **6** was also still effective against moiramide-resistant *E. coli tolC* but virtually ineffective against moiramide-resistant *S. aureus*. This result is wholly expected given that the secondary pharmacophore (the aminooxazole derivative) is not effective against Gram-positive bacteria due to a threonine residue at position 437 of biotin carboxylase (which is an isoleucine in Gram-negative bacteria) causing a loss in necessary hydrophobic contacts between the inhibitor and the binding pocket.[9] Lastly, while the antibacterial activity of dual-ligand **6** is similar to moiramide B in most strains there was an increase in potency for dual-ligand **6** with an MIC of 4 μg/mL against *E. faecalis*, whereas moiramide B (**4**) showed an MIC of 8 μg/mL. The absence of any apparent antibacterial activity of dual-ligand **5** is unexpected as dual-ligand **5** did, in fact inhibit the holoenzyme ACC. We speculated that dual-ligand **5** might be impaired in its ability to diffuse through the bacterial membrane due to the presence of the longer, hydrophobic linker.

2.2.5 Effect of PMBN on the Antibacterial Activity of Dual-Ligand 5

Polymyxin B nonapeptide (PMBN) is a cationic cyclic peptide that is a non-bactericidal version of the antibiotic polymyxin B (PMB). PMBN binds to the bacterial lipopolysaccharide (LPS) found in the outer membrane of Gram-negative bacteria which leads to increased susceptibility to the passage of hydrophobic antibiotics.[35-36] Therefore, the effect of PMBN on the antibacterial activity of dual-ligand **5** was examined to determine whether or not an inability to diffuse across the bacterial membrane was the reason for the lack of observed antibacterial activity.

The antibacterial activity of dual-ligand **5** when co-incubated in *E. coli* with PMBN is shown in Figure 2.7. As expected, there was no antibacterial activity observed for dual-ligand **5** when inoculated in *E. coli* without PMBN. However, with increasing amounts of PMBN, dual-ligand **5** did inhibit bacterial growth (Figure 2.7).

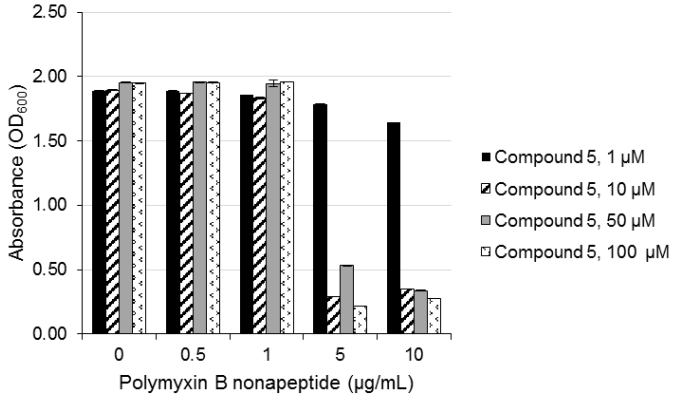

Figure 2.7. Effect of polymyxin B nonapeptide (PMBN) on the antibacterial activity of dual-ligand **5**. Increasing amounts of PMBN (0, 0.5, 1, 5, 10 μg/mL) were added to different fixed concentrations of dual-ligand **5** (1, 10, 50, 100 μM) and the solutions were inoculated with *E. coli* and incubated at 37 °C. After a 4 hour incubation, the absorbance at 600 nm was measured.

Concentrations of 10, 50, and 100 μM of dual-ligand **5** inhibited growth of *E. coli* when inoculated with at least 5 μg/mL of PMBN. There was no significant inhibition of growth with only 1 μM of dual-ligand **5**, even with the addition of PMBN. Control experiments showed no growth inhibition when *E. coli* was inoculated with only PMBN at the highest concentration (10 μg/mL) used in the assay. These results strongly suggest that the lack of antibacterial activity of dual-ligand **5**, even at high concentrations, was due to an inability to diffuse across the bacterial membrane. Thus, the antibacterial activity of dual-ligand **5** in the presence of PMBN can be attributed to the ability of dual-ligand **5** to enter the cell and inhibit ACC. This result implies synergy between PMBN

and dual-ligand **5** which can be beneficial when developing combination therapies targeting Gram-negative pathogens.[37-38]

2.2.6 Single-step Resistance Studies

One of the potential advantages of a dual-ligand antibacterial agent versus a molecule directed against a single target is a lower likelihood of developing resistance. To this end, the spontaneous resistance frequencies were determined for rifampin, aminooxazole **2**, moiramide B (**4**), and dual-ligand **6** against the *E. coli tolC* mutant (Figure 2.8). Compared to the control rifampin, aminooxazole **2** had a lower frequency of resistance and in general, was found to be a poor inhibitor in these assays. In contrast, the mutant prevention concentrations (MPC) for moiramide B (**4**) and dual-ligand **6** were 16 mg/L and 64 mg/L, respectively. This allowed for the calculation of mutant selection windows (MSWs) for these compounds where the MSW is the MPC/MIC ratio, with an ideal drug having an MSW of 1.[39] The MSW values for moiramide B and dual-ligand **6** were 32 and 8, respectively. Thus, dual-ligand **6** has a narrower MSW suggesting it has more restriction for selection of resistance. Lastly, when dosed at 8x the MIC value, moiramide B and dual-ligand **6** both exhibited an observed resistance frequency of $<2.5 \times 10^{-10}$. This number was too low to determine any significant difference between the two compounds. Therefore, it could not be assessed if dual-ligand **6** has a lower frequency of resistance when compared to the two "parent" compounds. Nonetheless, when compared to rifampin and aminooxazole **2**, dual-ligand **6** clearly has a much lower potential for spontaneous resistance development.

Compound	MIC[a] (mg/L)	MPC[b] (mg/L)	MSW[c]	Resistance Frequency[d]
Rifampin	8	>64	>8	7×10^{-9}
2	16	>128	>8	1.75×10^{-9}
4	0.5	16	32	$<2.5 \times 10^{-10}$
6	8	64	8	$<2.5 \times 10^{-10}$

[a]Determined from broth microdilution in MHII broth.
[b]MPC is the drug dose at which resistant mutants (using 4×10^9 CFU) were no longer obtained.
[c]MSW is the ratio of the MPC to the MIC.
[d]Resistance frequency is the number of resistant colonies observed over the total number of CFU plated at 8x MIC

Figure 2.8. Results of single-step resistance selection studies with the *E. coli tolC* strain.

2.3 CONCLUSIONS

The studies in this report provide "proof-of-concept" that a dual-ligand inhibitor of the multifunctional enzyme ACC can act as an antibacterial agent. First, the synthesis of the dual-ligand inhibitor led to significant improvements in the synthetic protocol for the moiramide B (**4**) moiety. Second, incorporating two known inhibitors for the two enzymes comprising ACC, biotin carboxylase and carboxyltransferase, into a single chemical entity yielded a potent (nM inhibition constant) inhibitor of the enzyme. An unexpected but potentially far-reaching finding was that the aminooxazole **2**, exhibited noncompetitive inhibition of biotin carboxylase with respect to ATP in ACC, but competitive inhibition in the isolated biotin carboxylase subunit. This indicates that inhibitors of biotin carboxylase discovered using the isolated subunit may react differently with ACC. Third, the finding that dual-ligand **5** had little to no antibacterial activity, while dual-ligand **6** exhibited antibacterial activity against Gram-negative and Gram-positive organisms indicates that the choice of the linking component is critical for determining whether dual-ligand inhibitors which show activity in biochemical assays will also show antibacterial activity. Based on our results, we speculate that the more hydrophobic the linker is, the less likely it is to diffuse across the bacterial membrane.

While the pharmacophore involving aminooxazole **2** was not as potent as the moiramide B (**4**) moiety, it did retain appreciable antibacterial activity *in vitro*. Importantly, many novel aminooxazole derivatives were recently reported as part of a recent virtual screening study[40] which identified several million aminooxazole derivatives that could potentially be linked to moiramide B (**4**) to generate a wide array of dual-ligand hybrids. These new dual-ligands could, in turn, be screened for potent broad spectrum antibacterial activity using the tools and techniques described herein. Future studies will seek to test this proposal directly and will undoubtedly provide new and important information about the activity of dual-ligand inhibitors against this novel target.

2.4 EXPERIMENTAL SECTION

2.4.1 Materials and Methods

All chemicals and reagents were purchased from Sigma-Aldrich, Fisher, Acros, NovaBiochem, Matrix, Combi-Blocks or Fluka and used without further purification. Diisopropylethylamine and triethylamine were dried and distilled from CaH_2 and stored over KOH pellets. Dry methanol was distilled from Mg turnings and stored over 3Å molecular sieves. All reactions were performed under a dry nitrogen atmosphere unless otherwise noted. Flash chromatography was performed using 230-400 mesh silica gel (40-63 μm) from Sigma-Aldrich. Thin layer chromatography (TLC) was performed on aluminum-backed 60 F_{254} silica plates from EMD Chemicals, Inc. Optical rotations were recorded on a Jasco P-2000 digital polarimeter. Circular dichroism (CD) spectrum was recorded on a Jasco J-815 Circular Dichroism spectrometer. ^{1}H and ^{13}C NMR spectra were recorded at room temperature on a Bruker AV-400 or AV-500 spectrometer. All NMR experiments were performed in deuterated solvents and the chemical shifts are

reported in standard δ notation as parts per million, using tetramethylsilane (TMS), $CDCl_3$, DMSO-d_6, or acetone-d_6 as an internal standard for ^1H and ^{13}C NMR, with coupling constants (*J*) reported in Hertz (Hz). High resolution mass spectrometry (HRMS) was carried out using an Agilent 6210 electrospray ionization-time-of-flight (ESI-TOF) mass spectrometer.

Synthesis of (*E*)-4-[(benzylideneamino)methyl]phenol (**9**). Benzaldehyde **7** (413 μL, 431 mg, 4.06 mmol, 1.00 equiv.) was added to a suspension of 3Å molecular sieves (150 mg/100 mg amine), triethylamine (736 μL, 534 mg, 5.28 mmol, 1.30 equiv.), and 4-hydroxybenzylamine **8** (500 mg, 4.06 mmol, 1.00 equiv.) in dry methanol (1.0 mL/100 mg amine) at rt under N_2. The mixture was stirred at rt for 18 h. The molecular sieves were removed by filtration through a pad of Celite®, washing well with dry methanol and the filtrate was concentrated *in vacuo* to give **9** as a light brown solid (556 mg, 65%).[3] ^1H NMR (DMSO-d_6, 400 MHz) δ 4.64 (s, 2H), 6.72 (d, *J* = 8.4 Hz, 2H), 7.11 (d, *J* = 8.4 Hz, 2H), 7.41-7.49 (m, 3H), 7.70-7.81 (m, 2H), 8.44 (s, 1H), 9.33 (br s, 1H); ^{13}C NMR (DMSO-d_6, 100 MHz) δ 64.1, 115.6, 128.4, 129.1, 129.6, 130.1, 131.1, 136.6, 156.7, 161.5. HRMS (ESI-TOF) calcd for $C_{14}H_{14}NO$ $(M+H)^+$: 212.1070, obsd: 212.1070.

Synthesis of 4-[(benzylamino)methyl]phenol (**10**). Sodium borohydride (154 mg, 4.06 mmol, 1.80 equiv.) was added in portions to a solution of **9** (556 mg, 2.63 mmol, 1.00 equiv.) in dry methanol (5 mL) at 0 °C. The mixture was stirred for 18 h under N_2 while allowing to warm to rt. The mixture was concentrated and then partitioned between CH_2Cl_2 (10 mL) and water (10 mL). The aqueous layer was further extracted

[3]No Rf was obtained for imine compound as product hydrolyzed on silica.

with CH_2Cl_2 (2 x 10 mL). The combined organic layers were washed with brine, dried over $MgSO_4$, filtered, and concentrated to give **10** as a light brown solid (470 mg, 84%). R_f 0.27 (3:2 CH_2Cl_2:EtOAc). ^{1}H NMR (acetone-d_6, 400 MHz) δ 3.69 (s, 2H), 3.77 (s, 2H), 5.55 (s, 1H), 6.80 (d, J = 8.4 Hz, 2H), 7.19 (d, J = 8.4, 2H), 7.23 (d, J = 7.4 Hz, 1H), 7.30 (t, J = 7.4 Hz, 2H), 7.37 (d, J = 7.4 Hz, 2H); ^{13}C NMR (acetone-d_6, 100 MHz) δ 52.2, 52.5, 115.3, 126.7, 128.2, 128.3, 129.5, 130.9, 140.7, 156.7. HRMS (ESI-TOF) calcd for $C_{14}H_{16}NO$ $(M+H)^+$: 214.1226, obsd: 214.1225.

Synthesis of 2-aminooxazole-5-carboxylic acid (**12**).[10] Ethyl 2-aminooxazole-5-carboxylate **11** (2.00 g, 12.8 mmol) was added to 2M aqueous NaOH (50 mL) and stirred at rt for 2 h. The mixture was heated to 60 °C and stirred for an additional 2 h. Concentrated hydrochloric acid was added dropwise to the reaction mixture until it became acidic by pH paper (pH ~3-4) and a colorless precipitate began to form. The mixture was cooled in the freezer for 1 h. The resulting solid was collected by filtration and washed with acetonitrile to give **12** as a colorless solid (1.60 g, 98%). R_f 0.24 (6:4:1 $CHCl_3$:MeOH:H_2O). ^{1}H NMR (DMSO-d_6, 400 MHz) δ 7.38 (s, 2H), 7.44 (s, 1H); ^{13}C NMR (DMSO-d_6, 100 MHz) δ 136.0, 137.1, 159.1, 164.1. HRMS (ESI-TOF) calcd for $C_4H_5N_2O_3$ $(M+H)^+$: 129.0295, obsd: 129.0296.

General procedure for the synthesis of aminooxazole derivatives (**2** and **13**). Amine (1.00 equiv.) was added to a solution of **12** (1.00 equiv.) and triethylamine (2.00 equiv.) in dry DMF (10 mL). HATU (1.00 equiv.) was added to the solution and the mixture stirred for 20 h under N_2. The mixture was partitioned between EtOAc (25 mL) and water (20 mL). The aqueous layer was further extracted with EtOAc (2 x 20 mL). The combined organic layers were washed with sat'd aq. $NaHCO_3$ (15 mL), brine (15

mL), dried over $MgSO_4$, filtered, and concentrated. The resulting residue was dissolved in EtOAc (20 mL) and placed in a freezer overnight. The resulting precipitate was collected by filtration, washed with EtOAc, and dried.

Synthesis of 2-amino-*N*,*N*-dibenzyloxazole-5-carboxamide (**2**).[10] Starting from dibenzylamine (249 μL, 256 mg, 1.30 mmol), carboxylic acid **12** (166 mg, 1.30 mmol), triethylamine (362 μL, 262 mg, 2.59 mmol) and HATU (493 mg, 1.30 mmol), the general procedure gave **2** as a colorless solid (124 mg, 31%). R_f 0.16 (3:2 CH_2Cl_2:EtOAc). ^{1}H NMR (DMSO-d_6, 400 MHz) δ 4.65 (br s, 4H), 7.06-7.41 (m, 13H); ^{13}C NMR (DMSO-d_6, 100 MHz) δ 49.9, 52.5, 127.7, 128.5, 128.6, 129.1, 134.9, 137.4, 137.7, 159.0, 163.1. HRMS (ESI-TOF) calcd for $C_{18}H_{18}N_3O_2$ $(M+H)^+$: 308.1394, obsd: 308.1399.

Synthesis of 2-amino-*N*-benzyl-*N*-(4-hydroxybenzyl)oxazole-5-carboxamide (**13**). Starting from amine **10** (1.20 g, 5.64 mmol), carboxylic acid **12** (721 mg, 5.64 mmol), triethylamine (1.57 mL, 1.14 g, 11.3 mmol), and HATU (2.14 g, 5.64 mmol), the general procedure gave **13** as a colorless solid (633 mg, 35%). R_f 0.57 (9:1 CH_2Cl_2:MeOH). ^{1}H NMR (DMSO-d_6, 400 MHz) δ 4.51 (s, 2H), 4.59 (s, 2H), 6.73 (d, J = 8.1 Hz, 2H), 7.42 (m, 10H), 9.40 (s, 1H); ^{13}C NMR (DMSO-d_6, 100 MHz) δ 49.3, 115.8, 127.6, 129.1, 134.7, 137.5, 137.8, 157.1, 158.8, 163.1. HRMS (ESI-TOF) calcd for $C_{18}H_{18}N_3O_3$ $(M+H)^+$: 324.1343, obsd: 324.1371.

Synthesis of (4*S*)-methyl-succinic anhydride (**15**). Acetyl chloride (4.53 mL, 4.75 g, 60.6 mmol, 4.00 equiv.) was added to (4*S*)-methylsuccinic acid **14** (2.00 g, 15.1 mmol, 1.00 equiv.) and heated gently at reflux for 6 h. Excess acetyl chloride and acetic acid were removed *in vacuo* to give **15** as a colorless solid (1.70 g, 97%).[24] R_f 0.76 (9:1 CH_2Cl_2:MeOH). $[\alpha]_D^{24}$ -33.0 (*c* 1.77, $CHCl_3$) [Lit.[24] $[\alpha]_D^{24}$ -36.3 (*c* 1.77, $CHCl_3$)]. ^{1}H

NMR ($CDCl_3$, 400 MHz) δ 1.30 (d, *J* = 7.2 Hz, 3H), 2.45-2.56 (m, 1H), 2.99-3.17 (m, 2H); ^{13}C NMR ($CDCl_3$, 100 MHz) δ 16.1, 35.6, 36.0, 169.9, 174.3. HRMS (ESI, -ve, TOF) calcd for $C_5H_5O_3$ $(M-H)^+$: 113.0244, obsd: 113.0244.

Synthesis of (4*S*)-methyl-*N*-*O*-benzylsuccinimide (**20**).[13] Triethylamine (1.08 mL, 787 mg, 7.78 mmol, 1.05 equiv.) was added to a solution of **15** (845 mg, 7.41 mmol, 1.00 equiv.) in CH_2Cl_2 (5 mL) at 0 °C followed by addition of *O*-benzylhydroxylamine hydrochloride **19** (1.24 g, 7.78 mmol, 1.05 equiv.). The mixture was warmed to rt overnight under N_2 and then 1,1'-carbonyldiimidazole (1.32 g, 8.15 mmol, 1.10 equiv.) was added in portions. The mixture was stirred at rt for 1.5 h and then heated at reflux for 30 min. The mixture was cooled to rt and the organic layer was washed with 10% hydrochloric acid (2 x 10 mL). The organic layer was washed with brine (10 mL), dried over $MgSO_4$, filtered, and concentrated to give **20** as a colorless solid (1.44 g, 89%). R_f 0.64 (4:1 EtOAc:Hex). $[\alpha]_D^{23}$ -2.0 (*c* 0.72, $CHCl_3$) [Lit.[24] $[\alpha]_D^{24}$ –4.9 (*c* 0.72, $CHCl_3$)]. ^1H NMR ($CDCl_3$, 400 MHz) δ 1.25 (d, *J* = 7.2 Hz, 3H), 2.20 (dd, *J* = 17.5, 3.6 Hz, 1H), 2.67-2.80 (m, 1H), 2.82 (dd, *J* = 17.6, 8.9 Hz, 1H), 5.13 (s, 2H), 7.28-7.40 (m, 3H), 7.43-7.56 (m, 2H); ^{13}C NMR ($CDCl_3$, 100 MHz) δ 16.7, 32.0, 33.7, 78.5, 128.5, 129.5, 130.1, 133.2, 170.6, 174.7. HRMS (ESI-TOF) calcd for $C_{12}H_{13}NaNO_3$ $(M+Na)^+$: 242.0788, obsd: 242.0804.

Synthesis of (3*S*)-Boc-L-valine-(4*S*)-methyl-*N*-*O*-benzylsuccinimide (**21**).[13, 24] A solution of Boc-L-valine (992 mg, 4.56 mmol, 1.00 equiv.) and 1,1'-carbonyldiimidazole (814 mg, 5.02 mmol, 1.10 equiv.) in dry THF (4 mL) was stirred at rt for 2 h under N_2. A solution of **20** (1.00 g, 4.56 mmol, 1.00 equiv.) in dry THF (8 mL) was added to the acylimidazole mixture at rt. This combined solution was then added dropwise over 45

min to a stirring solution of lithium hexamethyldisilazide (9.13 mL, 1.00 M, 9.13 mmol, 2.00 equiv.) in dry THF (6 mL) under N_2 at -78 °C. After the addition was complete, the mixture was stirred at -78 °C for an additional 15 min and then quenched with sat'd aq. ammonium chloride (5 mL). The reaction mixture was allowed to warm to rt and then partitioned between Et_2O (20 mL) and water (20 mL). The organic phase was washed with brine (20 mL), dried over $MgSO_4$, filtered, and concentrated. The resulting residue was purified by flash chromatography on silica gel eluting with 3:1 Hex:EtOAc to give **21** as a colorless solid (800 mg, 42%). R_f 0.45 (2:1 Hex:EtOAc). $[\alpha]_D^{23}$ -30.1 (*c* 0.70, $CHCl_3$) [Lit.[24] $[\alpha]_D^{23}$ -33.9 (*c* 0.70, $CHCl_3$)]. ^{1}H NMR ($CDCl_3$, 400 MHz) δ 0.78 (d, *J* = 6.7 Hz, 3H), 0.99 (d, *J* = 6.7 Hz, 3H), 1.23 (d, *J* = 7.4 Hz, 3H), 1.46 (s, 9H), 2.24-2.41 (m, 1H), 3.14-3.30 (m, 1H), 3.71 (d, *J* = 4.0 Hz, 1H), 4.44 (dd, *J* = 8.8, 4.8 Hz, 1H), 5.09 (s, 2H), 5.60 (d, *J* = 8.6 Hz, 1H), 7.30-7.39 (m, 3H), 7.40-7.46 (m, 2H); ^{13}C NMR ($CDCl_3$, 100 MHz) δ 15.6, 17.3, 19.6, 28.3, 29.6, 34.5, 55.0, 65.1, 78.7, 80.2, 128.6, 129.6, 130.2, 132.9, 156.0, 166.6, 173.1, 201.9. HRMS (ESI-TOF) calcd for $C_{22}H_{30}NaN_2O_6$ $(M+Na)^+$: 441.1996, obsd: 441.1994.

Synthesis of (3*S*)-Boc-L-valine-(4*S*)-methyl-succinimide (**22**).[24] A catalytic amount of 5% Pd/C (127 mg, 20% w/w) was added to a solution of **21** (637 mg, 1.52 mmol, 1.00 equiv.) in dry methanol (10 mL) and the mixture stirred under H_2 for 1 h. The reaction mixture was filtered through a pad of Celite®, washed with methanol, and concentrated. The residue was dissolved in acetonitrile (3 mL) and added dropwise to a stirred solution of 2-bromoacetophenone (303 mg, 1.52 mmol, 1.00 equiv.) in acetonitrile (5 mL) at rt. A solution of triethylamine (318 μL, 231 mg, 2.28 mmol, 1.50 equiv.) in acetonitrile (1 mL) was added dropwise over 2 h and the reaction mixture was stirred at rt

overnight. The mixture was concentrated and then partitioned between CH_2Cl_2 (25 mL) and 5% hydrochloric acid (2 x 20 mL). The organic layer was washed with brine (20 mL), dried over $MgSO_4$, filtered, concentrated, and purified by flash chromatography on silica gel eluting with 5:1 CH_2Cl_2:EtOAc to give **22** as a yellow solid (303 mg, 64%). R_f 0.63 (3:1 CH_2Cl_2:EtOAc). $[\alpha]_D^{24}$ -26.0 (*c* 1.005, $CHCl_3$) [Lit.[24] $[\alpha]_D^{23}$ -41.8 (*c* 0.66, $CHCl_3$)]. ^{1}H NMR ($CDCl_3$, 400 MHz) δ 0.79 (d, *J* = 6.7 Hz, 3H), 1.02 (d, *J* = 6.7 Hz, 3H), 1.31 (d, *J* = 7.4 Hz, 3H), 1.45 (s, 9H), 2.15-2.23 (m, 1H), 3.14-3.22 (m, 1H), 3.93 (d, *J* = 5.3 Hz, 1H), 4.61 (dd, *J* = 9.0, 4.0 Hz, 1H), 5.80 (d, *J* = 9.2 Hz, 1H), 9.82 (s, 1H); ^{13}C NMR ($CDCl_3$, 100 MHz) δ 15.3, 16.9, 19.7, 28.3, 29.7, 38.4, 59.0, 64.9, 80.3, 156.1, 172.1, 179.1, 202.2. HRMS (ESI-TOF) calcd for $C_{15}H_{24}NaN_2O_5$ $(M+Na)^+$: 335.1577, obsd: 335.1582.

General procedure for the synthesis of amines **23** and **25**.[24] Trifluoroacetic acid (2.0 mL) was added dropwise to a solution of Boc-protected amine (**22** or **24**) (1.00 equiv.) in CH_2Cl_2 (2.0 mL) at 0 °C and stirring continued at 0 °C for 2 h followed by the addition of toluene (10 mL) and removal of solvent *in vacuo*. The resulting residue was purified by flash chromatography on silica gel with the less polar byproducts being flushed with 2-3 columns lengths of 1:1 CH_2Cl_2:EtOAc and product being eluted with 9:1 CH_2Cl_2:MeOH.

Synthesis of (3*S*)-L-valine-(4*S*)-methyl-succinimide (**23**). Starting from Boc-protected amine **22** (200 mg, 0.64 mmol), the general procedure gave **23** as a light yellow foam (121 mg, 89%). R_f 0.50 (6:4:1 $CHCl_3$:MeOH;H_2O). HRMS (ESI-TOF) calcd for $C_{10}H_{16}N_2O_3$ $(M+H)^+$: 213.1234, obsd: 213.1238.

Synthesis of (3*S*)-β-phenylalanine-L-valine-(4*S*)-methyl-succinimide (**25**). Starting from Boc-protected amine **24** (183 mg, 0.398 mmol), the general procedure gave **25** as a light pink solid (141 mg, 98%). R_f 0.64 (6:4:1 $CHCl_3$:MeOH;H_2O). HRMS (ESI-TOF) calcd for $C_{19}H_{26}N_3O_4$ $(M+H)^+$: 360.1918, obsd: 360.1927.

Synthesis of (3*S*)-*N*-Boc-3-amino-β-phenylalanine-L-valine-(4*S*)-methyl-succinimide (**24**).[13] (*S*)-*N*-Boc-3-amino-3-phenylpropanoic acid (255 mg, 0.96 mmol, 1.20 equiv.) was added to a solution of **23** (170 mg, 0.80 mmol, 1.00 equiv.) in dry DMF (5.0 mL) at 0 °C. HATU (366 mg, 0.96 mmol, 1.20 equiv.) was added to the solution and the mixture began stirring under N_2. A solution of *N*,*N*-diisopropylethylamine (349 μL, 259 mg, 2.00 mmol, 2.50 equiv.) in dry DMF (1.5 mL) was added dropwise to the reaction over 1 h, while maintaining the temperature at 0 °C. The reaction was stirred for an additional 30 min at 0 °C before allowing the reaction mixture to warm to rt where stirring was continued for 20 h under N_2. The solvent was removed *in vacuo* and the mixture was partitioned between EtOAc (20 mL) and water (20 mL). The organic layer was washed with sat'd aq. $NaHCO_3$ (20 mL) and brine (20 mL), dried over $MgSO_4$, filtered, concentrated and purified by flash chromatography on silica gel eluting with 3:2 Hex:EtOAc to give **24** as a colorless solid (166 mg, 45%). R_f 0.25 (1:1 Hex:EtOAc). $[\alpha]_D^{20}$ -53.2 (*c* 1.00, $CHCl_3$). ^{1}H NMR (DMSO-d_6, 400 MHz) δ 0.77 (d, *J* = 6.6 Hz, 3H), 0.85 (d, *J* = 6.6 Hz, 3H), 1.11 (d, *J* = 7.3 Hz, 3H), 1.34 (s, 9H), 2.23-2.37 (m, 1H), 2.42-2.50 (m, 1H), 2.71 (dd, *J* = 13.9, 9.3 Hz, 1H), 2.84-3.03 (m, 1H), 3.99 (d, *J* = 5.4 Hz, 1H), 4.71 (dd, *J* = 7.6, 5.3 Hz, 1H), 4.79-4.95 (m, 1H), 7.12-7.39 (m, 6H), 8.01 (d, *J* = 8.3 Hz, 1H), 11.37 (br s, 1H); ^{13}C NMR (DMSO-d_6, 100 MHz) δ 15.0, 17.5, 20.0, 28.6, 28.8,

43.0, 52.1, 58.3, 63.4, 78.3, 126.6, 127.3, 128.7, 144.0, 155.0, 170.4, 174.2, 180.5, 203.7. HRMS (ESI-TOF) calcd for $C_{24}H_{34}N_3O_6$ $(M+H)^+$: 460.2442, obsd: 460.2428.

Synthesis of moiramide B (**4**). Sorbic acid (75 mg, 0.67 mmol, 1.20 equiv.), TBTU (215 mg, 0.67 mmol, 1.20 equiv.) and *N*,*N*-diisopropylethylamine (242 μL, 180 mg, 1.39 mmol, 2.50 equiv.) were added to a solution of **25** (200 mg, 0.56 mmol, 1.00 equiv.) in dry DMF (2 mL) and the mixture stirred for 20 h under N_2. The mixture was partitioned between EtOAc (10 mL) and water (6 mL). The organic layer was washed with sat'd aq. $NaHCO_3$ (5 mL), brine (5 mL), dried over $MgSO_4$, filtered, and concentrated. The resulting residue was purified by flash chromatography on silica gel eluting with 2% NH_4OH in 9:1 EtOAc:MeOH to give **4** as a colorless solid (81 mg, 32%).[24] R_f 0.54 (100% EtOAc). $[\alpha]_D^{24}$ -77.5 (*c* 1.00, MeOH) [Lit.[24] $[\alpha]_D^{25}$ -96.6 (*c* 0.28, MeOH)]. CD (*c* 1 μM, MeOH) $\lambda_{max}(\theta)$ 213.0 (+9.68), 238.0 (-21.08), 292.0 (+0.69), 320.0 (-1.26). CD spectrum displayed λ_{max} values in good agreement with the literature though no concentrations were reported.[11, 24] ^{1}H NMR (DMSO-d_6, 400 MHz) δ 0.74 (d, *J* = 6.7 Hz, 3H), 0.79 (d, *J* = 6.7 Hz, 3H), 1.06 (d, *J* = 7.4 Hz, 3H), 1.77 (d, *J* = 6.4 Hz, 3H), 2.19-2.34 (m, 1H), 2.62 (dd, *J* = 14.1, 5.9 Hz, 1H), 2.76 (dd, *J* = 14.2, 8.7, 1H), 2.83-2.97 (m, 1H), 3.92 (d, *J* = 5.4 Hz, 1H), 4.62 (dd, *J* = 8.0, 5.6 Hz, 1H), 5.14-5.29 (m, 1H), 5.91 (d, *J* = 15.2, 1H), 6.06 (dq, *J* = 14.9, 6.8 Hz, 1H), 6.18 (dd, *J* = 14.9, 11.0 Hz, 1H), 6.94 (dd, *J* = 14.9, 11.0 Hz, 1H), 7.10-7.37 (m, 5H), 8.11 (d, *J* = 8.4 Hz, 1H), 8.41 (d, *J* = 8.4 Hz, 1H), 11.35 (br s, 1H); ^{13}C NMR (DMSO-d_6, 100 MHz) δ 15.0, 17.7, 18.7, 19.9, 28.6, 39.5, 42.4, 50.3, 58.2, 63.5, 123.3, 126.9, 127.3, 128.6, 128.7, 130.3, 137.2, 139.9, 143.3, 164.9, 170.3, 174.2, 180.5, 203.8. HRMS (ESI-TOF) calcd for $C_{25}H_{32}N_3O_5$ $(M+H)^+$: 454.2336, obsd: 454.2347.

General procedure for the synthesis of allyl ester linker derivatives (**27** and **30**).[29] Concentrated sulfuric acid (2.00 equiv.) was added to a solution of acid (1.00 equiv.) in allyl alcohol. The solution was heated at reflux for 6 h. The mixture was cooled to rt, diluted with Et_2O (25 mL), and washed with sat'd aq. $NaHCO_3$ (2 x 20 mL). The aqueous phase was back-extracted with Et_2O (15 mL). The combined organic layers were washed with brine (10 mL), dried over $MgSO_4$, filtered and concentrated. The resulting oil was purified by flash chromatography on silica gel eluting with 4:1 Hex:EtOAc.

Synthesis of allyl 16-hydroxyhexadecanoate (**27**). According to the general procedure, concentrated sulfuric acid (391 μL, 720 mg, 7.34 mmol), 16-hydroxyhexadecanoic acid **26** (1.00 g, 3.67 mmol), and allyl alcohol (35 mL) gave **27** as a colorless solid (704 mg, 61%). R_f 0.61 (1:1 Hex:EtOAc). ^{1}H NMR ($CDCl_3$, 400 MHz) δ 1.20-1.35 (m, 22H), 1.53-1.65 (m, 4H), 2.33 (t, J = 7.6 Hz, 2H), 3.64 (t, J = 6.6 Hz, 2H), 4.58 (d, J = 5.7 Hz, 2H), 5.24 (d, J = 10.4 Hz, 1H), 5.32 (d, J = 17.2 Hz, 1H), 5.92 (ddt, J = 17.2, 10.4, 5.7 Hz, 1H); ^{13}C NMR ($CDCl_3$, 100 MHz) δ 24.9, 25.7, 29.1, 29.2, 29.4, 29.6, 32.8, 34.2, 62.9, 64.9, 118.0, 132.3, 173.5. HRMS (ESI-TOF) calcd for $C_{19}H_{36}NaO_3$ $(M+Na)^+$: 335.2557, obsd: 335.2559.

Synthesis of allyl 8-hydroxyoctanoate (**30**). According to the general procedure, concentrated sulfuric acid (133 μL, 245 mg, 2.50 mmol), 8-hydroxyoctanoic acid **29** (200 mg, 1.25 mmol), and allyl alcohol (8 mL) gave **30** as a yellow oil (148 mg, 59%). R_f 0.54 (1:1 Hex:EtOAc). ^{1}H NMR ($CDCl_3$, 400 MHz) δ 1.29-1.38 (m, 7H), 1.55 (p, J = 6.7 Hz, 2H), 1.64 (p, J = 6.9 Hz, 2H), 2.34 (t, J = 7.5 Hz, 2H), 3.61 (t, J = 6.6 Hz, 2H), 4.57 (d, J = 5.7 Hz, 2H), 5.23 (d, J = 10.4 Hz, 1H), 5.31 (d, J = 17.2 Hz, 1H), 5.92 (ddt, J = 17.2,

10.4, 5.7 Hz, 1H); ^{13}C NMR ($CDCl_3$, 100 MHz) δ 24.8, 25.5, 28.9, 29.0, 32.6, 34.2, 62.7, 64.9, 118.1, 132.2, 173.5. HRMS (ESI-TOF) calcd for $C_{11}H_{20}NaO_3$ $(M+Na)^+$: 223.1305, obsd: 223.1302.

General procedure for the synthesis of iodoalkanoic linker derivatives (**28** and **31**). Polymer-bound triphenylphosphine (100-200 mesh, polystyrene crosslinked with 2% divinylbenzene: ~3 mmol/g loading; 2.18 equiv.) was suspended in dry CH_2Cl_2 (10 mL). Iodine (2.18 equiv.) was added in portions until the dark color persisted. The mixture was stirred at rt under N_2 for 15 min. Imidazole (2.48 equiv.) was added and the reaction stirred for an additional 15 min. A solution of compound **27** or **30** (1.00 equiv.) in dry CH_2Cl_2 (5 mL) was added and the mixture was heated at reflux for 30 min. The mixture was filtered to remove the resin and resin-bound byproducts and the resin was washed with CH_2Cl_2 (15 mL). The filtrate was washed with sat'd aq. $Na_2S_2O_3$ (15 mL) and water (15 mL). The organic layer was dried over $MgSO_4$, filtered, and concentrated.

Synthesis of allyl 16-iodohexadecanoate (**28**). Starting from polymer-bound triphenylphosphine (2.19 g, 8.36 mmol), iodine (2.12 g, 8.36 mmol), imidazole (647 mg, 9.51 mmol), and allyl ester linker **27** (1.20 g, 3.83 mmol), the general procedure gave **28** as a yellow solid (1.26 g, 78%). R_f 0.74 (2:1 Hex:EtOAc). ^{1}H NMR ($CDCl_3$, 400 MHz) δ 1.21-1.33 (m, 22H), 1.38 (p, J = 7.0 Hz, 2H), 1.62 (p, J = 7.0 Hz, 2H), 1.81 (p, J = 7.2 Hz, 2H), 2.31 (t, J = 7.5 Hz, 2H), 3.17 (t, J = 7.0 Hz, 2H), 4.56 (d, J = 5.6 Hz, 2H), 5.21 (d, J = 10.6 Hz, 1H), 5.30 (d, J = 17.1 Hz, 1H), 5.91 (ddt, J = 17.1, 10.6, 5.6 Hz, 1H); ^{13}C NMR ($CDCl_3$, 100 MHz) δ 7.0, 24.9, 28.5, 29.1, 29.2, 29.4, 29.5, 29.6, 29.6, 30.5, 33.6, 34.2, 64.8, 117.9, 132.4, 173.2.

Synthesis of allyl 8-iodooctanoate (**31**). Starting from polymer-bound triphenylphosphine (394 mg, 1.50 mmol), iodine (382 mg, 1.50 mmol), imidazole (116 mg, 1.71 mmol), and allyl ester linker **30** (138 mg, 0.690 mmol), the general procedure gave **31** as a yellow oil (178 mg, 83%). R_f 0.48 (1:1 Hex:EtOAc). ^{1}H NMR ($CDCl_3$, 400 MHz) δ 1.22-1.33 (m, 7H), 1.40 (p, J = 6.6 Hz, 2H), 1.64 (p, J = 7.3 Hz, 2H), 1.82 (p, J = 7.2 Hz, 2H), 2.34 (t, J = 7.5 Hz, 2H), 3.18 (t, J = 7.0 Hz, 2H), 4.58 (d, J = 5.7 Hz, 2H), 5.24 (d, J = 10.4 Hz, 1H), 5.32 (d, J = 17.2 Hz, 1H), 5.92 (ddt, J = 17.2, 10.4, 5.7 Hz, 1H); ^{13}C NMR ($CDCl_3$, 100 MHz) δ 7.2, 24.8, 28.2, 28.9, 30.3, 33.4, 34.1, 65.0, 118.1, 132.3, 173.3.

General procedure for the synthesis of aminooxazole conjugated to linker derivatives (**32-33**). Cesium hydroxide (1.00 equiv.) was added to a solution of **13** (1.00 equiv.) in dry DMF (5 mL). Linker derivative (**28** or **31**) (1.00 equiv.) in dry THF (2 mL) was added to the reaction and the mixture was heated at reflux for 24 h. Once cooled to rt, the mixture was filtered and the precipitate was washed with THF. The solvent was removed *in vacuo* and the residue was partitioned between EtOAc (10 mL) and water (10 mL) and the organic layer was dried over $MgSO_4$, filtered, and concentrated.

Synthesis of allyl 16-{4-[(2-amino-*N*-benzyloxazole-5-carboxamido)methyl] phenoxy}hexadecanoate (**32**). Starting from cesium hydroxide (224 mg, 1.33 mmol), aminooxazole **13** (430 mg, 1.33 mmol), and linker **28** (562 mg, 1.33 mmol), the general procedure gave a residue that was purified by flash chromatography on silica gel eluting with 3:1 EtOAc:Hex that gave **32** as a pale yellow solid (166 mg, 20%). R_f 0.18 (3:1 EtOAc:Hex). ^{1}H NMR ($CDCl_3$, 400 MHz) δ 1.18-1.36 (m, 22H), 1.44 (p, J = 7.2 Hz, 2H), 1.63 (p, J = 6.9 Hz, 2H), 1.75 (p, J = 7.1 Hz, 2H), 2.32 (t, J = 7.5 Hz, 2H), 3.93 (t, J

= 6.3 Hz, 2H), 4.53-4.68 (m, 6H), 5.22 (d, *J* = 10.4 Hz, 1H), 5.30 (d, *J* = 17.2 Hz, 1H), 5.91 (ddt, *J* = 17.2, 10.4, 5.7 Hz, 1H), 6.00 (br s, 2H), 6.85 (d, *J* = 7.9 Hz, 2H), 7.02-7.38 (m, 8H); ^{13}C NMR ($CDCl_3$, 100 MHz) δ 25.0, 26.1, 29.1, 29.3, 29.5, 29.6, 29.7, 34.3, 49.1, 50.2, 64.9, 68.1, 114.8, 118.1, 127.6, 127.8, 128.5, 128.9, 132.3, 133.3, 138.1, 158.7, 159.5, 162.0, 173.6. HRMS (ESI-TOF) calcd for $C_{37}H_{52}N_3O_5$ $(M+H)^+$: 618.3901, obsd: 618.3883.

Synthesis of allyl 8-{4-[(2-amino-*N*-benzyloxazole-5-carboxamido)methyl] phenoxy}octanoate (**33**). Starting from cesium hydroxide (257 mg, 1.53 mmol), aminooxazole **13** (494 mg, 1.53 mmol), and linker **31** (474 mg, 1.53 mmol), the general procedure gave a residue that was purified by flash chromatography on silica gel eluting with 4:1 EtOAc:Hex that gave **33** as a yellow oil (160 mg, 21%). R_f 0.43 (2.5:1 EtOAc:Hex). ^{1}H NMR ($CDCl_3$, 400 MHz) δ 1.25-1.52 (m, 7H), 1.65 (p, *J* = 6.8 Hz, 2H), 1.77 (p, *J* = 6.9 Hz, 2H), 2.34 (t, *J* = 7.5 Hz, 2H), 3.93 (t, *J* = 6.3 Hz, 2H), 4.48-4.69 (m, 6H), 5.22 (d, *J* = 10.4 Hz, 1H), 5.31 (d, *J* = 17.1 Hz, 1H), 5.90 (ddt, *J* = 17.1, 10.4, 5.4 Hz, 1H), 6.00 (br s, 2H), 6.85 (d, *J* = 8.0 Hz, 2H), 6.96-7.41 (m, 8H); ^{13}C NMR ($CDCl_3$, 100 MHz) δ 24.9, 25.9, 29.0, 29.1, 29.2, 34.2, 49.2, 65.0, 68.0, 114.8, 118.2, 127.6, 128.9, 132.3, 133.3, 138.4, 158.7, 159.5, 161.7, 173.5. HRMS (ESI-TOF) calcd for $C_{29}H_{36}N_3O_5$ $(M+H)^+$: 506.2649, obsd: 506.2656.

General procedure for the synthesis of allyl deprotected aminooxazole-linker derivatives (**34-35**). A 2M aqueous NaOH solution (5 mL) was added to a solution of aminooxazole-linker derivative (**32-33**) (1.00 equiv.) in methanol (5 mL) and THF (2 mL) and the mixture was stirred at rt for 18 h. Concentrated hydrochloric acid was added dropwise to the reaction mixture until it became acidic by pH paper (pH ~3-4). The

aqueous layer was extracted with EtOAc (3 x 10 mL) and the combined organic layers were washed with brine (6 mL), dried over $MgSO_4$, filtered, and concentrated.

Synthesis of 16-{4-[(2-amino-*N*-benzyloxazole-5-carboxamido)methyl]phenoxy} hexadecanoic acid (**34**). Compound **32** (89 mg, 0.144 mmol) gave **34** as a yellow solid (74 mg, 89%) and was taken into the next step without further purification. R_f 0.42 (4:1 EtOAc:Hex). HRMS (ESI-TOF) calcd for $C_{34}H_{48}N_3O_5$ $(M+H)^+$: 578.3588, obsd: 578.3573.

Synthesis of 8-{4-[(2-amino-*N*-benzyloxazole-5-carboxamido)methyl]phenoxy} octanoic acid (**35**). Compound **33** (160 mg, 0.317 mmol) gave **35** as a yellow oil (104 mg, 71%) and was taken into the next step without further purification. R_f 0.23 (4:1 EtOAc:Hex). HRMS (ESI-TOF) calcd for $C_{26}H_{32}N_3O_5$ $(M+H)^+$: 466.2336, obsd: 466.2324.

Synthesis of dual-ligand inhibitor with 15C-linker (**5**). Compound **34** (69 mg, 0.120 mmol, 1.00 equiv.), HOBt (48 mg, 0.359 mmol, 3.00 equiv.), EDC (35 mg, 0.179 mmol, 1.50 equiv.), and triethylamine (50 μL, 36 mg, 0.359 mmol, 3.00 equiv.) were added to a solution of **25** (109 mg, 0.303 mmol, 2.50 equiv.) in dry DMF (3 mL) and the mixture stirred for 20 h under N_2. The mixture was partitioned between EtOAc (15 mL) and water (10 mL). The organic layer was washed with sat'd aq. $NaHCO_3$ (10 mL), brine (10 mL), dried over $MgSO_4$, filtered, concentrated, and purified by flash chromatography on silica gel eluting with 2:1 EtOAc:Hex → 4:1 EtOAc:Hex to give **5** as a yellow solid (21 mg, 19%). R_f 0.70 (92:8 CH_2Cl_2:MeOH). $[\alpha]_D^{24}$ -28.5 (*c* 0.425, MeOH). ^{1}H NMR (CD_3OD, 400 MHz) δ 0.79 (d, *J* = 6.7 Hz, 3H), 0.90 (d, *J* = 6.7 Hz, 3H), 1.16 (d, *J* = 7.3 Hz, 3H), 1.20-1.41 (m, 22H), 1.42-1.52 (m, 2H), 1.53-1.65 (m, 2H), 1.70-1.82 (m, 2H),

2.11-2.29 (m, 2H), 2.32-2.47 (m, 1H), 2.63-2.93 (m, 3H), 3.06-3.20 (m, 1H), 3.95 (t, *J* = 5.9 Hz, 2H), 4.63 (s, 2H), 4.68 (s, 2H), 4.76 (d, *J* = 4.5 Hz, 1H), 5.28-5.43 (m, 1H), 6.80-6.91 (m, 2H), 7.05-7.40 (m, 13H). HRMS (ESI-TOF) calcd for $C_{53}H_{71}N_6O_8$ $(M+H)^+$: 919.5328, obsd: 919.5344.

Synthesis of dual-ligand inhibitor with 7C-linker (**6**). Compound **35** (104 mg, 0.224 mmol, 1.20 equiv.) was added to a solution of **25** (67 mg, 0.186 mmol, 1.00 equiv.) in dry DMF (3.0 mL) at 0 °C. HATU (85 mg, 0.224 mmol, 1.20 equiv.) was added to the solution and the mixture began stirring under N_2. A solution of *N*,*N*-diisopropylethylamine (97 μL, 72 mg, 0.559 mmol, 3.00 equiv.) in dry DMF (1.0 mL) was added dropwise to the reaction over 1 h at 0 °C. The reaction was stirred for an additional 30 min at 0 °C before allowing reaction to warm to rt where stirring was continued for 20 h under N_2. The solvent was removed *in vacuo* and the mixture was partitioned between EtOAc (10 mL) and water (10 mL). The organic layer was washed with sat'd aq. $NaHCO_3$ (10 mL) and brine (10 mL), dried over $MgSO_4$, filtered, concentrated, and purified by flash chromatography on silica gel eluting with 4:1 EtOAc:Hex → 100% EtOAc to give **6** as a yellow oil (26 mg, 17%). R_f 0.59 (92:8 CH_2Cl_2:MeOH). $[\alpha]_D^{24}$ -22.1 (*c* 1.17, MeOH). ^{1}H NMR (CD_3OD, 500 MHz) δ 0.74 (d, *J* = 6.7 Hz, 3H), 0.84 (d, *J* = 6.7 Hz, 3H), 1.11 (d, *J* = 7.4 Hz, 3H), 1.21-1.36 (m, 7H), 1.37-1.47 (m, 2H), 1.48-1.60 (m, 2H), 1.62-1.77 (m, 2H), 2.08-2.24 (m, 2H), 2.30-2.41 (m, 1H), 2.71-2.84 (m, 2H), 3.02-3.15 (m, 1H), 3.29 (s, 1H), 3.78-3.97 (m, 2H), 4.57 (s, 2H), 4.63 (s, 2H), 4.72 (d, *J* = 4.8 Hz, 1H), 5.24-5.39 (m, 1H), 6.83 (d, *J* = 7.4 Hz, 2H), 7.04-7.40 (m, 13H). HRMS (ESI-TOF) calcd for $C_{45}H_{55}N_6O_8$ $(M+H)^+$: 807.4076, obsd: 807.4077.

2.4.2 Kinetic Assays

Acetyl-CoA carboxylase was purified according to Broussard *et al*. from a strain of *E. coli* that overexpresses the four genes that encode the enzyme.[20] The activity of acetyl-CoA carboxylase was determined spectrophotometrically by measuring the production of ADP using pyruvate kinase and lactate dehydrogenase and following the oxidation of NADH at 340 nm. Each reaction mixture contained 17.5 units of lactate dehydrogenase, 10.5 units of pyruvate kinase, 0.5 mM phosphoenolpyruvate, 0.2 mM NADH, 20 mM $MgCl_2$, 15 mM potassium bicarbonate, and 100 mM HEPES (pH 8.0). For reactions measuring the effects of inhibition versus ATP, each reaction contained a concentration of 0.2 mM acetyl-CoA, with ATP concentrations ranging from 0.8 μM to 56 μM. For reactions measuring the effects of inhibition versus acetyl-CoA, each reaction contained a concentration of 5 μM ATP, with acetyl-CoA concentrations ranging from 50 μM to 1000 μM. All reactions were conducted in a total of 0.5 mL in a 1 cm pathlength quartz cuvette and all reactions were initiated by the addition of enzyme. Spectrophotometric data were collected using an Agilent Cary 60 UV-Vis spectrophotometer interfaced with a personal computer with a data acquisition program.

2.4.3 Kinetic Analysis

Data were analyzed by nonlinear regression using the computer programs of Cleland.[41] Data describing competitive inhibition were fitted to Eq. 1, where v is the initial velocity, V is the maximal velocity, K_m is the Michaelis constant, I is the concentration of the inhibitor, and K_{is} is the slope inhibition constant.

Eq. 1 $$v = \frac{VA}{K_m\left(1+\frac{I}{K_{is}}\right)+A}$$

Data describing noncompetitive inhibition were fitted to Eq. 2, where v is the initial velocity, V is the maximal velocity, K_m is the Michaelis constant, I is the concentration of the inhibitor, and K_{is} and K_{ii} are the slope and intercept inhibition constants, respectively.

Eq. 2 $$v = \frac{VA}{K_m\left(1+\frac{I}{K_{is}}\right)+A\left(1+\frac{I}{K_{ii}}\right)}$$

2.4.4 Determination of MICs

Determination of MICs was conducted by Dr. Gregory Robertson at UT Southwestern Medical Center (Dallas, TX) in accordance with the Clinical and Laboratory Standards Institute (CLSI) methodology using the broth microdilution methods with cation-adjusted Mueller Hinton (MHII) medium.[42] The strains tested were used with permission from the strain collection of TenNor Therapeutics. Test organisms were streaked onto agar medium and incubated overnight at 35 °C. Experimental compounds were tested over a concentration range prepared by two-fold serial dilution after solubilizing compounds in 100% DMSO (or sterile water for gentamicin and kanamycin) to achieve a final stock concentration of 10 mg/L. A standardized inoculum of 5 x 10^5 CFU/mL in a volume of 0.1 mL was incubated with antibiotic for 18-24 h at 35 °C. The MIC was scored visually as the lowest concentration of antibiotic where no growth is apparent by visual inspection for turbidity.

2.4.5 Sensitization Assay using PMBN

A culture of *E. coli* strain JM109 was grown overnight in Luria broth (LB) at 37 °C. Culture tubes containing 2 mL of fresh LB media were inoculated with 10 μL of the saturated *E. coli* culture. Polymyxin B nonapeptide (PMBN) was dissolved in water to

achieve a 1 mM stock and inoculated into the tubes to generate final concentrations of 0.5, 1, 5, and 10 μg/mL. Dual-ligand **5** was dissolved in 100% DMSO to achieve a 5 mM stock solution and inoculated into the tubes to generate final concentrations of 1, 10, 50, and 100 μM. After inoculation, the culture tubes were incubated for 4 hours at 37 °C. Optical density (OD) readings were measured at 600 nm in 1 mL plastic cuvettes. Spectrophotometric data were collected using an Agilent Cary 60 UV-Vis spectrophotometer.

2.4.6 Generation of Spontaneous Resistant Mutant Strains and Resistance Studies

Single-step spontaneous resistance selections were undertaken by Dr. Gregory Robertson at UT Southwestern Medical Center on agar medium using overnight saturated cultures grown in cation-adjusted Mueller Hinton (MHII). Briefly, compounds were added to molten MHII agar after allowing time to cool to 55 °C. Compounds were dosed in two-fold increasing concentrations starting at 1x MIC. The test organism was grown overnight to saturation in MHII broth. The cells were concentrated by centrifugation and the viable number of CFU plated was determined by serial dilution and plating. Each drug plate received a total of 4×10^9 CFU/plate (i.e., 0.1 mL plated of 4×10^{10} CFU/mL in the concentrated culture). Plates were monitored for the appearance of drug-resistant colonies. For selection of spontaneous moiramide-resistance in the wild-type *S. aureus* and *E. coli tolC* backgrounds, moiramide was dosed at ~2x to 8x their respective MICs and potential drug-resistant isolates were evaluated after secondary passage through a drug-free intermediate. Stable moiramide-resistance was verified by broth microdilution MIC assays, as above. The mutant prevention concentration (MPC) was defined as the

lowest consecutive drug concentration capable of fully suppressing the emergence of antibiotic-resistant bacterial subpopulations.[43]

2.5 REFERENCES

(1) CDC. Antibiotic Resistance Threats in the United States, 2013. Atlanta, Georgia: U.S. Department of Health and Human Services, CDC, **2013**.

(2) Heath, R. J.; Rock, C. O., Fatty acid biosynthesis as a target for novel antibacterials. *Curr. Opin. Investig. Drugs* **2004,** *5*, 146-153.

(3) Zhang, Y. M.; White, S. W.; Rock, C. O., Inhibiting bacterial fatty acid synthesis. *J. Biol. Chem.* **2006,** *281*, 17541-17544.

(4) Campbell, J. W.; Cronan, J. E., Jr., Bacterial fatty acid biosynthesis: targets for antibacterial drug discovery. *Annu. Rev. Microbiol.* **2001,** *55*, 305-332.

(5) Cronan, J. E., Jr.; Waldrop, G. L., Multi-subunit acetyl-CoA carboxylases. *Prog. Lipid Res.* **2002,** *41*, 407-435.

(6) Tanabe, T.; Wada, K.; Okazaki, T.; Numa, S., Acetyl-coenzyme-A carboxylase from rat liver. Subunit structure and proteolytic modification. *Eur. J. Biochem.* **1975,** *57*, 15-24.

(7) Rock, C. O.; Cronan, J. E., *Escherichia coli* as a model for the regulation of dissociable (type II) fatty acid biosynthesis. *Biochim. Biophys. Acta* **1996,** *1302*, 1-16.

(8) Heath, R. J.; White, S. W.; Rock, C. O., Inhibitors of fatty acid synthesis as antimicrobial chemotherapeutics. *Appl. Microbiol. Biotechnol.* **2002,** *58*, 695-703.

(9) Miller, J. R.; Dunham, S.; Mochalkin, I.; Banotai, C.; Bowman, M.; Buist, S.; Dunkle, B.; Hanna, D.; Harwood, H. J.; Huband, M. D.; Karnovsky, A.; Kuhn, M.; Limberakis, C.; Liu, J. Y.; Mehrens, S.; Mueller, W. T.; Narasimhan, L.; Ogden, A.; Ohren, J.; Prasad, J. V.; Shelly, J. A.; Skerlos, L.; Sulavik, M.; Thomas, V. H.; VanderRoest, S.; Wang, L.; Wang, Z.; Whitton, A.; Zhu, T.; Stover, C. K., A class of selective antibacterials derived from a protein kinase inhibitor pharmacophore. *Proc. Natl. Acad. Sci. USA* **2009,** *106*, 1737-1742.

(10) Mochalkin, I.; Miller, J. R.; Narasimhan, L.; Thanabal, V.; Erdman, P.; Cox, P. B.; Prasad, J. V.; Lightle, S.; Huband, M. D.; Stover, C. K., Discovery of antibacterial biotin carboxylase inhibitors by virtual screening and fragment-based approaches. *ACS Chem. Biol.* **2009,** *4*, 473-483.

(11) Needham, J.; Kelly, M. T.; Ishige, M.; Andersen, R. J., Andrimid and moiramides A-C, metabolites produced in culture by a marine isolate of the bacterium

Pseudomonas fluorescens: Structure elucidation and biosynthesis. *J. Org. Chem.* **1994,** *59*, 2058-2063.

(12) Freiberg, C.; Brunner, N. A.; Schiffer, G.; Lampe, T.; Pohlmann, J.; Brands, M.; Raabe, M.; Habich, D.; Ziegelbauer, K., Identification and characterization of the first class of potent bacterial acetyl-CoA carboxylase inhibitors with antibacterial activity. *J. Biol. Chem.* **2004,** *279*, 26066-26073.

(13) Pohlmann, J.; Lampe, T.; Shimada, M.; Nell, P. G.; Pernerstorfer, J.; Svenstrup, N.; Brunner, N. A.; Schiffer, G.; Freiberg, C., Pyrrolidinedione derivatives as antibacterial agents with a novel mode of action. *Bioorg. Med. Chem. Lett.* **2005,** *15*, 1189-1192.

(14) Blanchard, C. Z.; Waldrop, G. L., Overexpression and kinetic characterization of the carboxyltransferase component of acetyl-CoA carboxylase. *J. Biol. Chem.* **1998,** *273*, 19140-19145.

(15) Li, S. J.; Cronan, J. E., Jr., Growth rate regulation of *Escherichia coli* acetyl coenzyme A carboxylase, which catalyzes the first committed step of lipid biosynthesis. *J. Bacteriol.* **1993,** *175*, 332-340.

(16) Silver, L. L., Multi-targeting by monotherapeutic antibacterials. *Nat. Rev. Drug Discov.* **2007,** *6*, 41-55.

(17) Pokrovskaya, V.; Baasov, T., Dual-acting hybrid antibiotics: a promising strategy to combat bacterial resistance. *Expert Opin. Drug Discov.* **2010,** *5*, 883-902.

(18) O'Connell, K. M.; Hodgkinson, J. T.; Sore, H. F.; Welch, M.; Salmond, G. P.; Spring, D. R., Combating multidrug-resistant bacteria: Current strategies for the discovery of novel antibacterials. *Angew. Chem. Int. Ed. Engl.* **2013**, 10706-10733.

(19) East, S. P.; Silver, L. L., Multitarget ligands in antibacterial research: progress and opportunities. *Expert Opin. Drug Discov.* **2013,** *8*, 143-156.

(20) Broussard, T. C.; Price, A. E.; Laborde, S. M.; Waldrop, G. L., Complex formation and regulation of *Escherichia coli* acetyl-CoA carboxylase. *Biochemistry* **2013,** *52*, 3346-3357.

(21) Li, H. Q.; Yan, T.; Yang, Y.; Shi, L.; Zhou, C. F.; Zhu, H. L., Synthesis and structure-activity relationships of *N*-benzyl-*N*-(X-2-hydroxybenzyl)-*N*'-phenylureas and thioureas as antitumor agents. *Bioorg. Med. Chem.* **2010,** *18*, 305-313.

(22) McWhorter, W.; Fredenhagen, A.; Nakanishi, K.; Komura, H., Stereocontrolled synthesis of andrimid and a structural requirement for the activity. *J. Chem. Soc., Chem. Commun.* **1989**, 299-301.

(23) Rama Rao, A. V.; Singh, A. K.; Varaprasad, C. V. N. S., A convenient diastereoselective total synthesis of andrimid. *Tetrahedron Lett.* **1991,** *32*, 4393-4396.

(24) Davies, S. G.; Dixon, D. J., Asymmetric syntheses of moiramide B and andrimid. *J. Chem. Soc., Perkin Trans. 1* **1998**, 2635-2643.

(25) Fredenhagen, A.; Tamura, S. Y.; Kenny, P. T. M.; Komura, H.; Naya, Y.; Nakanishi, K.; Niegyama, K.; Sugiura, M.; Kita, H., Andrimid, a new peptide antibiotic produced by an intracellular bacterial symbiont isolated from a brown planthopper. *J. Am. Chem. Soc.* **1987,** *109*, 4409-4411.

(26) Midgley, G.; Thomas, C. B., Selectivity of radical formation in the reaction of carbonyl-compounds with manganese (III) acetate. *J. Chem. Soc., Perkin Trans. 2* **1987**, 1103-1108.

(27) Bailey, P. D.; Morgan, K. M.; Smith, D. I.; Vernon, J. M., Spiro cyclisations of *N*-acyliminium ions involving an aromatic π-nucleophile. *Tetrahedron Lett.* **2003,** *59*, 3369-3378.

(28) Robin, S.; Zhu, J.; Galons, H.; Pham-Huy, C.; Claude, J. R.; Tomas, A.; Viossat, B., A convenient asymmetric synthesis of thalidomide. *Tetrahedron: Asymmetry* **1995,** *6*, 1249-1252.

(29) Aron, Z. D.; Overman, L. E., Total synthesis and properties of the crambescidin core zwitterionic acid and crambescidin 359. *J. Am. Chem. Soc.* **2005,** *127*, 3380-3390.

(30) Jobron, L.; Hummel, G., Solid-phase synthesis of new S-glycoamino acid building blocks. *Org. Lett.* **2000,** *2*, 2265-2267.

(31) Zhang, Q.; Wu, Y.; Wang, L.; Hu, B.; Li, P.; Liu, F., Effect of hapten structures on specific and sensitive enzyme-linked immunosorbent assays for *N*-methylcarbamate insecticide metolcarb. *Anal. Chim. Acta* **2008,** *625*, 87-94.

(32) Bennett, B. D.; Kimball, E. H.; Gao, M.; Osterhout, R.; Van Dien, S. J.; Rabinowitz, J. D., Absolute metabolite concentrations and implied enzyme active site occupancy in *Escherichia coli*. *Nat. Chem. Biol.* **2009,** *5*, 593-599.

(33) Freiberg, C.; Pohlmann, J.; Nell, P. G.; Endermann, R.; Schuhmacher, J.; Newton, B.; Otteneder, M.; Lampe, T.; Habich, D.; Ziegelbauer, K., Novel bacterial acetyl coenzyme A carboxylase inhibitors with antibiotic efficacy *in vivo*. *Antimicrob. Agents Chemother.* **2006,** *50*, 2707-2712.

(34) Robertson, G. T.; Bonventre, E. J.; Doyle, T. B.; Du, Q.; Duncan, L.; Morris, T. W.; Roche, E. D.; Yan, D.; Lynch, A. S., In vitro evaluation of CBR-2092, a novel rifamycin-quinolone hybrid antibiotic: microbiology profiling studies with

staphylococci and streptococci. *Antimicrob. Agents Chemother.* **2008,** *52*, 2324-2334.

(35) Viljanen, P.; Vaara, M., Susceptibility of Gram-negative bacteria to polymyxin B nonapeptide. *Antimicrob. Agents Chemother.* **1984,** *25*, 701-705.

(36) Tsubery, H.; Ofek, I.; Cohen, S.; Eisenstein, M.; Fridkin, M., Modulation of the hydrophobic domain of polymyxin B nonapeptide: effect on outer-membrane permeabilization and lipopolysaccharide neutralization. *Mol. Pharmacol.* **2002,** *62*, 1036-1042.

(37) Zavascki, A. P.; Goldani, L. Z.; Li, J.; Nation, R. L., Polymyxin B for the treatment of multidrug-resistant pathogens: a critical review. *J. Antimicrob. Chemother.* **2007,** *60*, 1206-1215.

(38) Velkov, T.; Roberts, K. D.; Nation, R. L.; Wang, J.; Thompson, P. E.; Li, J., Teaching 'old' polymyxins new tricks: new-generation lipopeptides targeting Gram-negative 'superbugs'. *ACS Chem. Biol.* **2014,** *9*, 1172-1177.

(39) Zhao, X.; Drlica, K., Restricting the selection of antibiotic-resistant mutant bacteria: measurement and potential use of the mutant selection window. *J. Infect. Dis.* **2002,** *185*, 561-565.

(40) Brylinski, M.; Waldrop, G. L., Computational redesign of bacterial biotin carboxylase inhibitors using structure-based virtual screening of combinatorial libraries. *Molecules* **2014,** *19*, 4021-4045.

(41) Cleland, W. W., Statistical analysis of enzyme kinetic data. *Methods Enzymol.* **1979,** *63*, 103-138.

(42) Clinical and Laboratory Standards Institute. **2006**. Methods for dilution antimicrobial susceptibility tests for bacteria that grow aerobically, approved standard, 7th ed. CLSI document M7-A7, vol. 26, no. 2. Clinical and Laboratory Standards Institute, Wayne, PA.

(43) Drlica, K., The mutant selection window and antimicrobial resistance. *J. Antimicrob. Chemother.* **2003,** *52*, 11-17.

2.6 SPECTRA

^{1}H NMR of Compound **9**

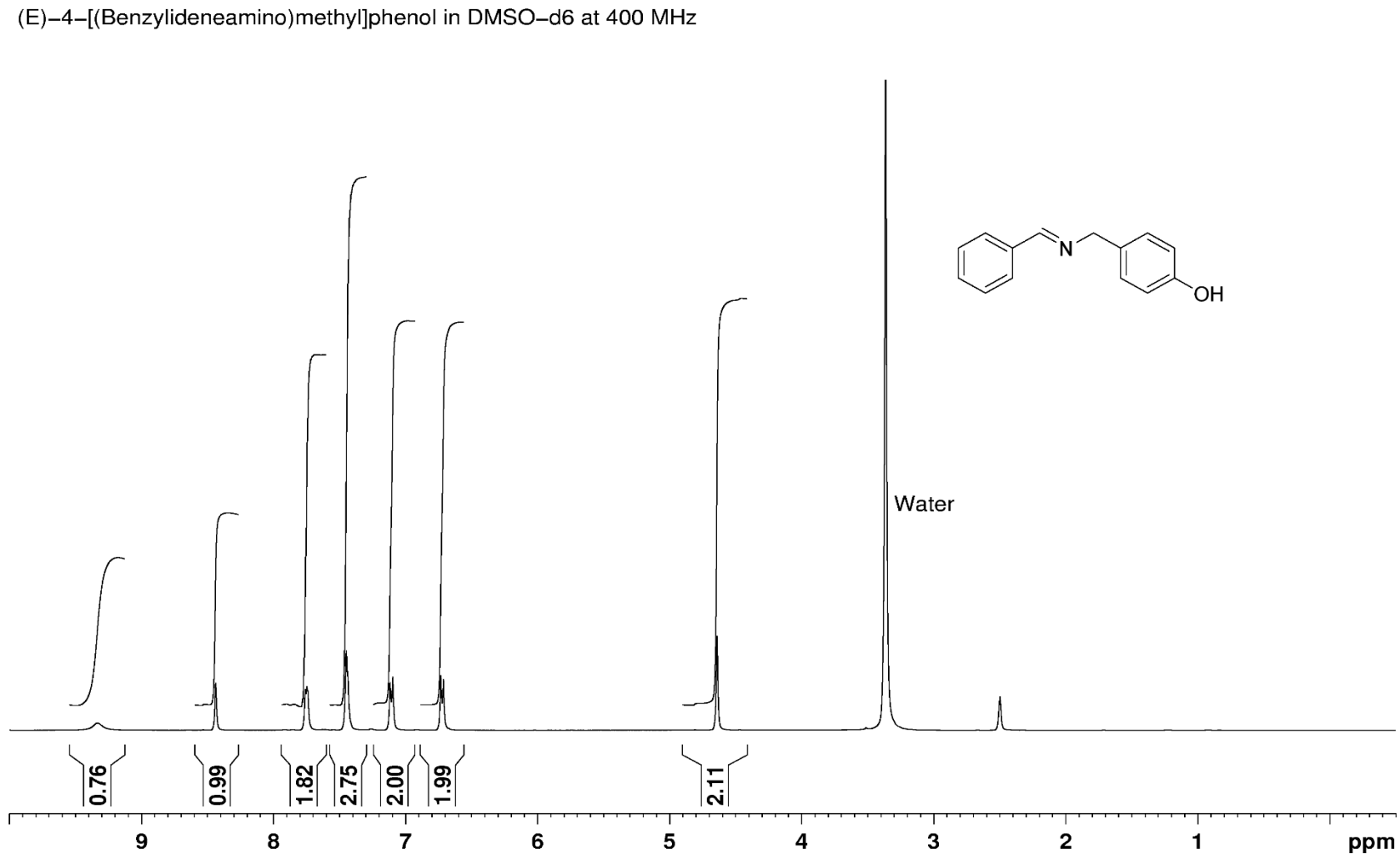

^{13}C NMR of Compound **9**

(E)−4−[(Benzylideneamino)methyl]phenol in DMSO−d6 at 100 MHz

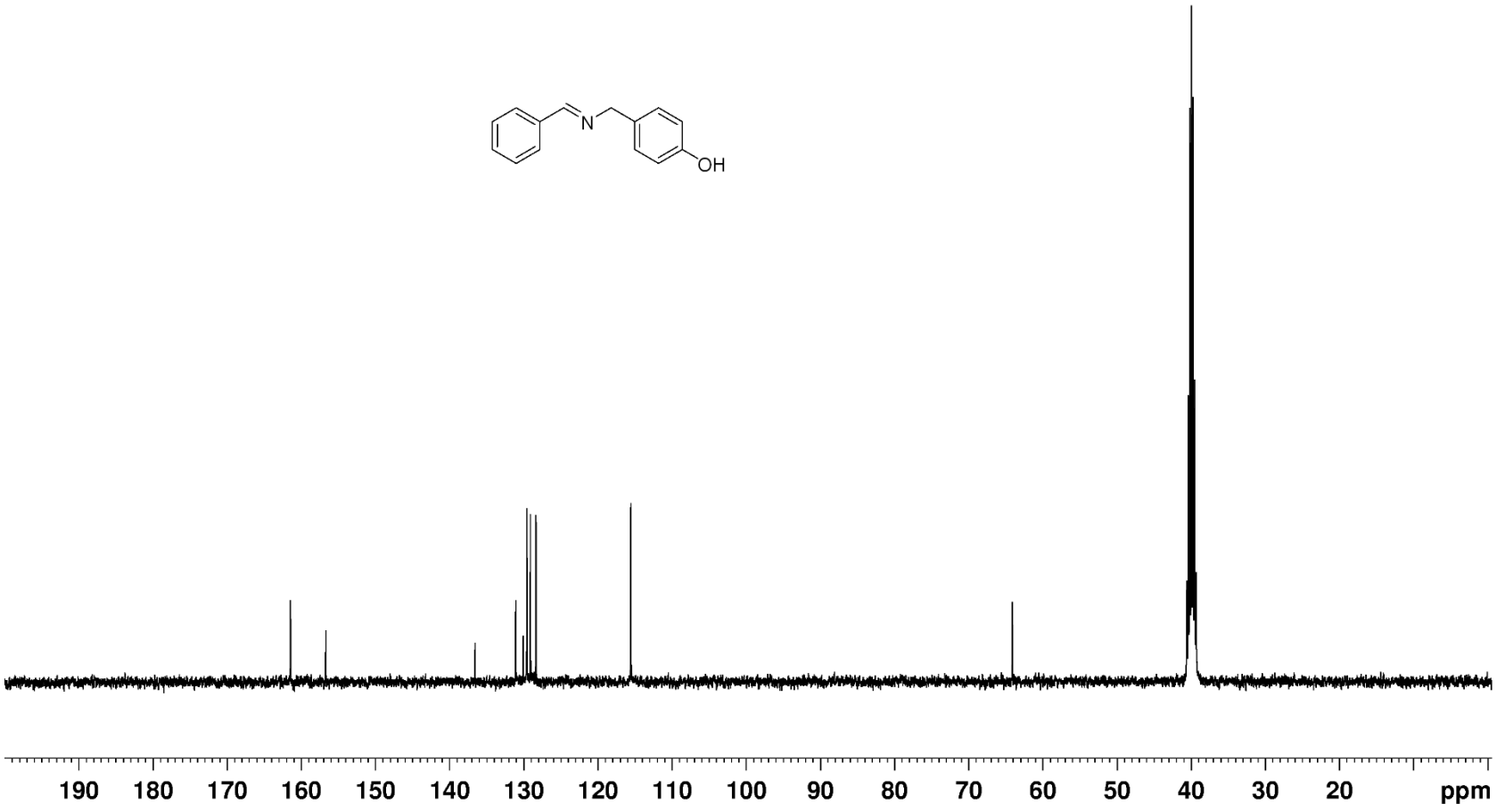

^{1}H NMR of Compound **10**

4–[(Benzylamino)methyl]phenol in acetone–d6 at 400 MHz

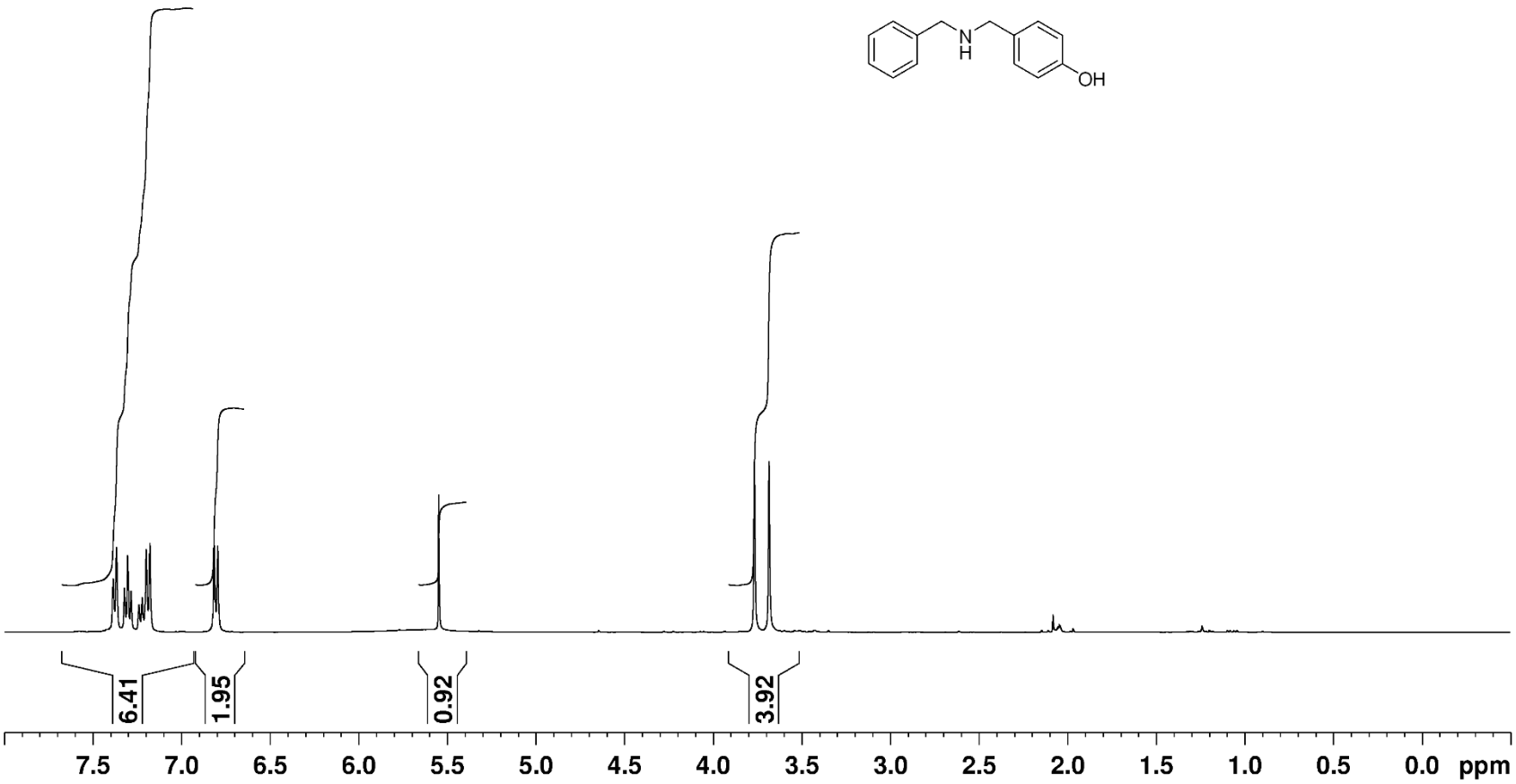

^{13}C NMR of Compound **10**

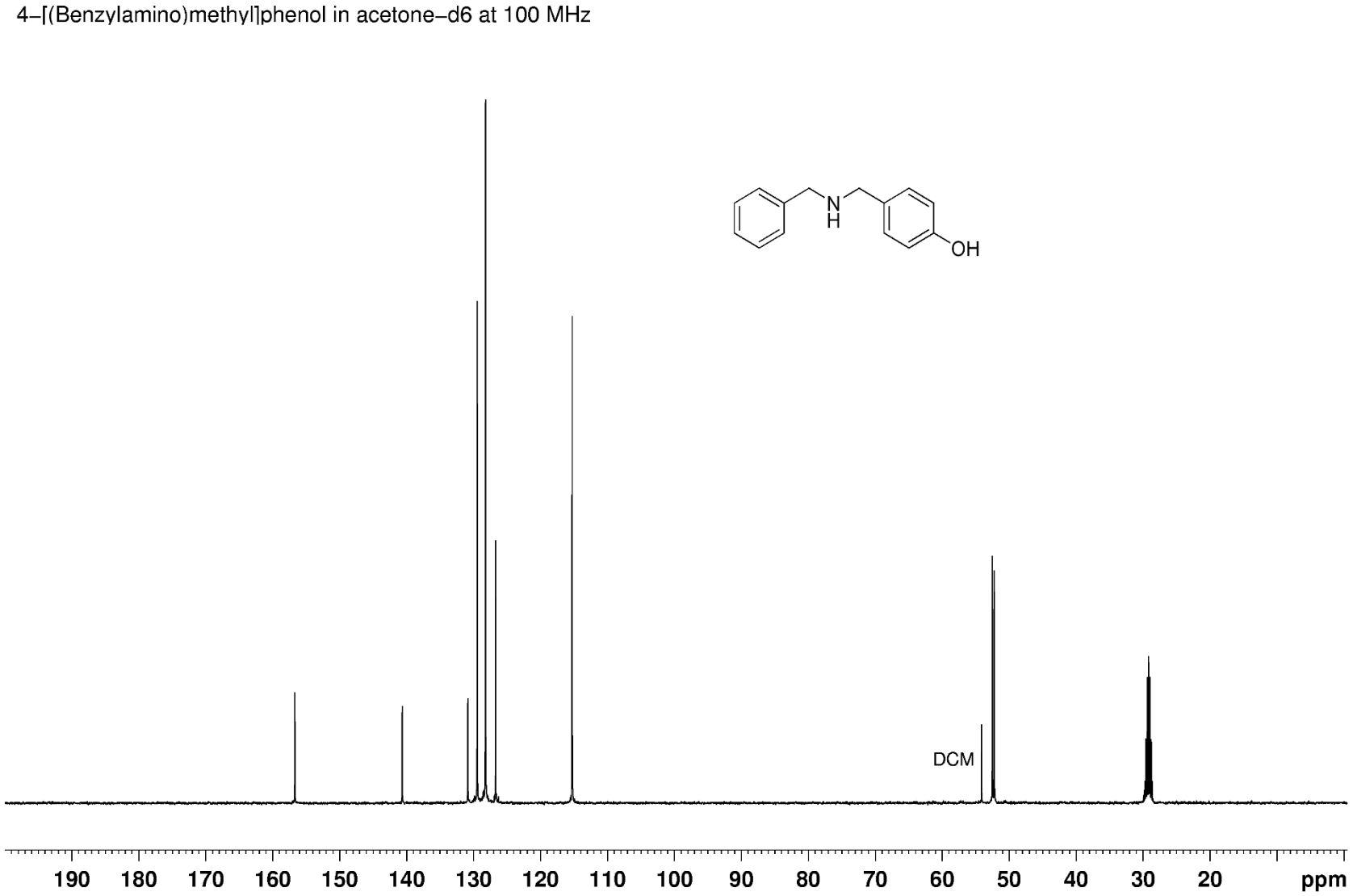

^{1}H NMR of Compound **12**

2–Aminooxazole–5–carboxylic acid in DMSO–d6 at 400 MHz

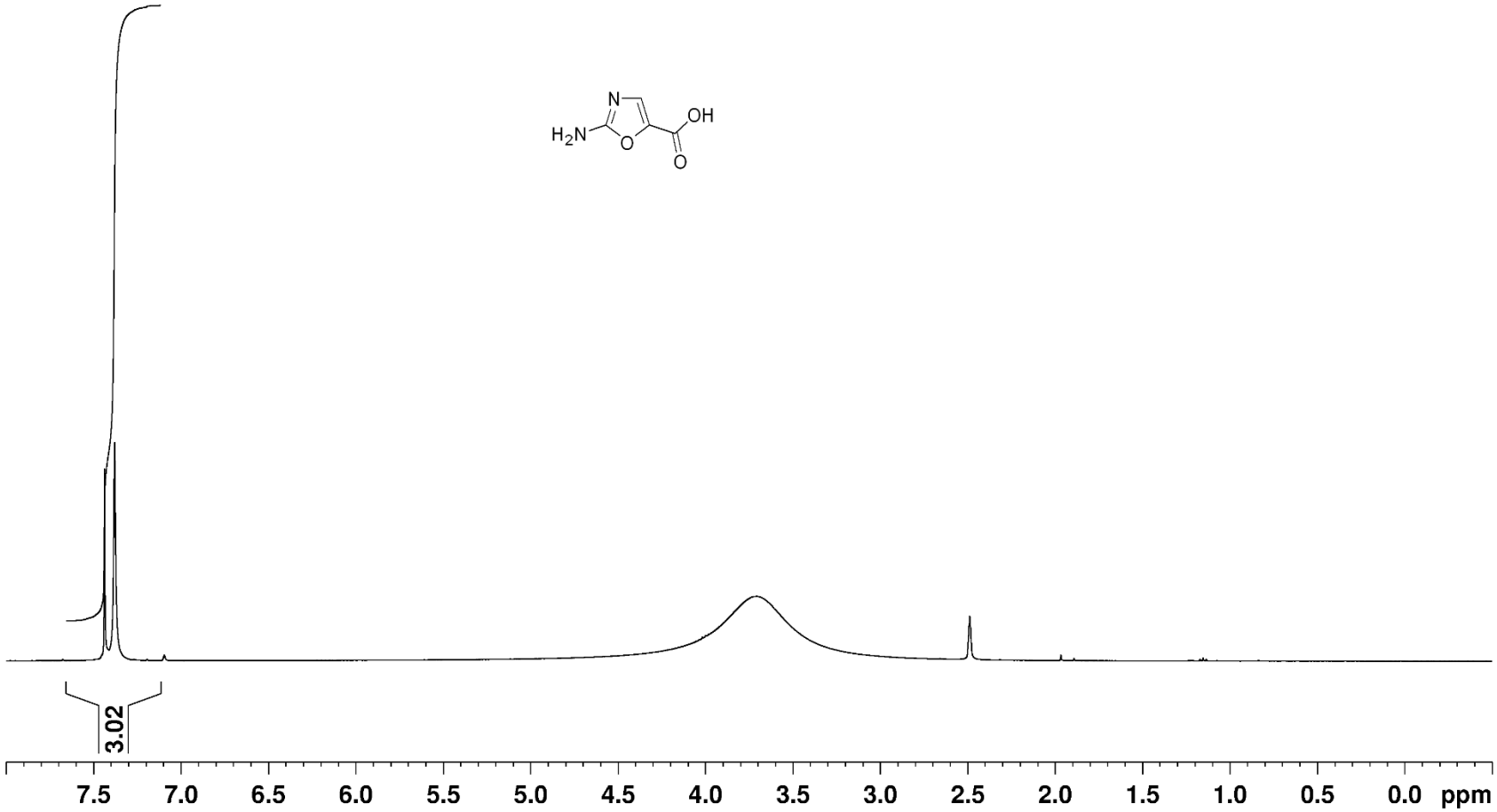

^{13}C NMR of Compound **12**

2–Aminooxazole–5–carboxylic acid in DMSO–d6 at 100 MHz

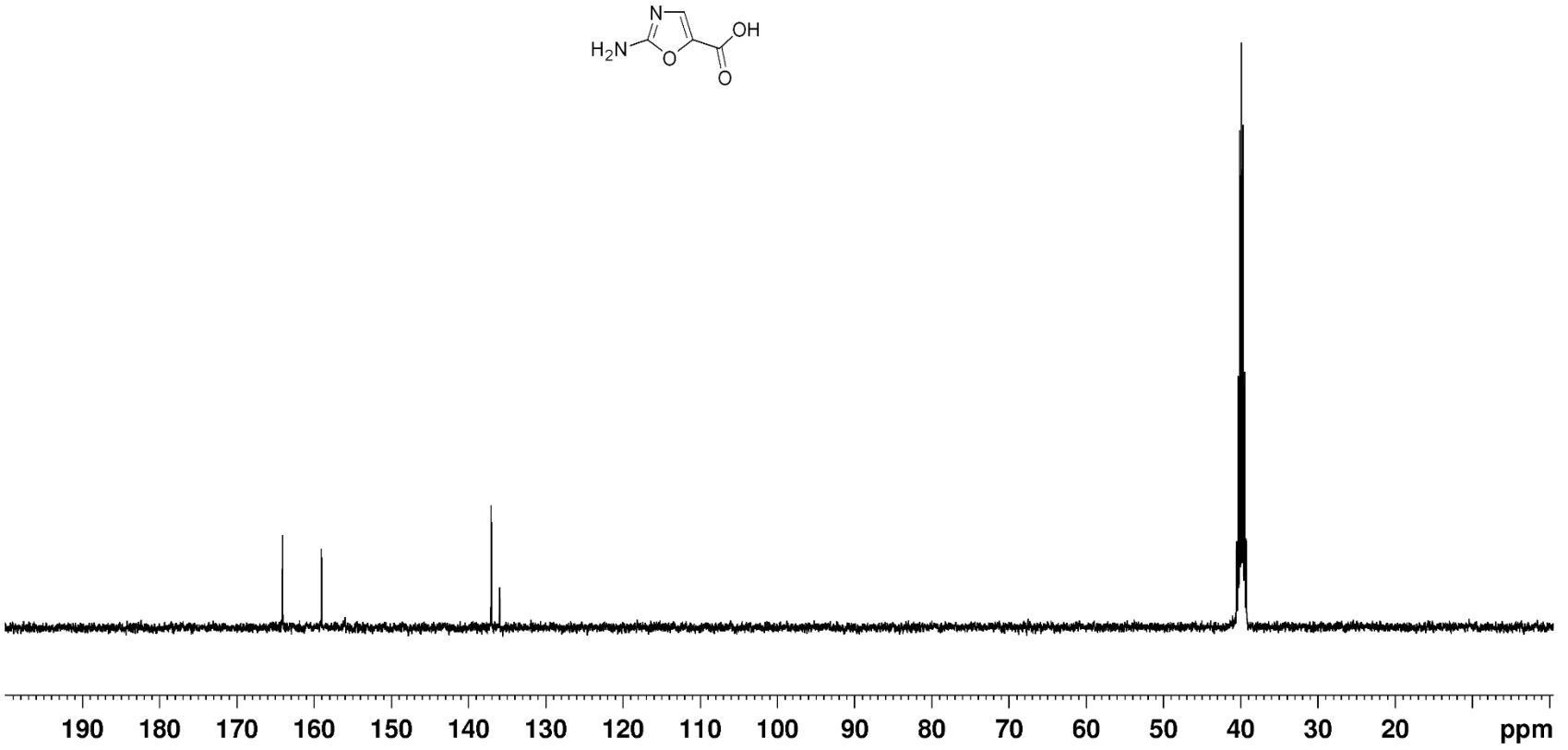

^{1}H NMR of Compound **2**

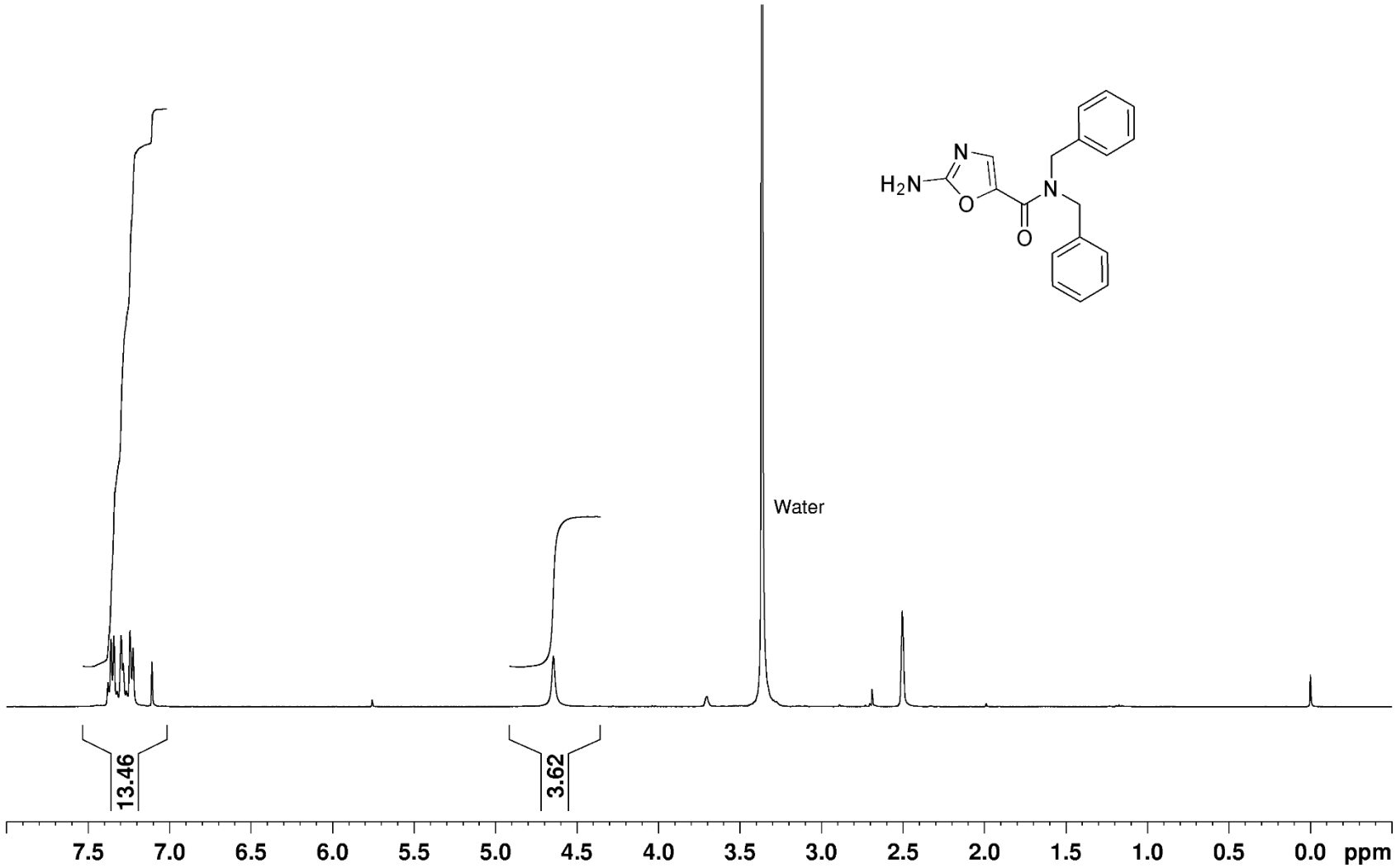

^{13}C NMR of Compound **2**

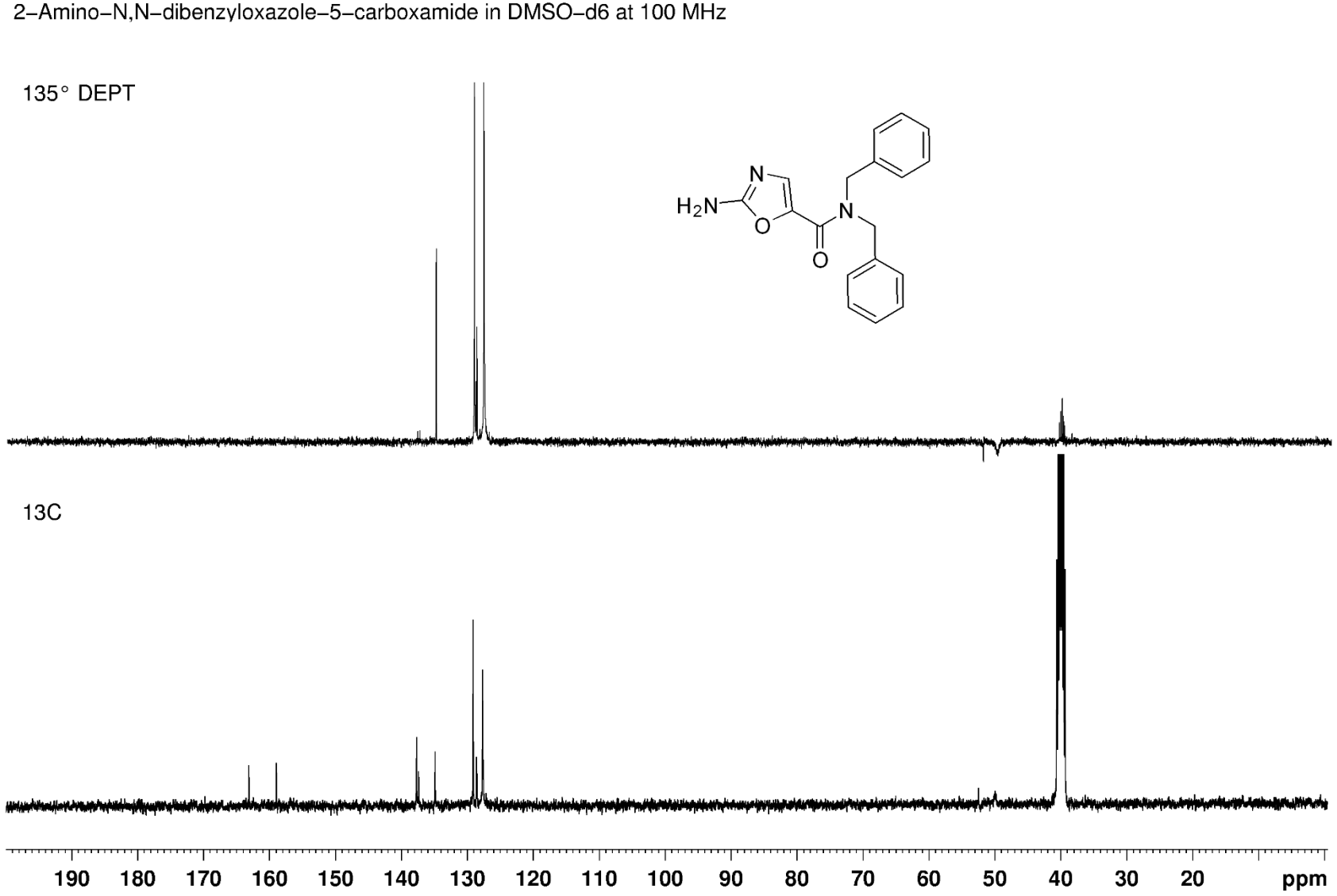

^{1}H NMR of Compound **13**

2–Amino–N–benzyl–N–(4–hydroxybenzyl)oxazole–5–carboxamide in DMSO–d6 at 400 MHz

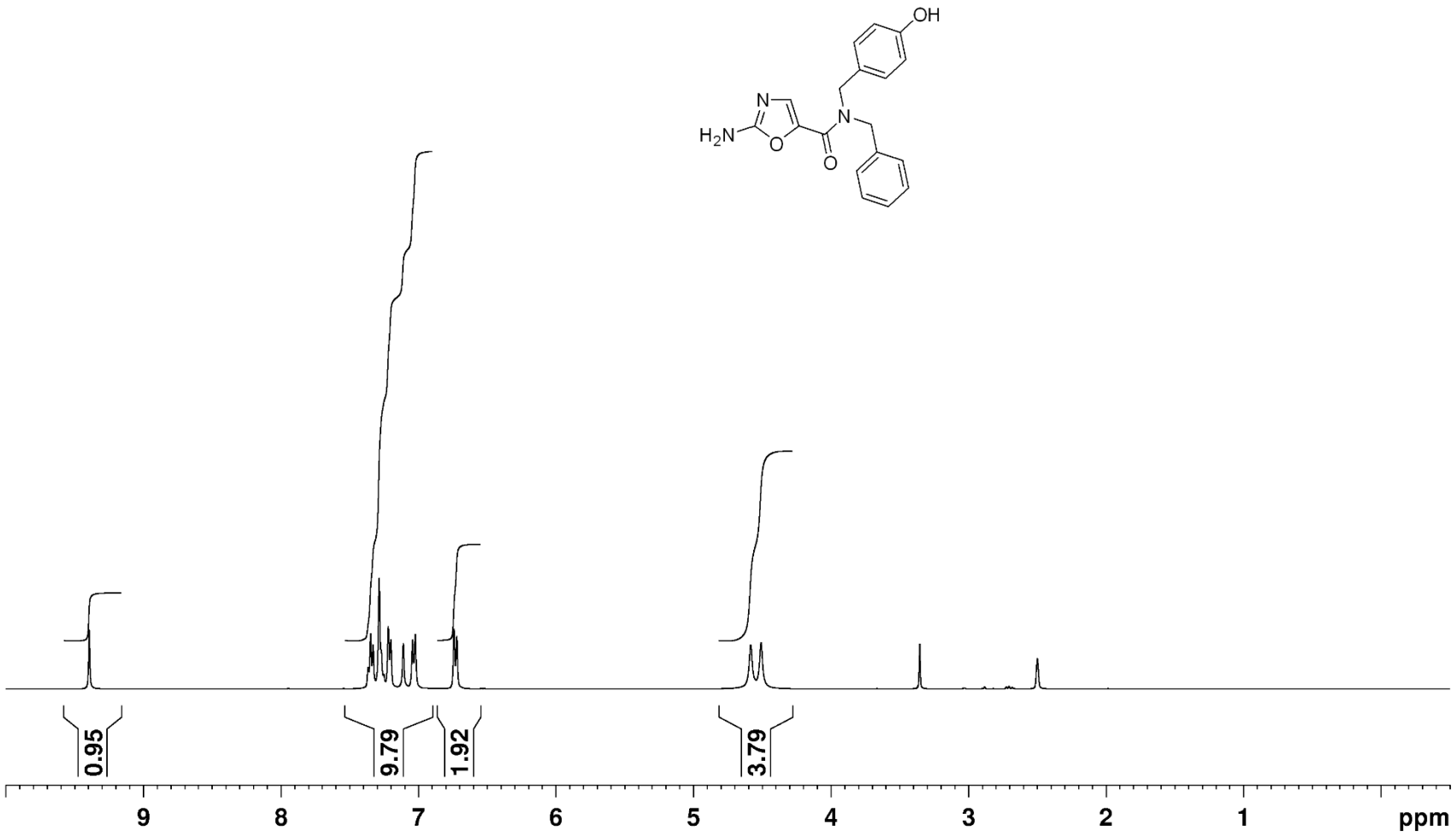

^{13}C NMR of Compound **13**

2–Amino–N–benzyl–N–(4–hydroxybenzyl)oxazole–5–carboxamide in DMSO–d6 at 100 MHz

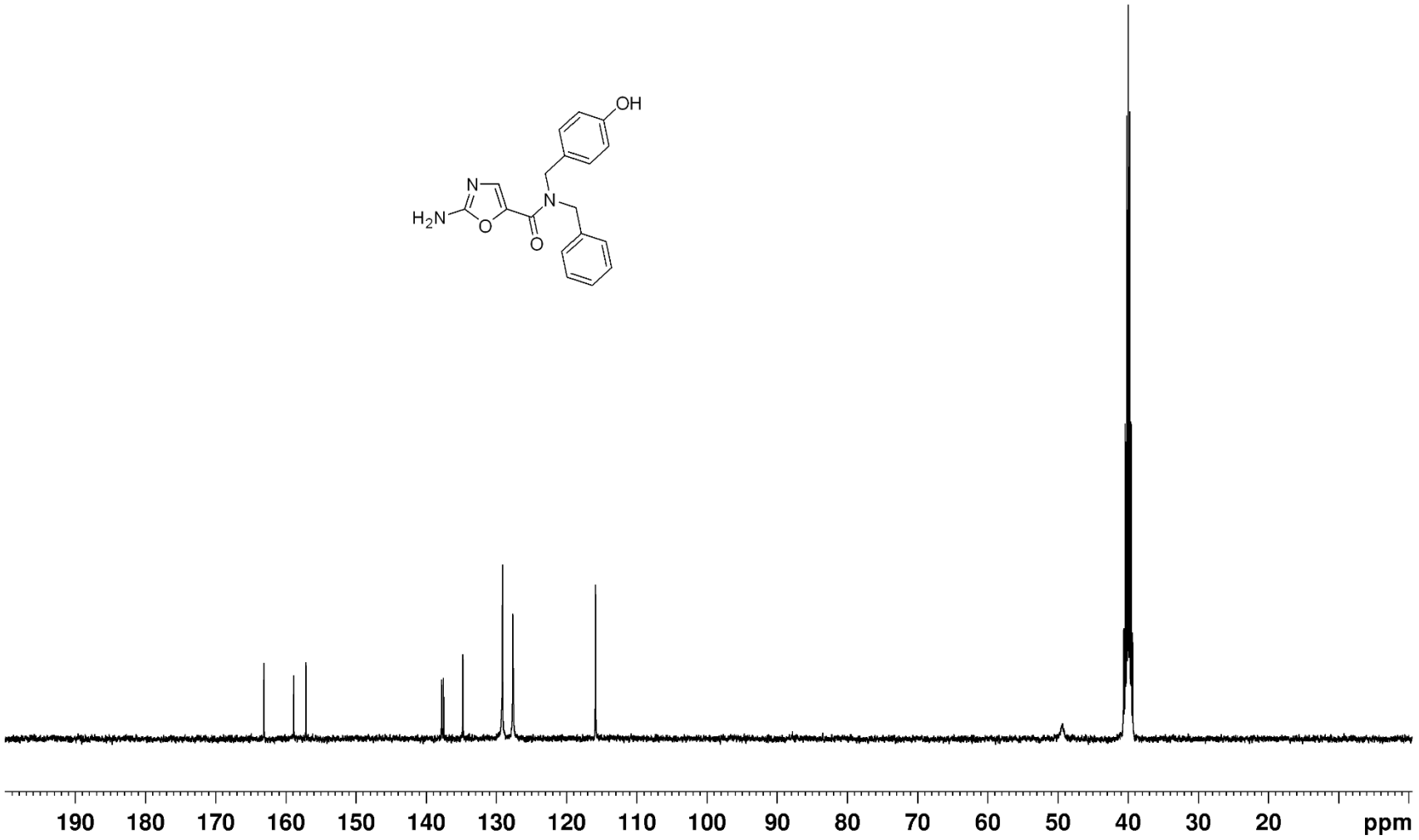

^{1}H NMR of Compound **15**

(4S)−Methyl−succinic anhydride in CDCl3 at 400 MHz

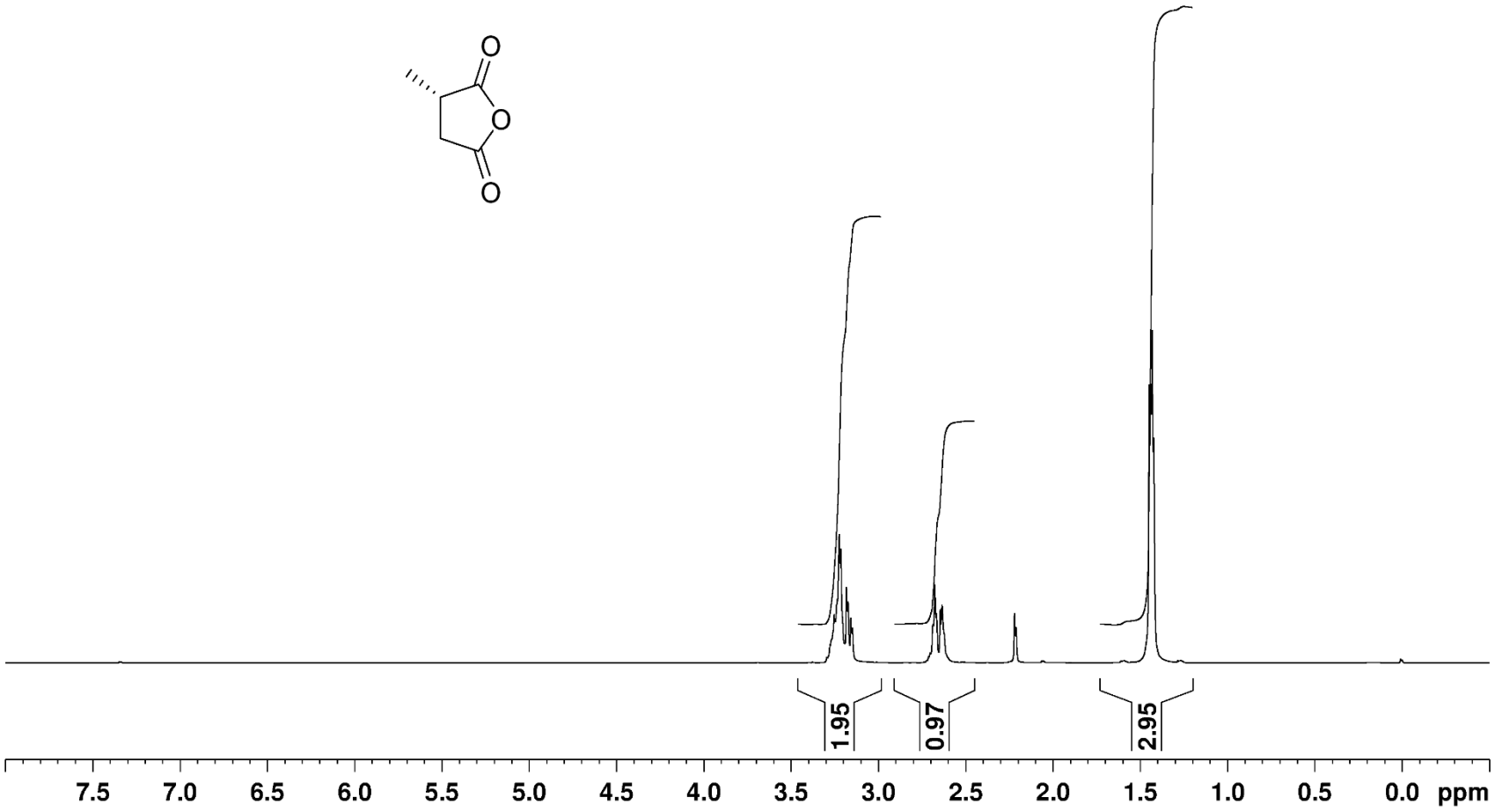

^{13}C NMR of Compound **15**

(4S)–Methyl–succinic anhydride in CDCl3 at 100 MHz

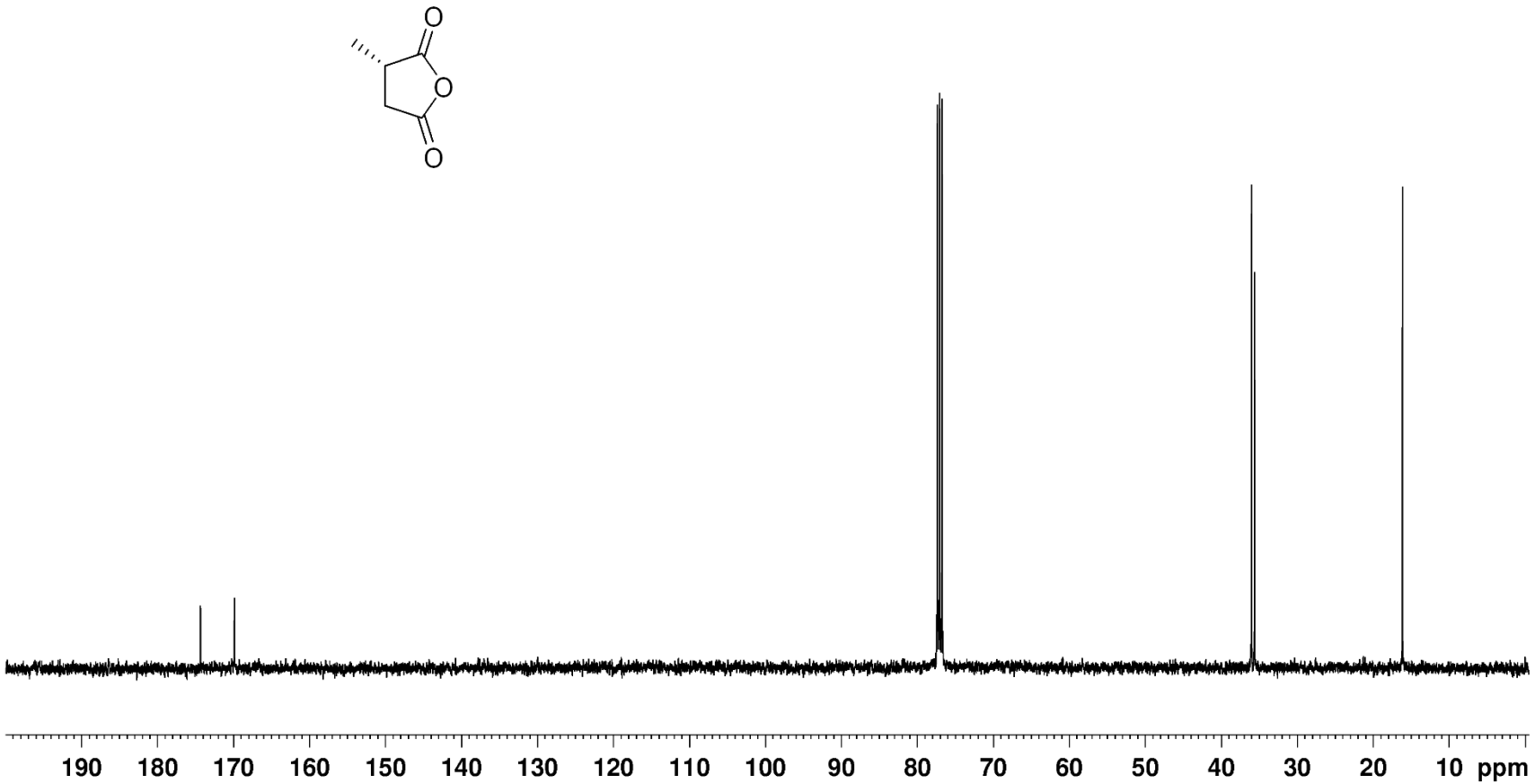

^{1}H NMR of Compound **20**

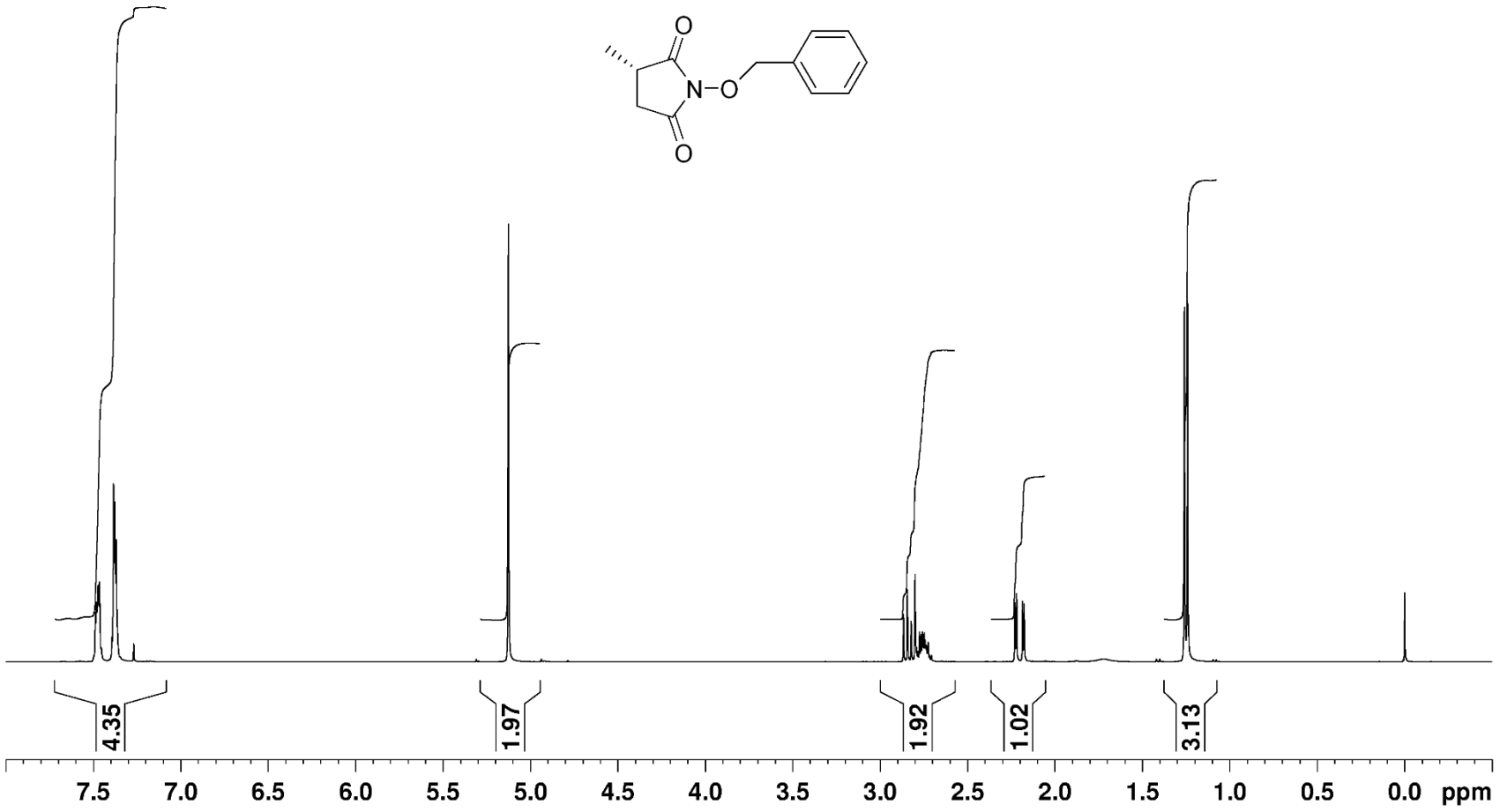

^{13}C NMR of Compound **20**

(4S)–Methyl–N–O–benzylsuccinimide in CDCl3 at 100 MHz

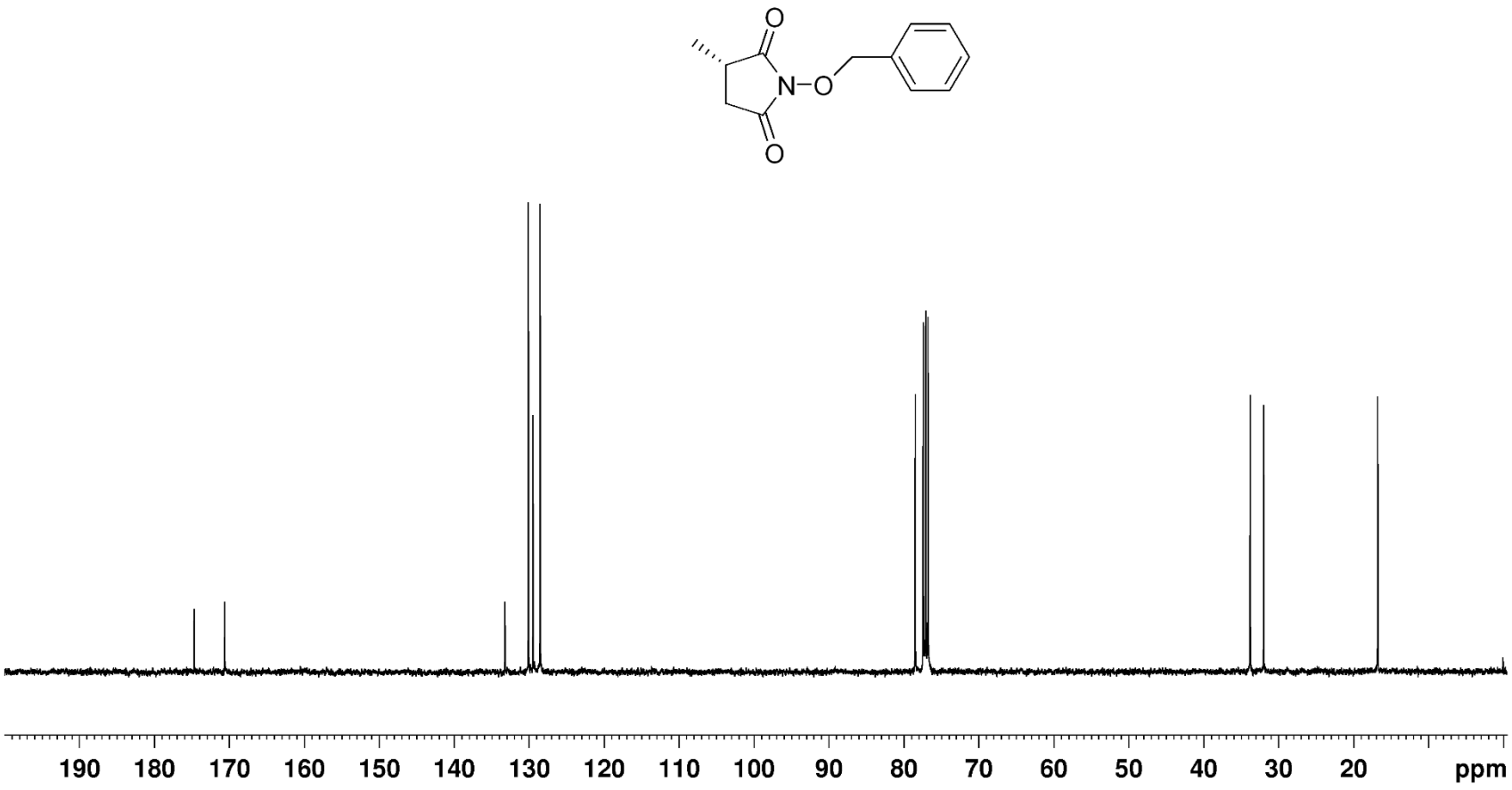

^{1}H NMR of Compound **21**

(3S)–Boc–L–valine–(4S)–methyl–N–O–benzylsuccinimide in CDCl3 at 400 MHz

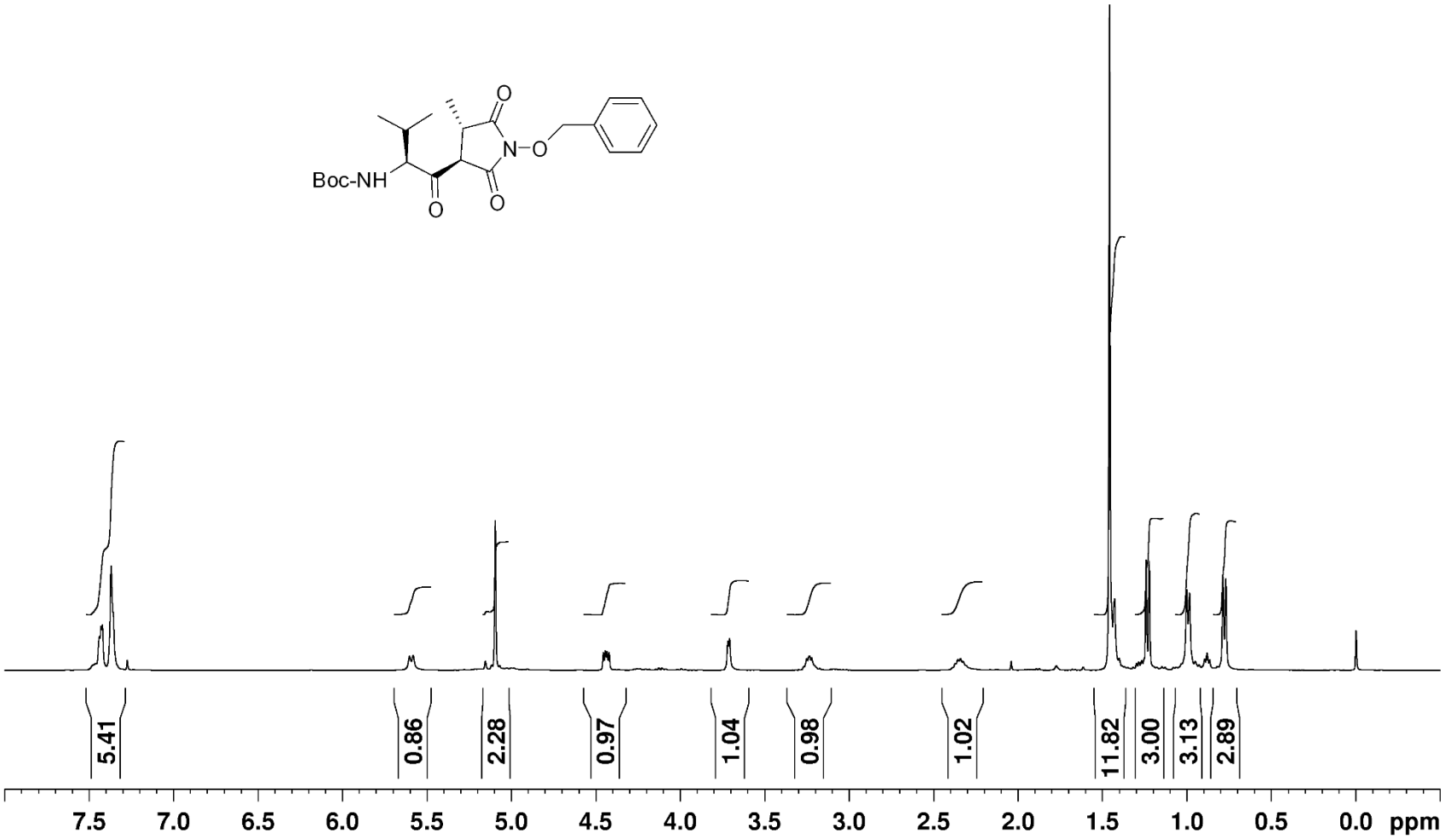

^{13}C NMR of Compound **21**

(3S)–Boc–L–valine–(4S)–methyl–N–O–benzylsuccinimide in CDCl3 at 100 MHz

* = diastereomer peaks

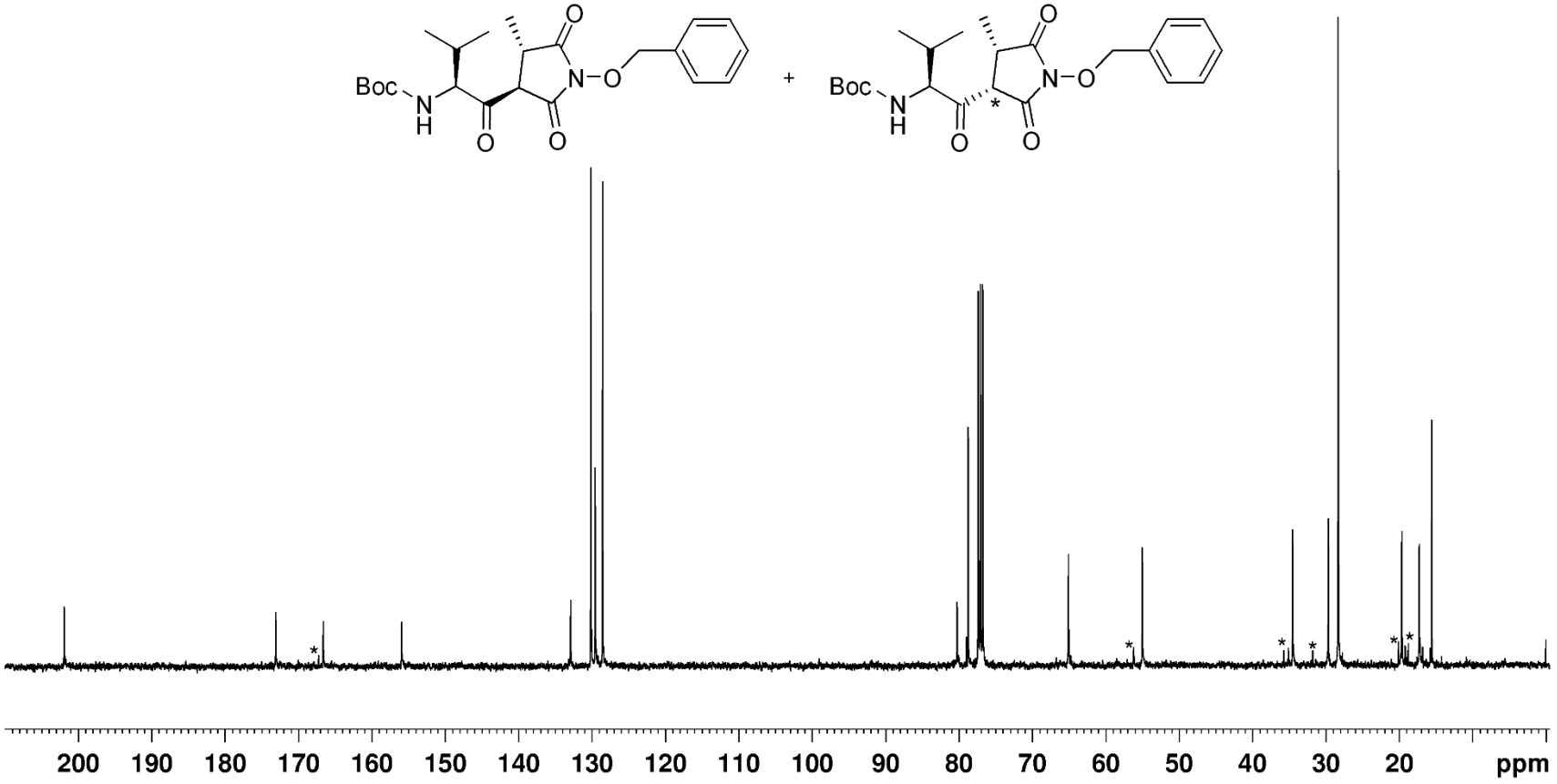

^{1}H NMR of Compound **22**

(3S)–Boc–L–valine–(4S)–methyl–succinimide in CDCl3 at 400 MHz

* = diastereomer peaks

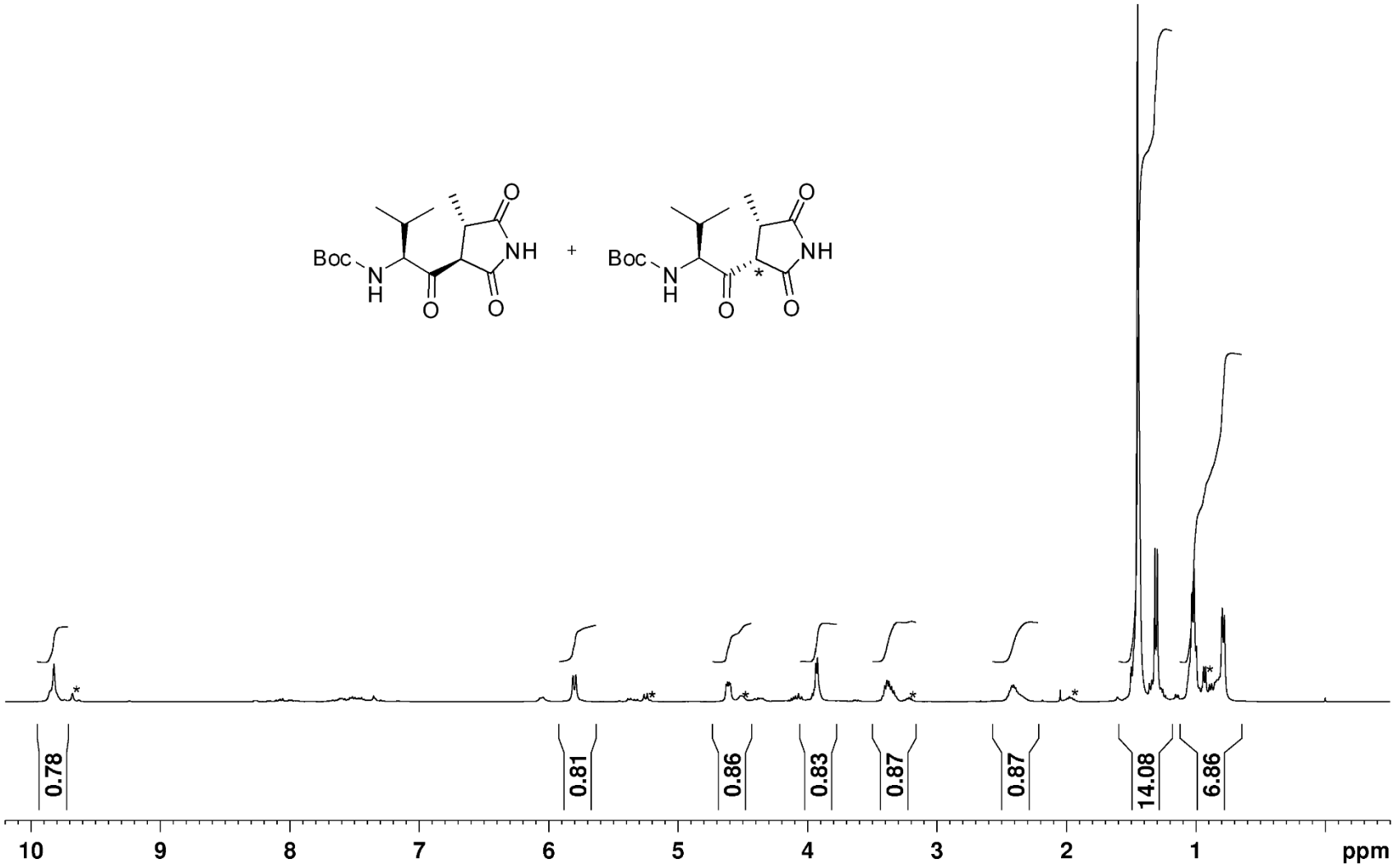

^{13}C NMR of Compound **22**

(3S)–Boc–L–valine–(4S)–methyl–succinimide in CDCl3 at 100 MHz

* = diastereomer peaks

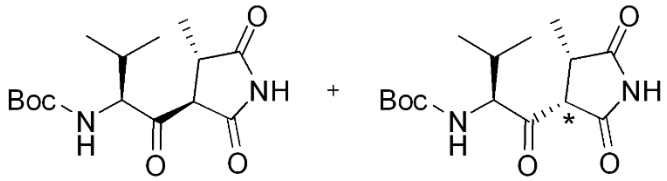

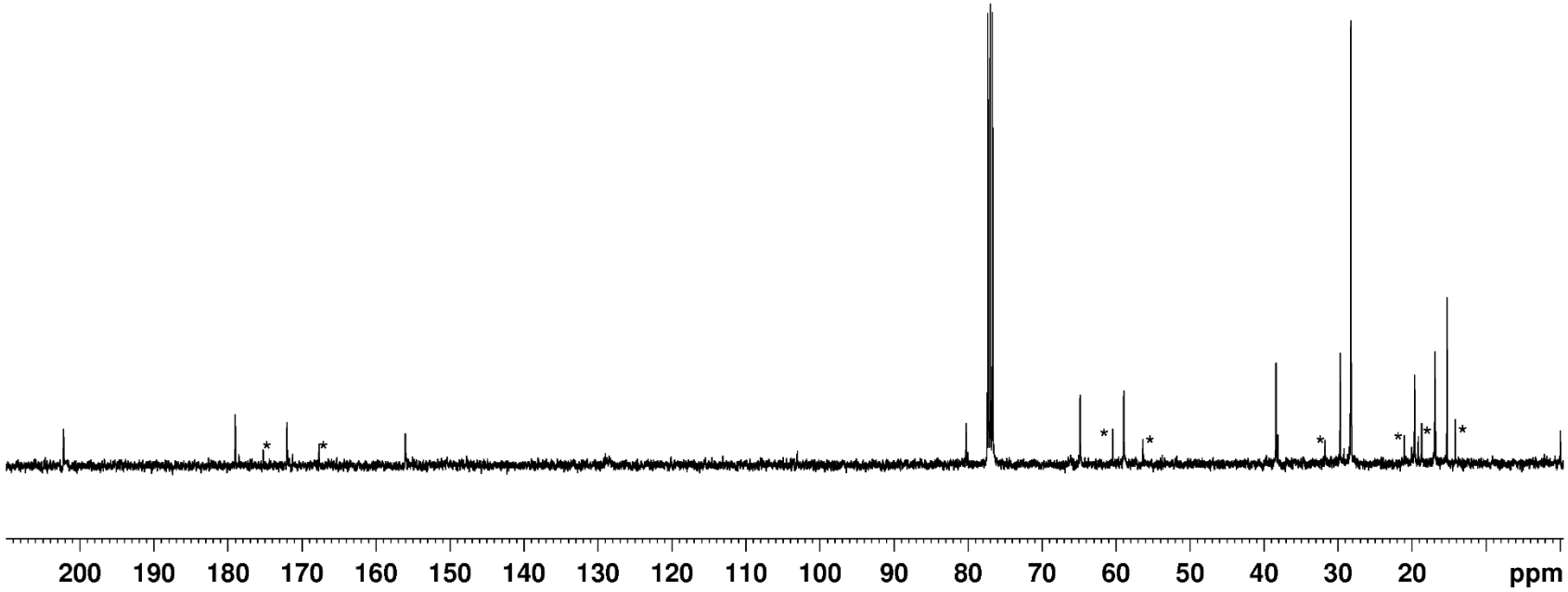

^{1}H NMR of Compound **24**

(3S)–N–Boc–3–amino– –phenylalanine–L–valine–(4S)–methyl–succinimide in DMSO–d6 at 400 MHz

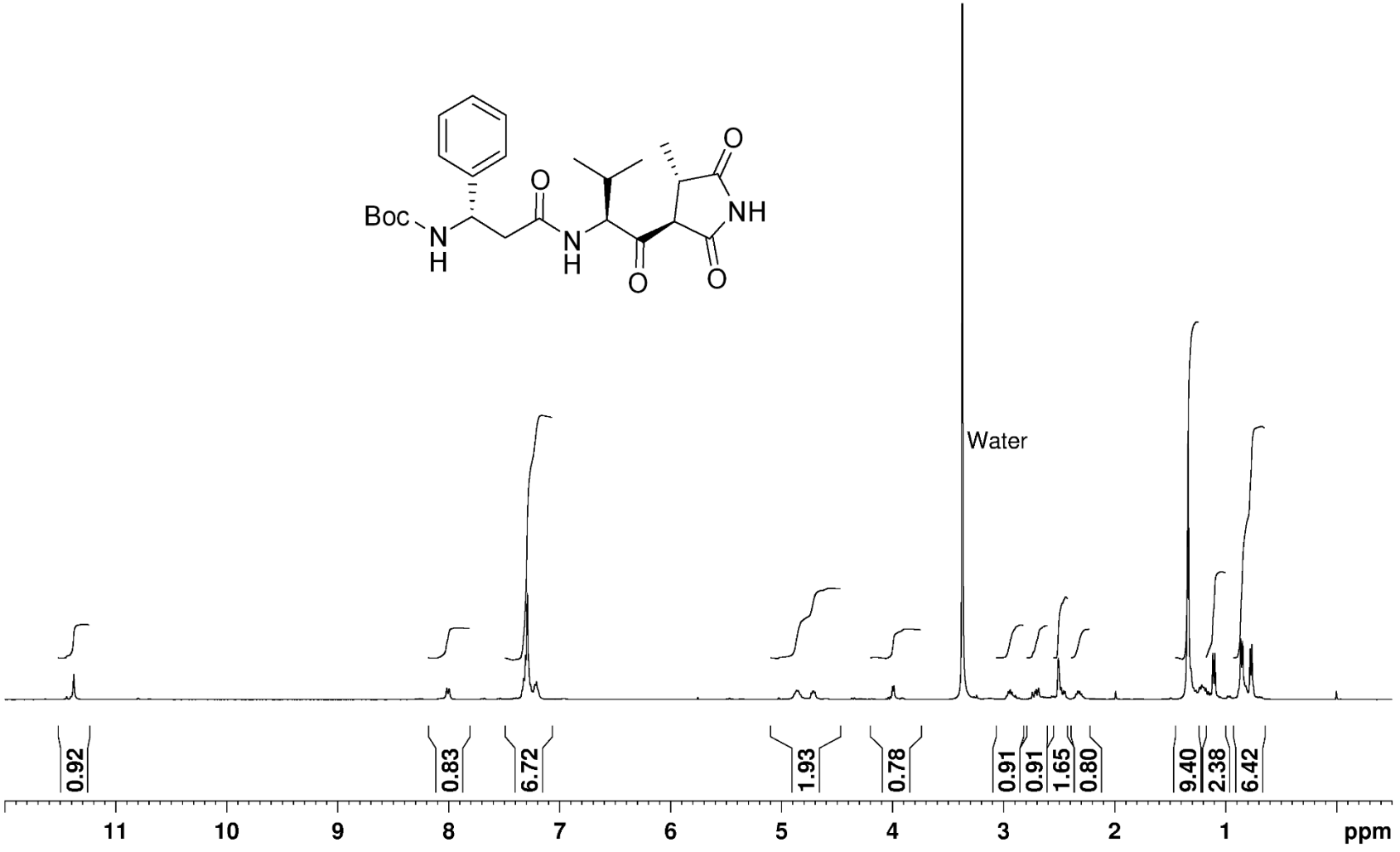

^{13}C NMR of Compound **24**

(3S)–N–Boc–3–amino– –phenylalanine–L–valine–(4S)–methyl–succinimide in DMSO–d6 at 100 MHz

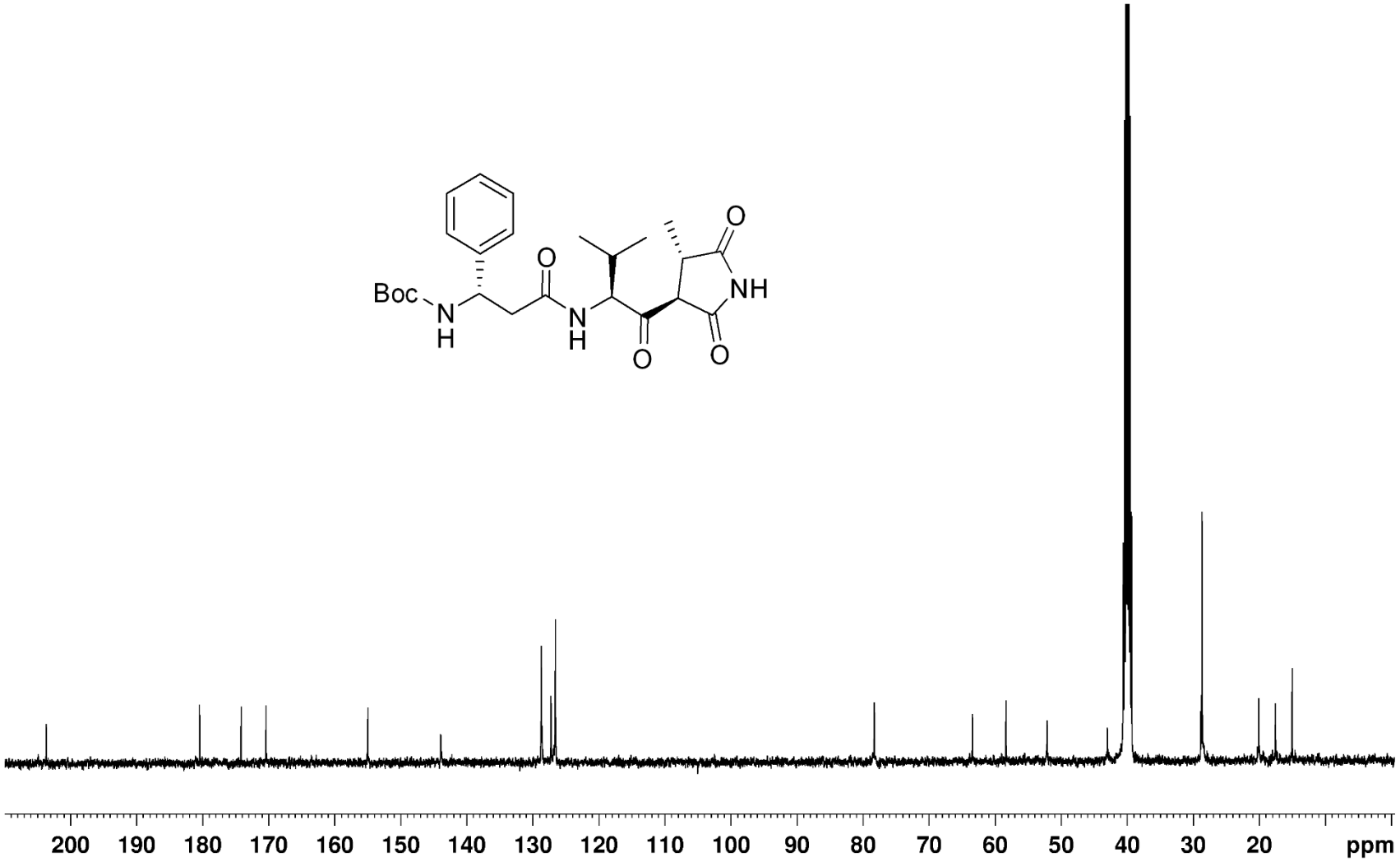

^{1}H NMR of Compound **4**

Moiramide B in DMSO–d6 at 400 MHz

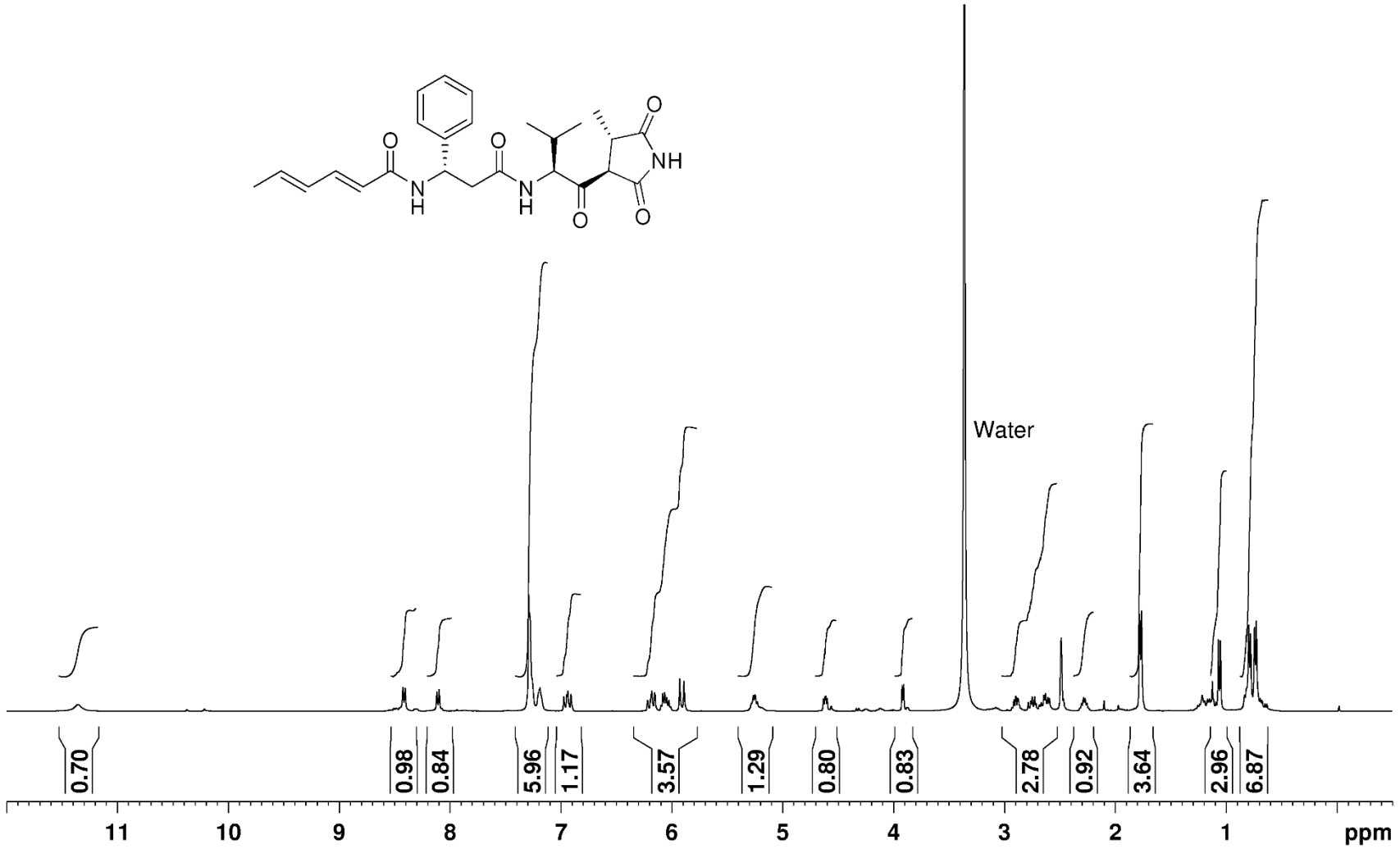

^{13}C NMR of Compound **4**

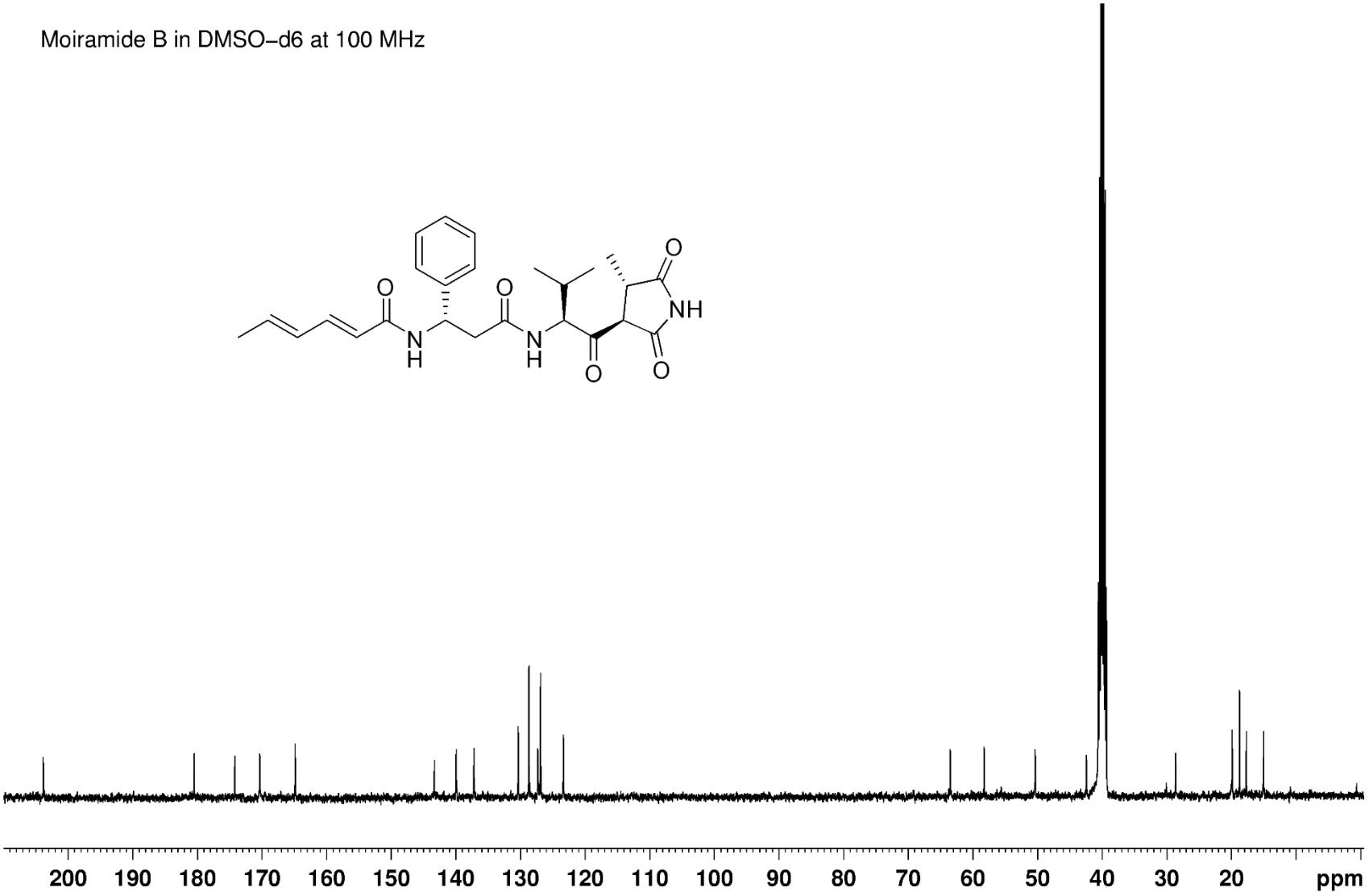

CD Spectrum of Compound **4**

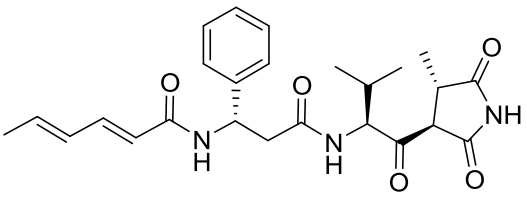

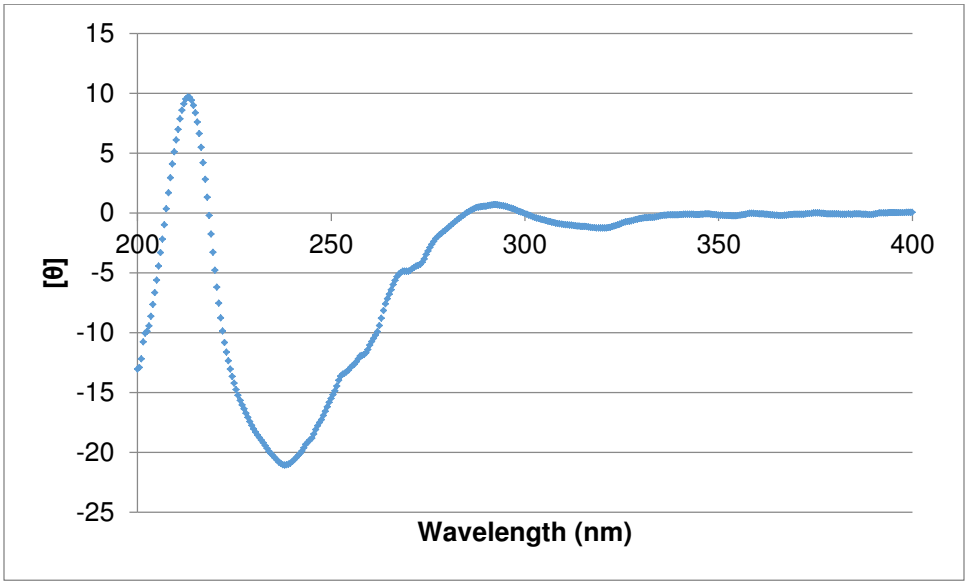

Wavelength (nm)	[θ]
213	9.6777
238	-21.0783
292	0.6904
320	-1.2602

^{1}H NMR of Compound **27**

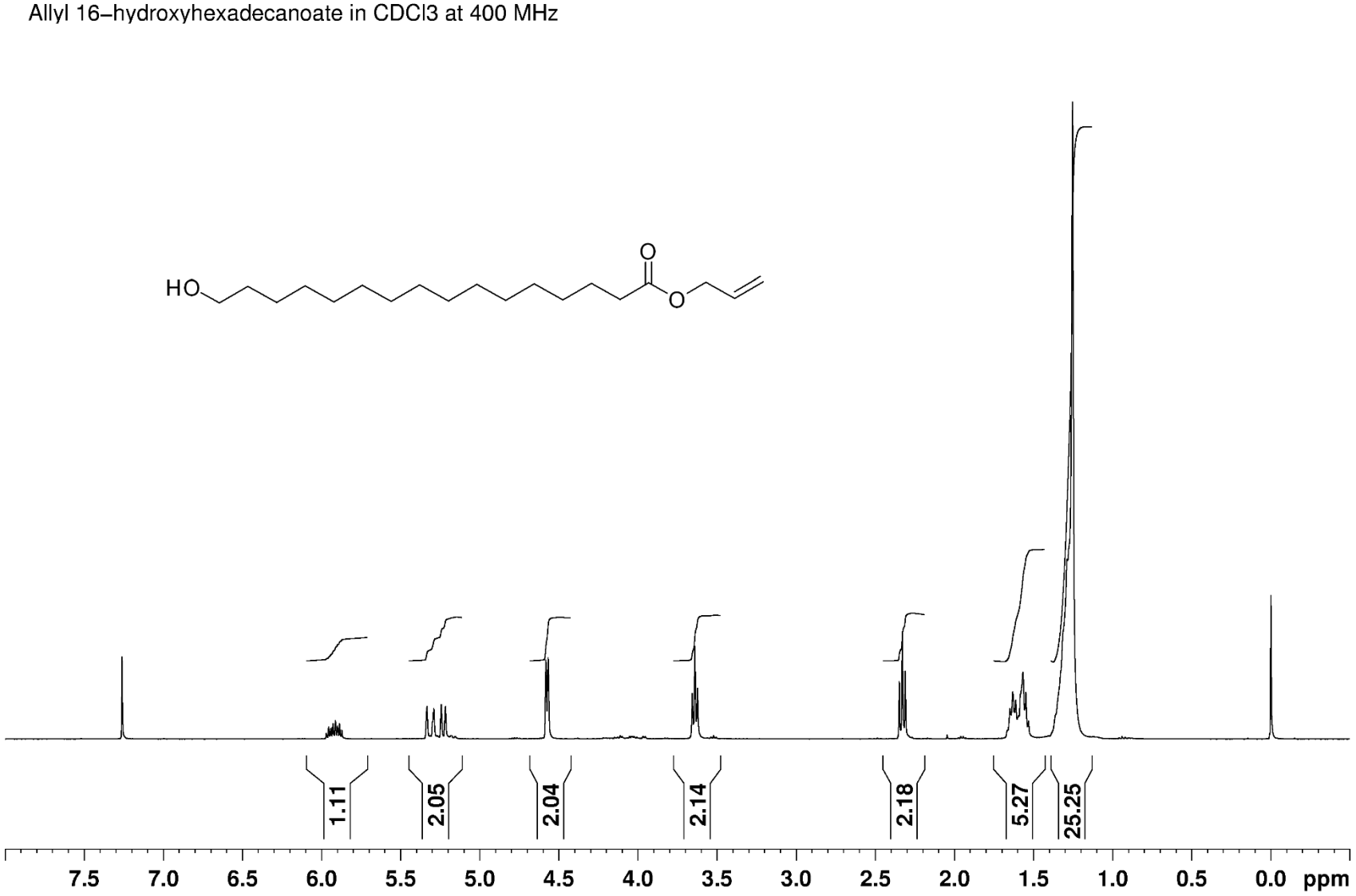

^{13}C NMR of Compound **27**

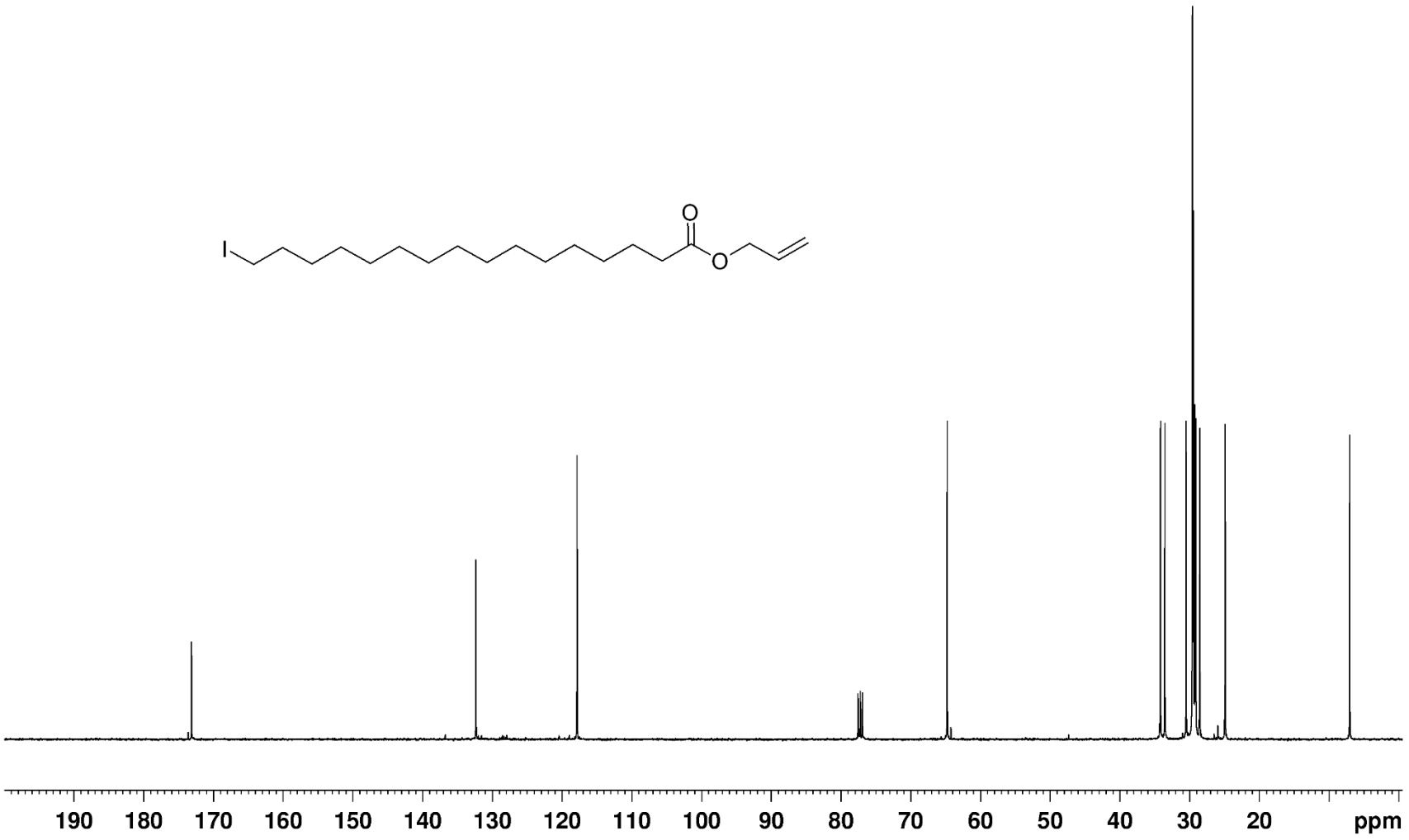

^{1}H NMR of Compound **28**

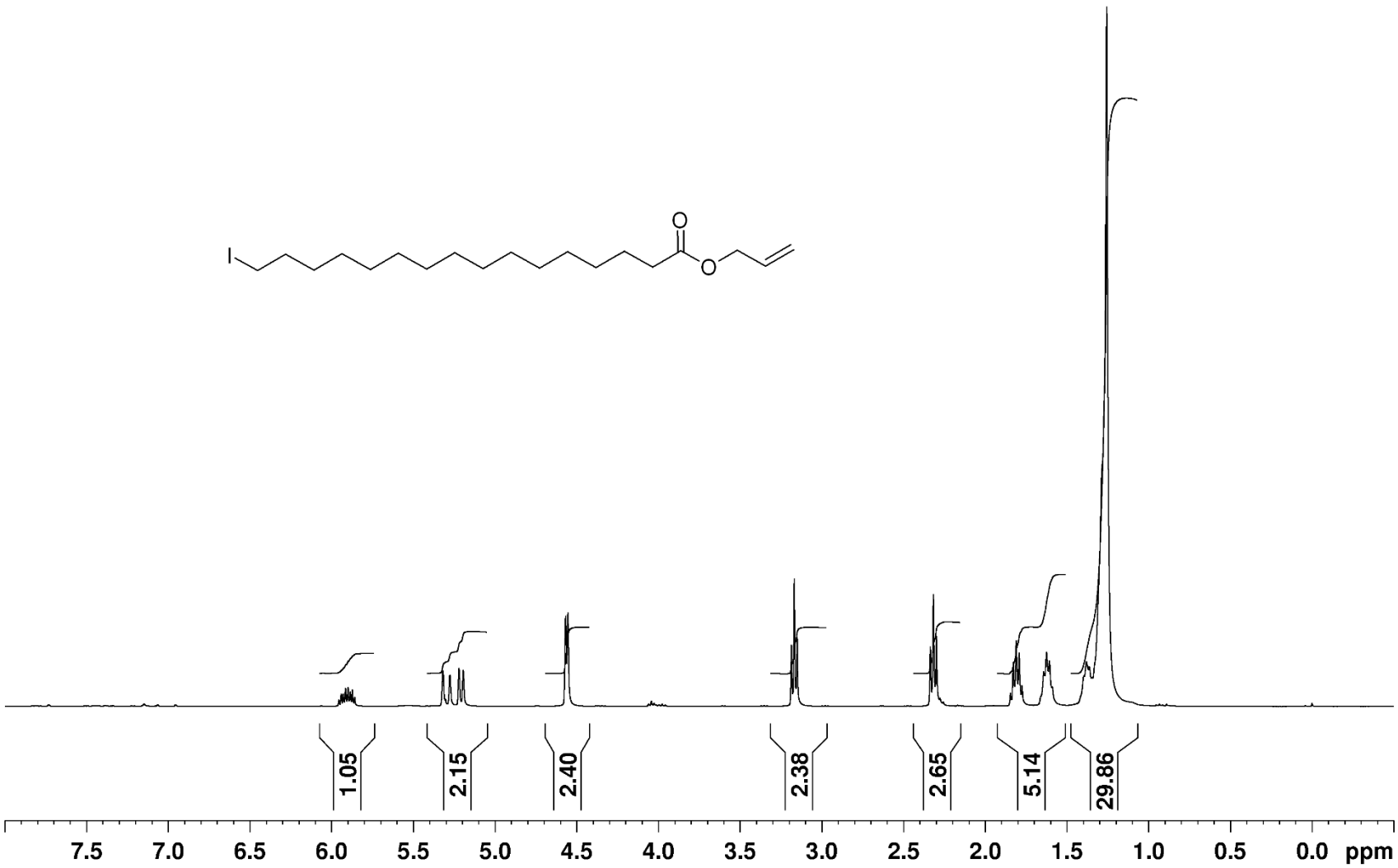

^{13}C NMR of Compound **28**

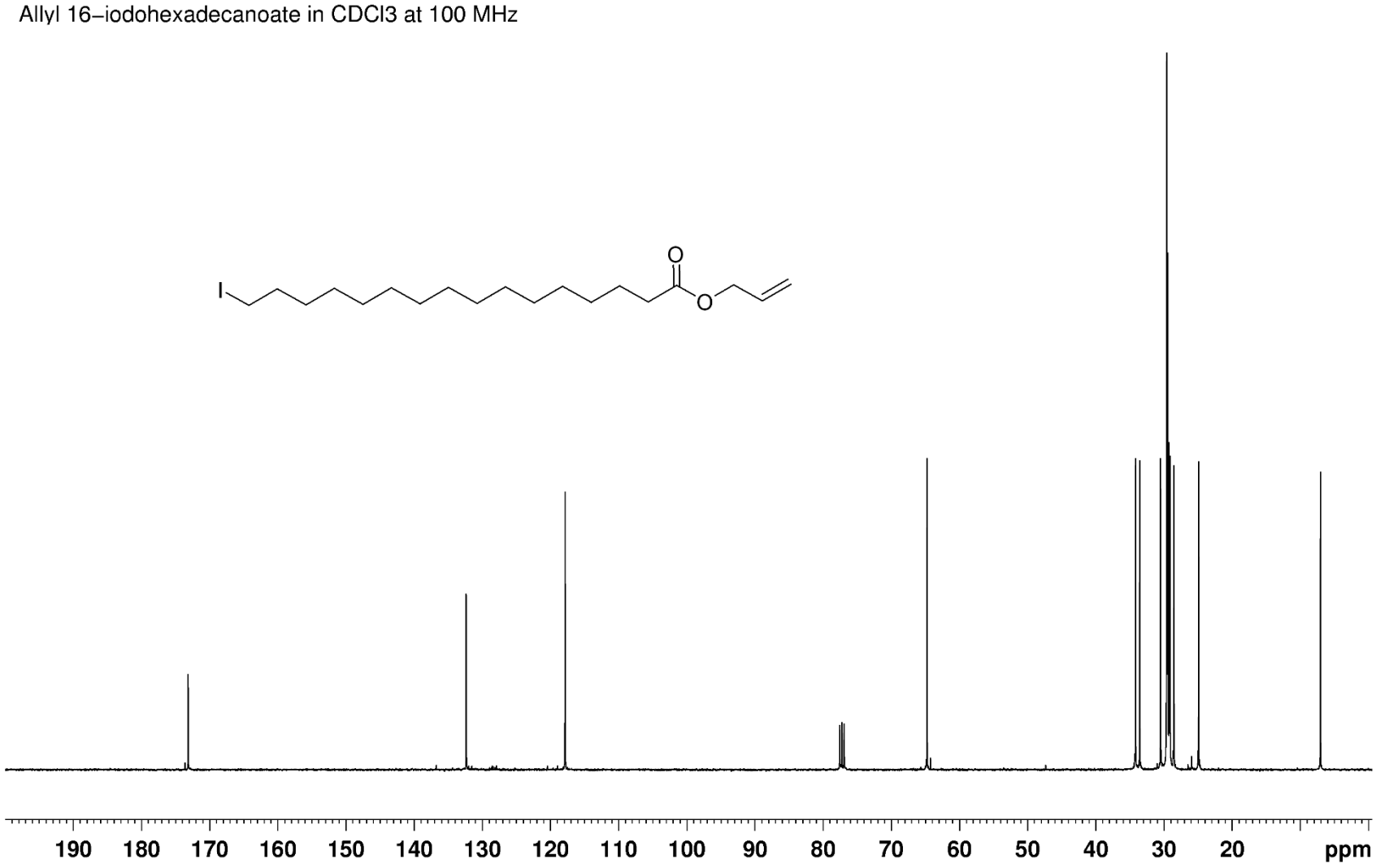

^{1}H NMR of Compound **30**

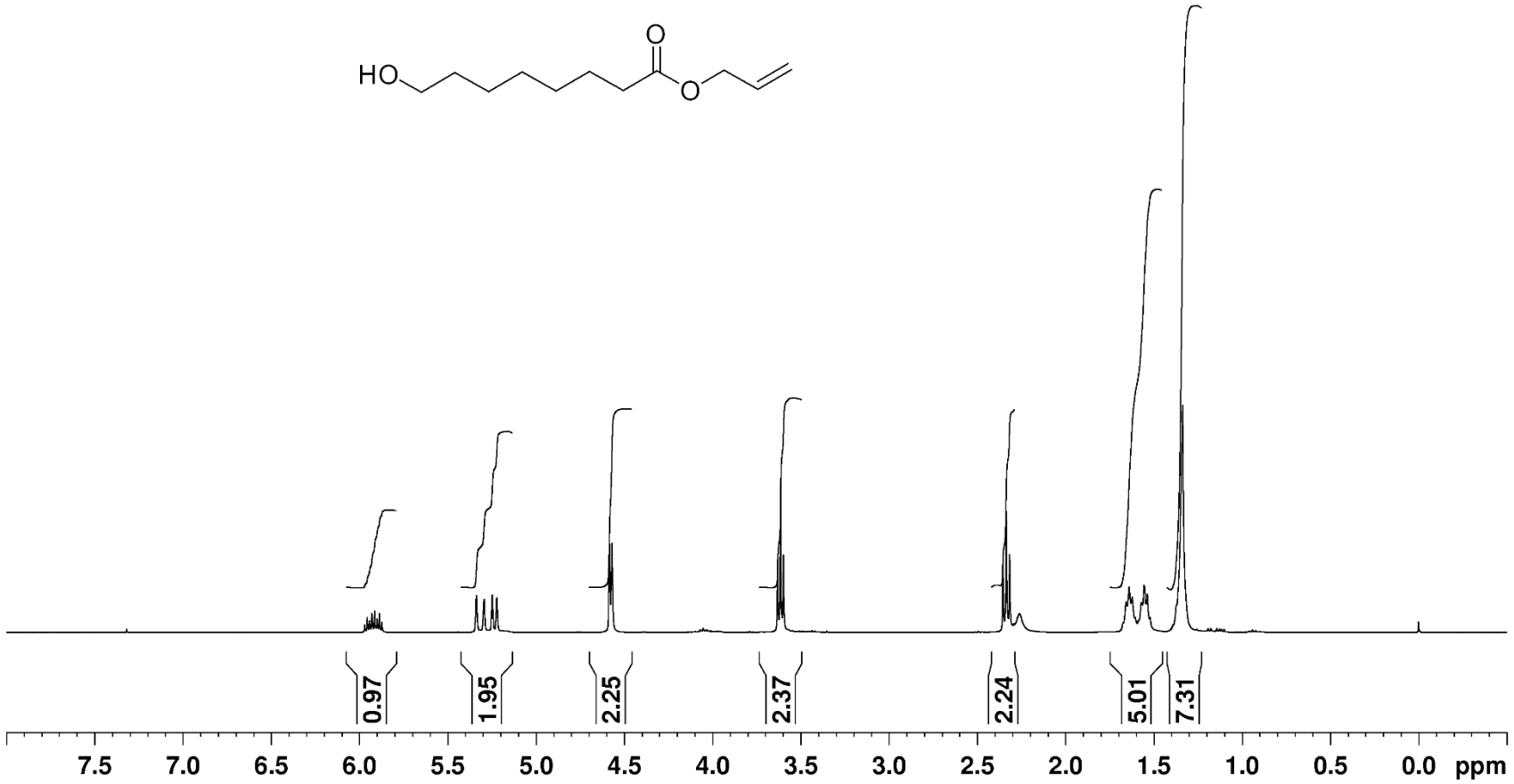

^{13}C NMR of Compound **30**

Allyl 8–hydroxyoctanoate in CDCl3 at 100 MHz

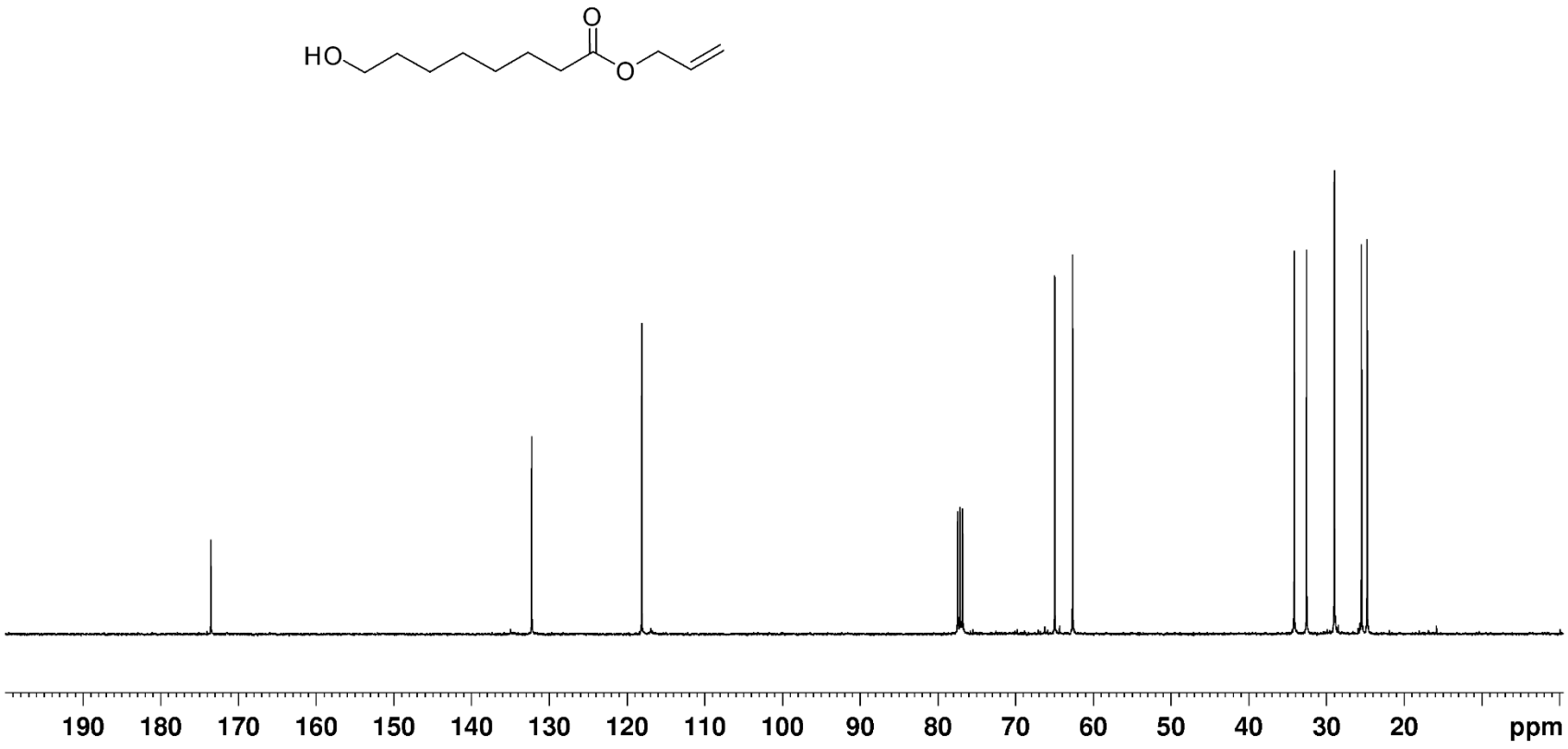

^{1}H NMR of Compound **31**

Allyl 8–iodooctanoate in CDCl3 at 400 MHz

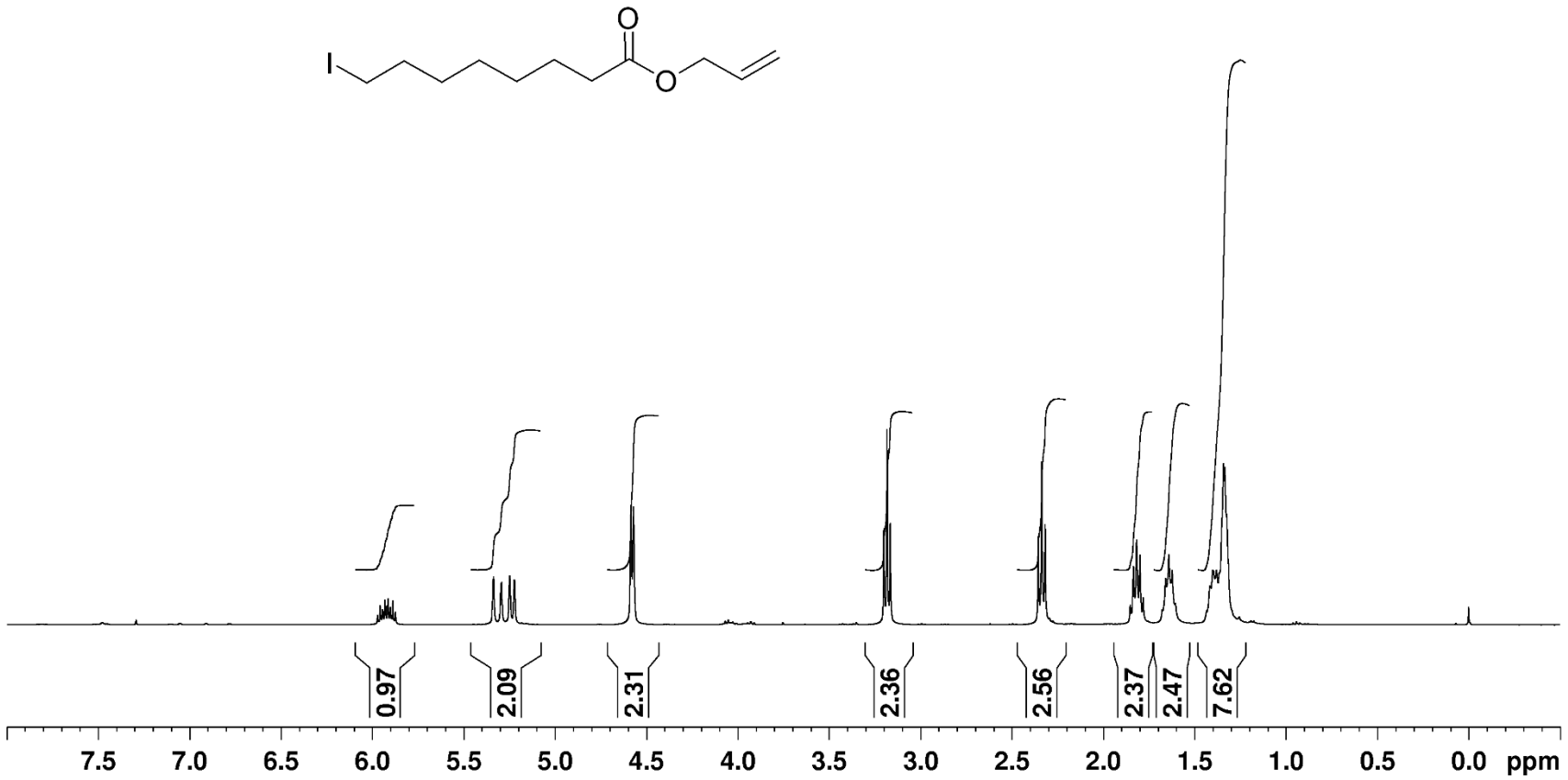

^{13}C NMR of Compound **31**

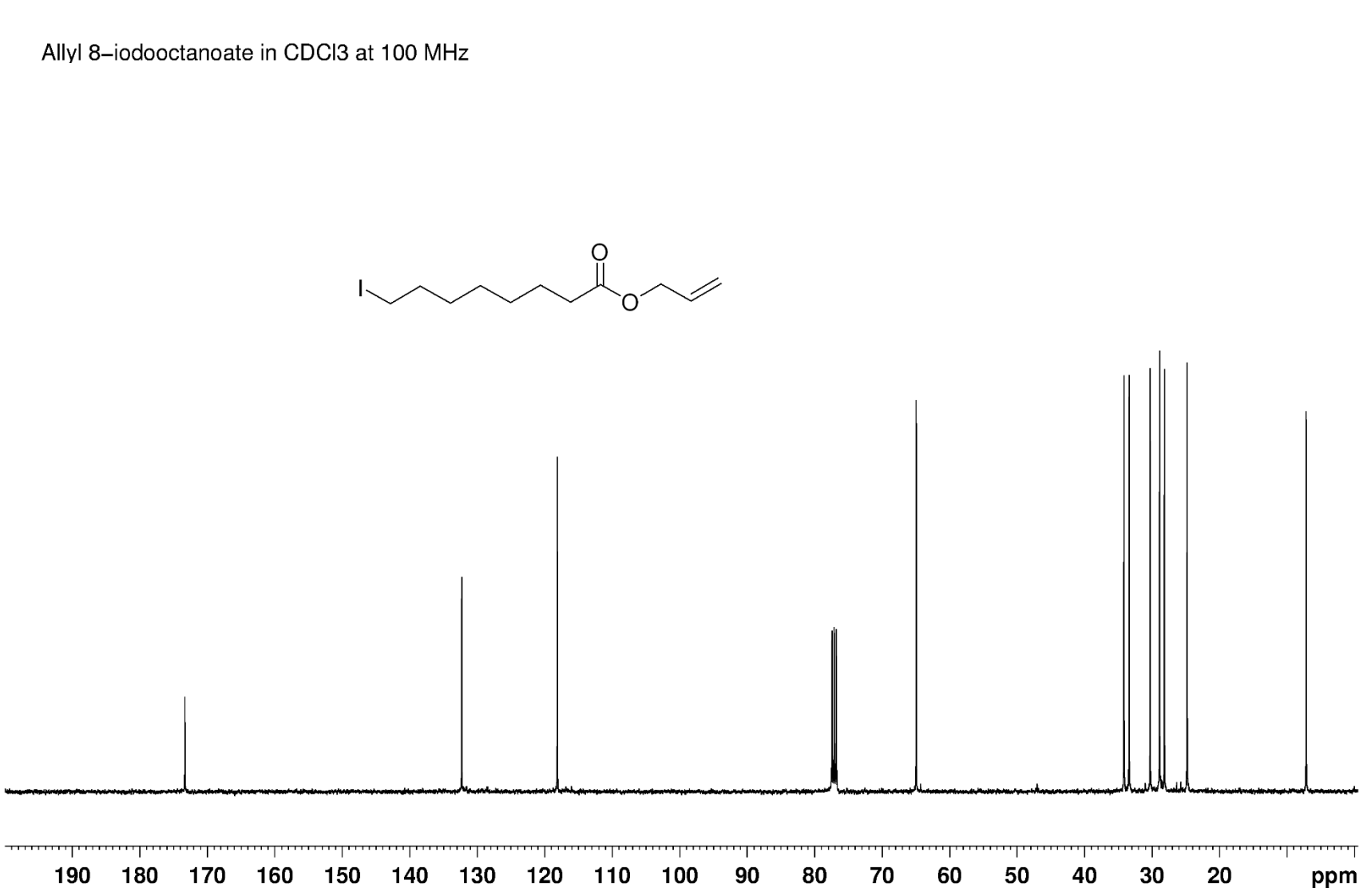

^{1}H NMR of Compound **32**

Allyl 16–{4–[(2–amino–N–benzyloxazole–5–carboxamido)methyl]phenoxy}hexadecanoate in CDCl3 at 400 MHz

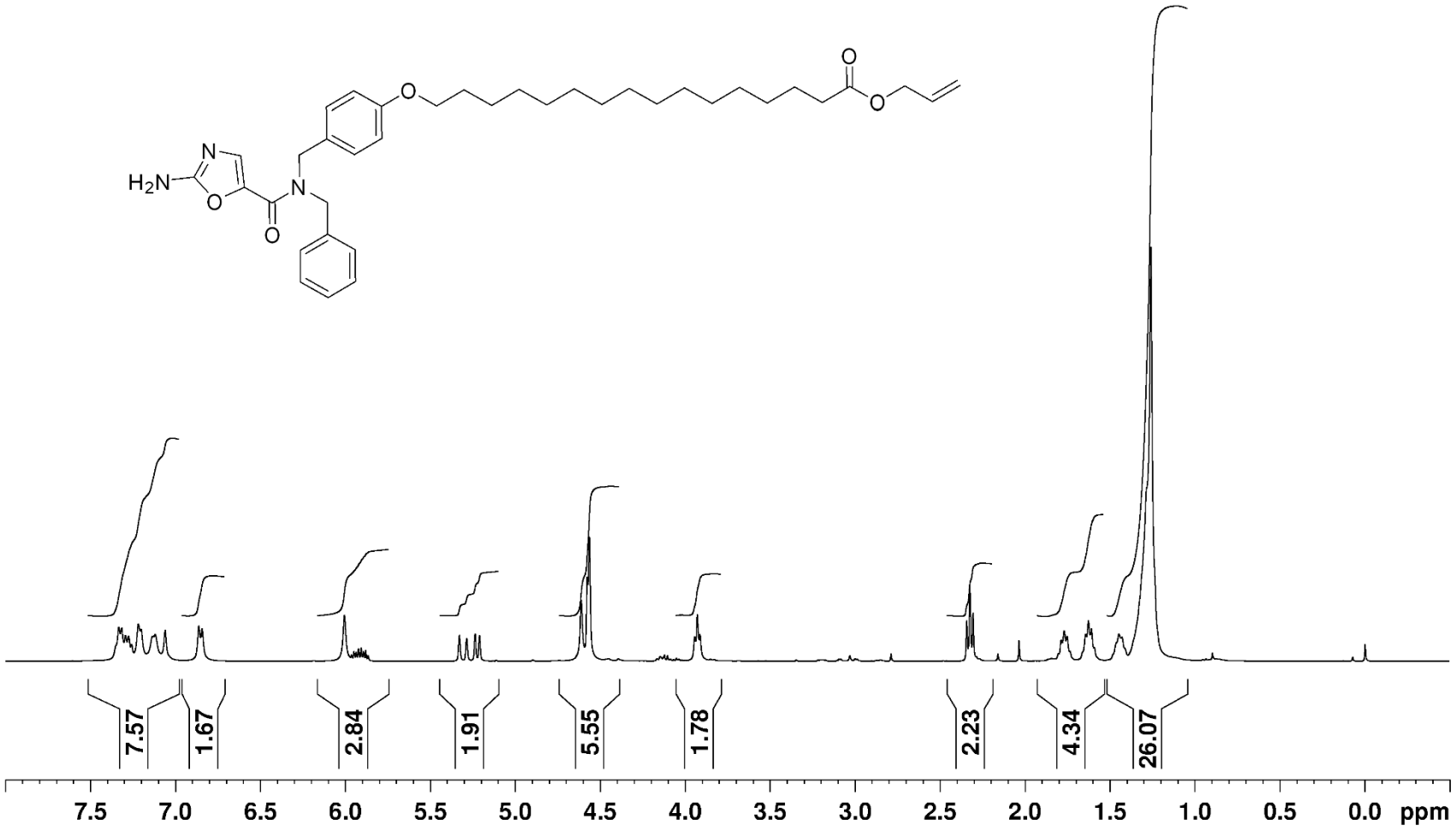

^{13}C NMR of Compound **32**

Allyl 16–{4–[(2–amino–N–benzyloxazole–5–carboxamido)methyl]phenoxy}hexadecanoate in CDCl3 at 100 MHz

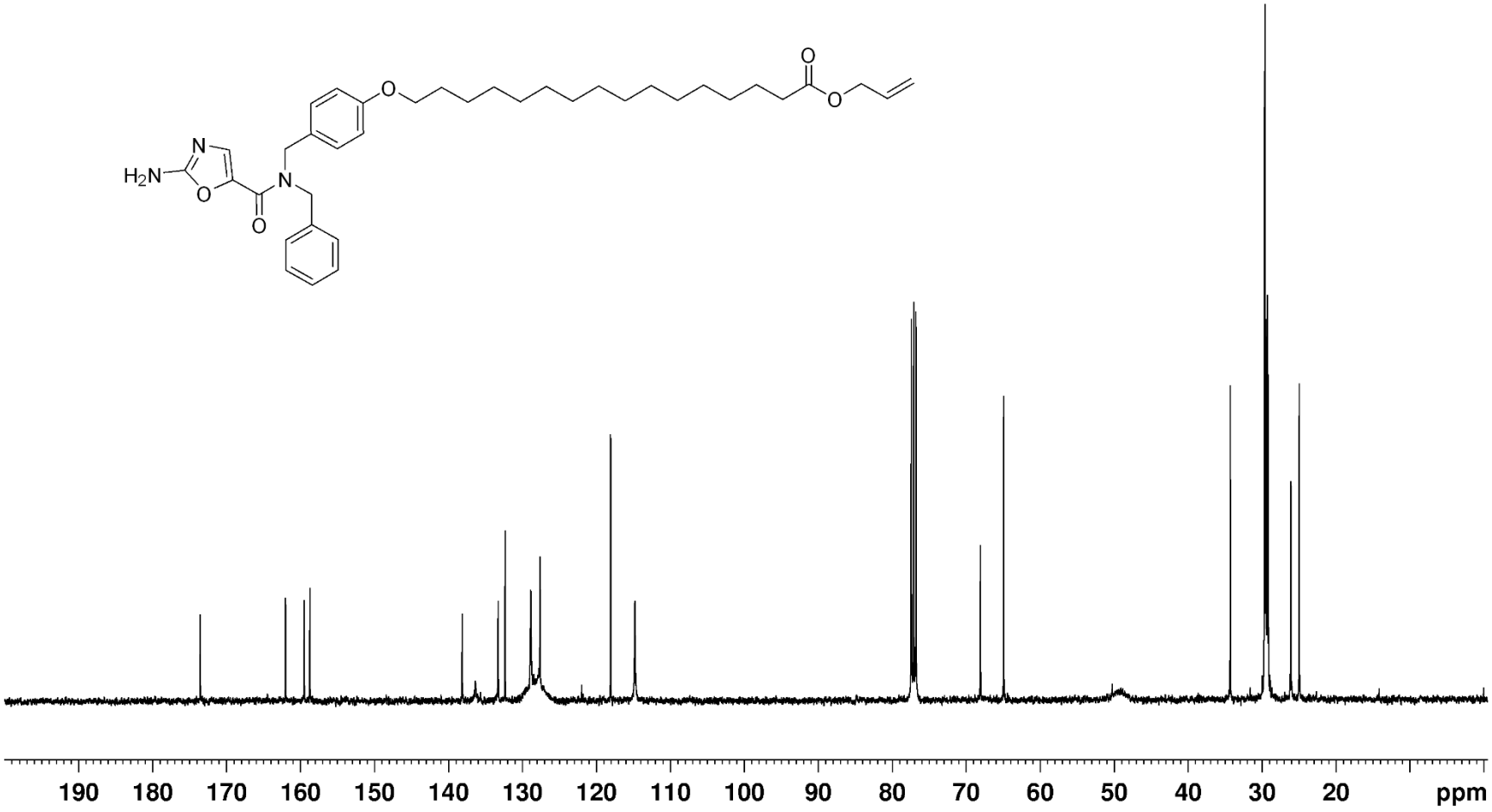

^{1}H NMR of Compound **33**

Allyl 8–{4–[(2–amino–N–benzyloxazole–5–carboxamido)methyl]phenoxy}octanoate in CDCl3 at 400 MHz

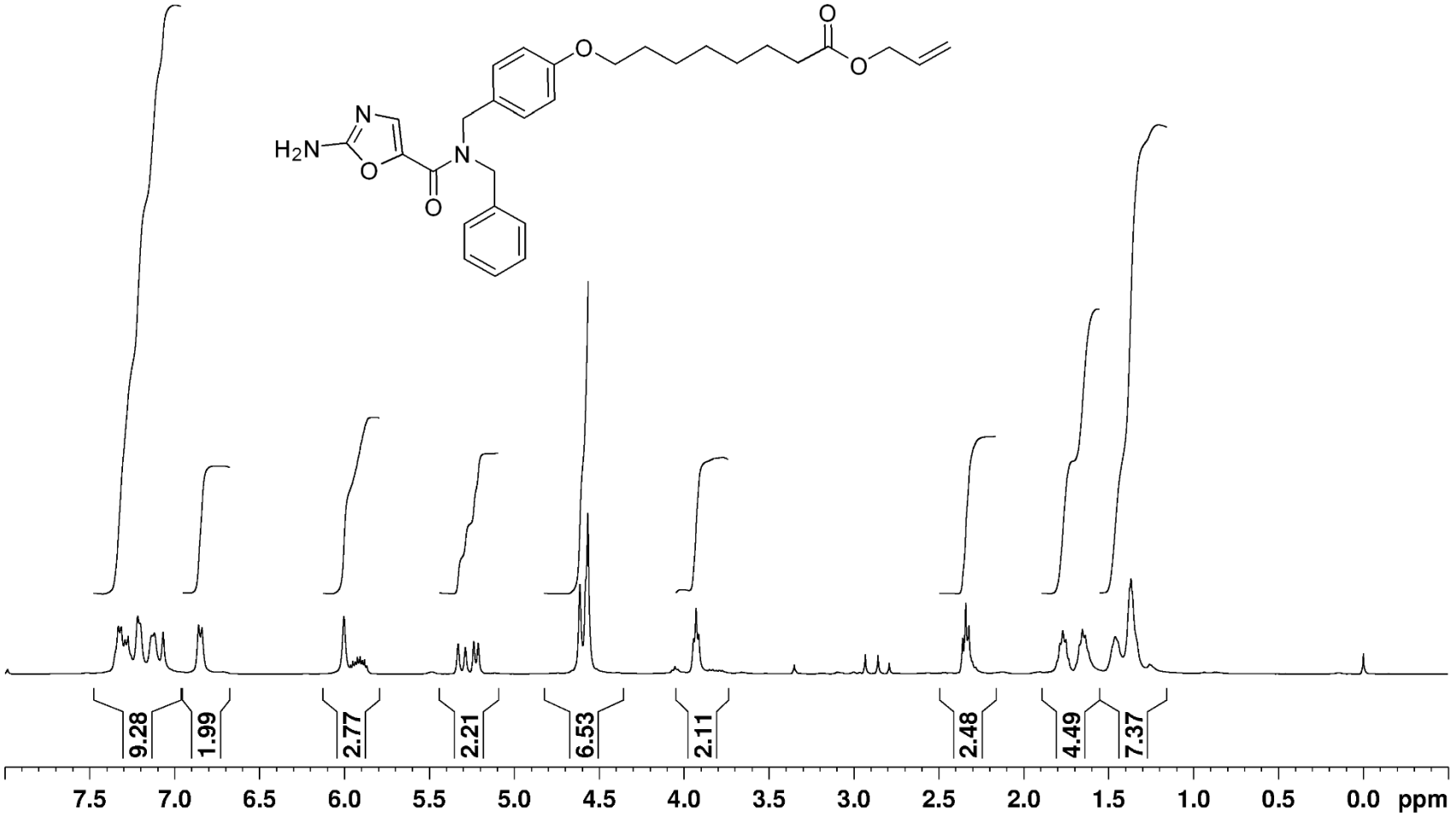

^{13}C NMR of Compound **33**

Allyl 8–{4–[(2–amino–N–benzyloxazole–5–carboxamido)methyl]phenoxy}octanoate in CDCl3 at 100 MHz

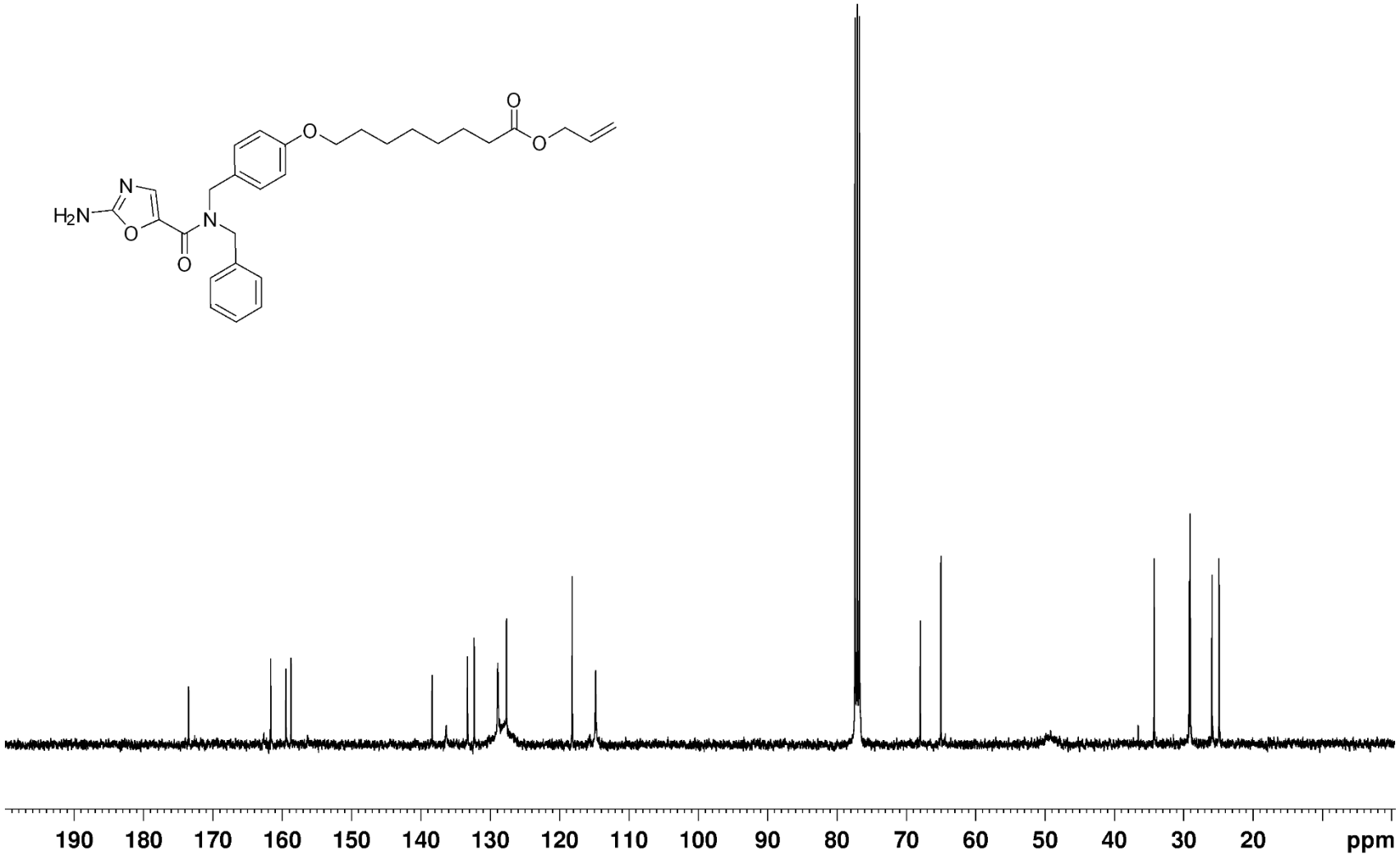

^{1}H NMR of Compound **5**

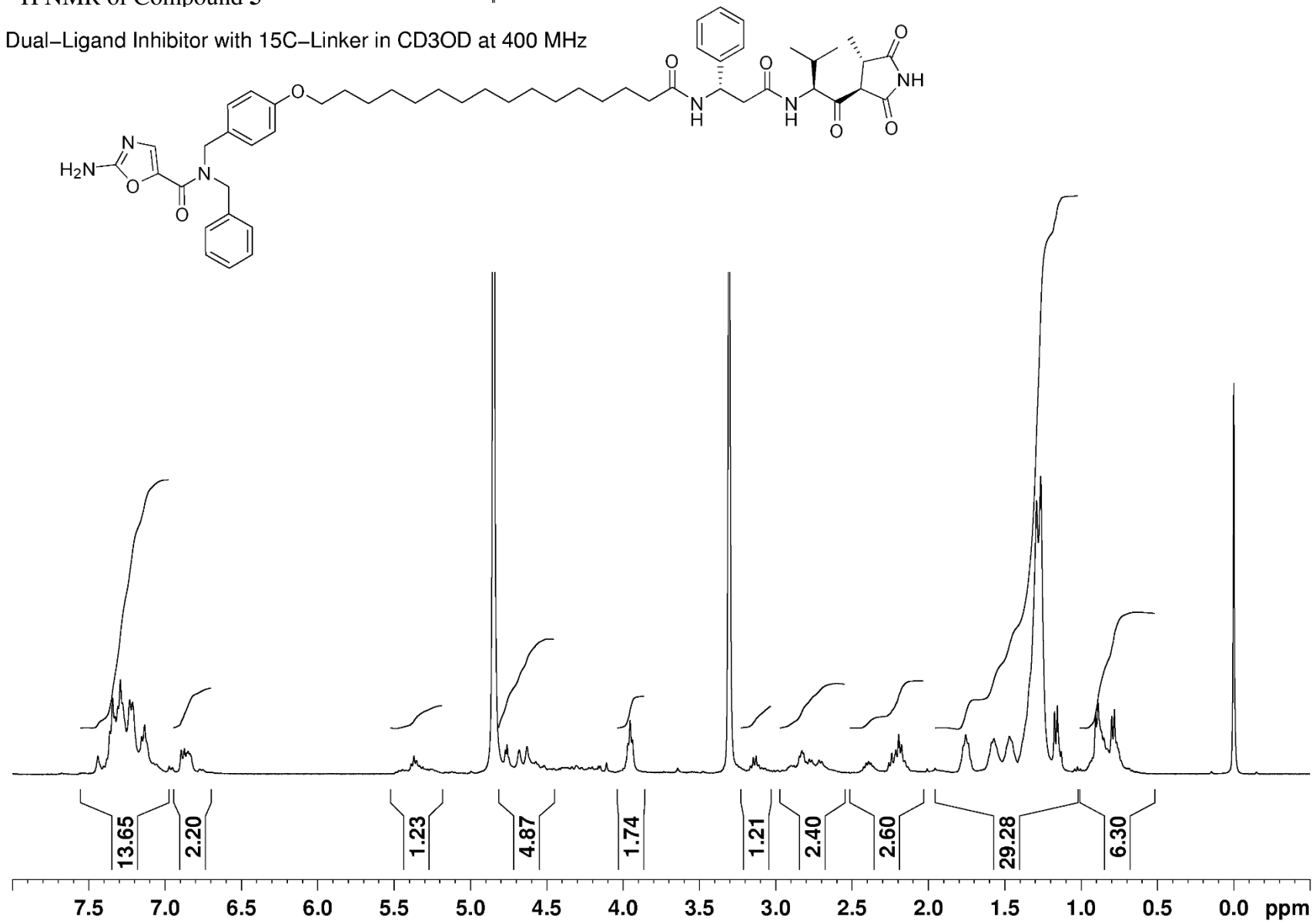

^{1}H NMR of Compound **6**

Dual–Ligand Inhibitor with 7C–Linker in CD3OD at 500 MHz

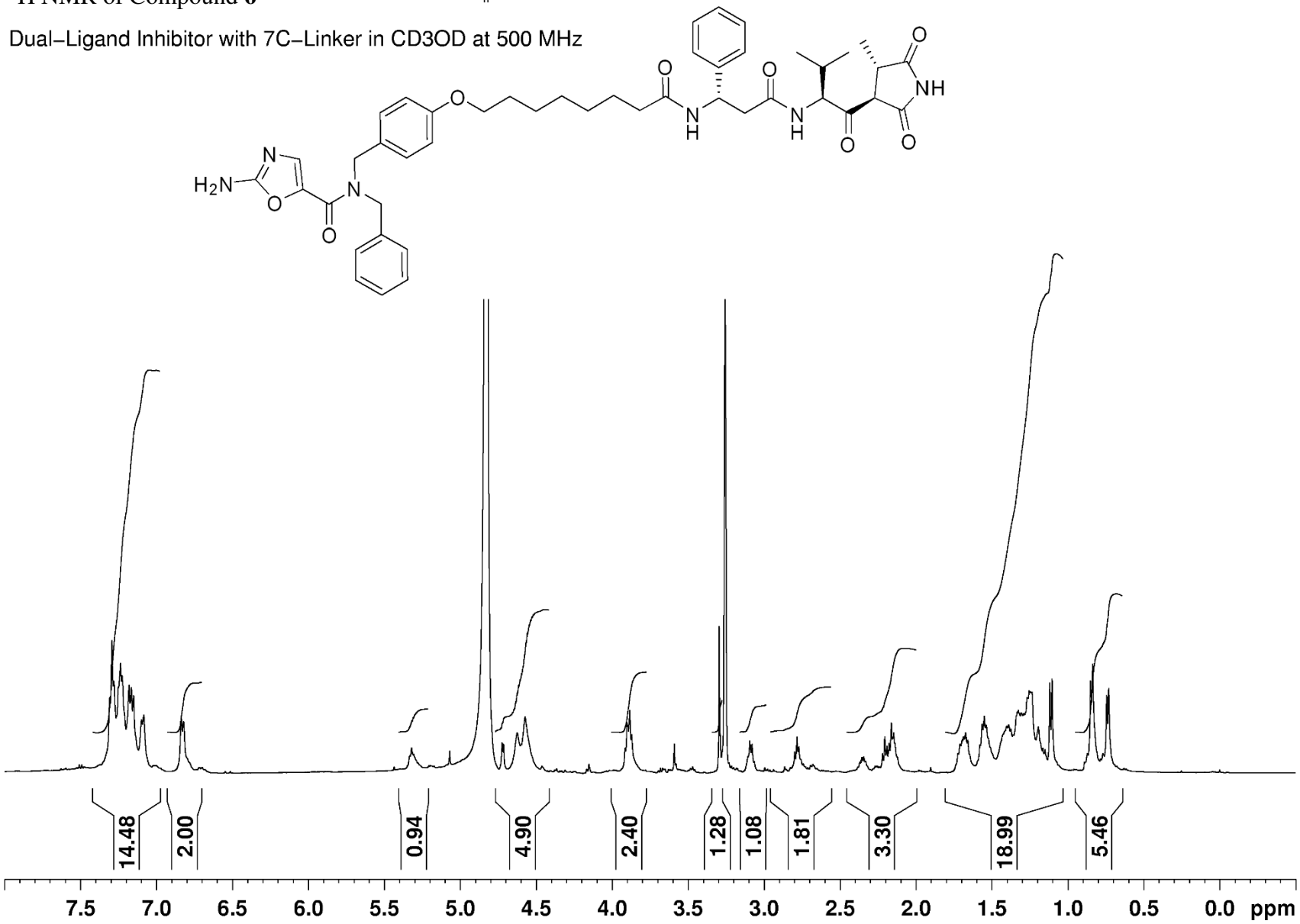

CHAPTER 3: MECHANISM OF ACTION FOR THE ANTIBACTERIAL AGENT MOIRAMIDE B

3.1 INTRODUCTION

As the frequency of antibiotic resistant bacteria steadily increases, there is an urgent need for new antibacterial agents. Fatty acid synthesis is required for membrane biogenesis in bacteria, so the enzymes in this pathway are targets for antibacterial development.[1] Acetyl-CoA carboxylase (ACC) catalyzes the committed and regulated step in fatty acid synthesis.[2] The bacterial form of the enzyme consists of three proteins: biotin carboxylase, biotin carboxyl carrier protein, and carboxyltransferase,[3] which catalyze the following two-step reaction.

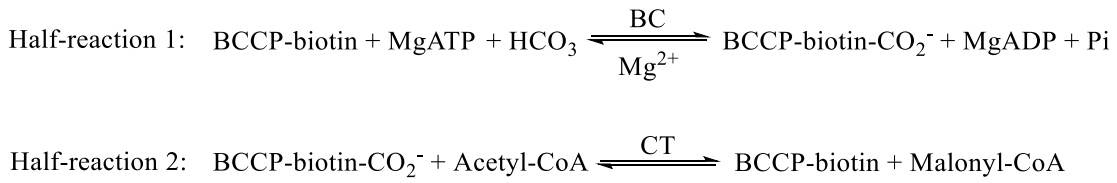

Scheme 3.1. The two half-reactions catalyzed by acetyl-CoA carboxylase.

Biotin carboxylase (BC) catalyzes the first half-reaction in Scheme 3.1, which involves the ATP-dependent phosphorylation of bicarbonate to form a reactive carboxyphosphate intermediate.[4] The carboxyl group is then transferred to the vitamin biotin, which *in vivo*, is covalently attached to the biotin carboxyl carrier protein (BCCP). The second half-reaction is catalyzed by the carboxyltransferase (CT) component, which transfers the carboxyl group from carboxybiotin to acetyl-CoA to make malonyl-CoA. Biotin carboxylase and carboxyltransferase can be purified and retain their activity when free biotin is used as a substrate instead of BCCP.[1]

Both the biotin carboxylase and the carboxyltransferase components of acetyl-CoA carboxylase can serve as targets for antibacterial agents. Biotin carboxylase is the target for three different types of antibacterial compounds: pyridopyrimidines[5], aminooxazoles[6] and benzimidazole-carboxamides[7]. In contrast, there is currently only one class of molecules known to inhibit carboxyltransferase, the natural products moiramide B and andrimid. Moiramide B is a pseudopeptide pyrrolidinedione that was isolated from the marine bacterium *Pseudomonas fluorescens* and was determined to be a potent broad-spectrum antibiotic.[8] Ten years after the discovery of the antibacterial potential of moiramide B, Freiberg *et al.* determined that carboxyltransferase was the target.[9] The inhibition of carboxyltransferase by moiramide B was competitive with respect to malonyl-CoA (K_i = 5 nM) and noncompetitive with respect to biocytin.[1,10]

The structure of moiramide B is composed of four distinct domains: 1) an unsaturated fatty acid chain, 2) the β-amino acid β-phenylalanine, 3) an L-valine derived β-ketoamide group, and 4) a pyrrolidinedione head group (Figure 3.1).

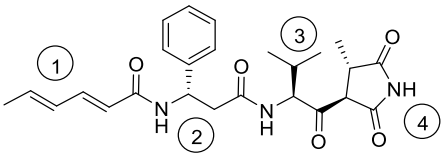

Figure 3.1. Structure of moiramide B with four domains: 1) unsaturated fatty acid chain, 2) β-amino acid β-phenylalanine, 3) L-valine derived β-ketoamide, and 4) pyrrolidinedione head group.

The assembly of moiramide B is likely genetically similar to the biosynthesis of andrimid, which utilizes a cluster of 21 genes encoding a hybrid polyketide synthase/non-

[1]The activity of carboxyltransferase is measured in the reverse or non-physiological direction where malonyl-CoA and biocytin (a biotin analog) are the substrates. The formation of the product acetyl-CoA is detected using the coupling enzymes, citrate synthase and malate dehydrogenase.

ribosomal peptide synthetase.[11] The biosynthesis starts with the tail (domain 1) and proceeds to the head (domain 4), whereas synthetic procedures for moiramide B start with the head (domain 4) and conclude with the tail (domain 1).[12-13] Given the significant resources that a bacterium must commit to produce each of the domains of moiramide B, why have these particular molecular structures survived natural selection? In other words, how do each of the domains of moiramide B contribute to its overall potent antibacterial activity? The objective of this study is to dissect moiramide B into molecular fragments and determine the function of those fragments with respect to the inhibition of carboxyltransferase and the antibacterial properties.

3.2 RESULTS AND DISCUSSION

3.2.1 Three-dimensional Structure of Moiramide B Bound to Carboxyltransferase

The first approach for determining the function of each of the molecular fragments was to determine the structure of moiramide B bound to carboxyltransferase. Synthetic procedures outlining the production of moiramide B in milligram quantities for crystallization trials have recently been described (Chapter 2). Carboxyltransferase from *E. coli*[10] was cocrystallized with the synthetically produced moiramide B (Figure 3.2), X-ray diffraction data were collected at the Advanced Photon Source and the structure was solved by molecular replacement. The data collection and refinement statistics are shown in Figure 3.3.

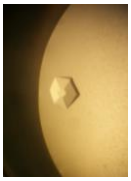

Figure 3.2. Crystal of moiramide B bound to carboxyltransferase. The crystallization conditions were: 0.1 M MES (pH 6.5), 0.1 M malonate, and 20% w/v polyacrylic acid 2100. The space group was $P6_522$.

Data Collection	
Wavelength (Å)	0.97918
Resolution (Å)	3.53
Temperature (K)	100
Space group	$P\,6_522$
Cell dimensions	
a (Å)	156.170
c (Å)	193.158
Number of CT subunits per asymmetric unit	1
Unique reflections	17 327
R_{pim} [a,b] (%)	5.8 (54.9)
Completeness (%)	98.5 (99.0)
Redundancies	7.2 (7.4)
$I/\sigma(I)$	11.1 (1.5)
Refinement Statistics	
Resolution range (Å)	135 - 3.53
Number of reflections	16 439
σ cutoff used in refinement	none
R_{work}/R_{free} [c] (%)	21.00/25.93
Number of refined atoms	
Protein	4445
Heterogen atoms	34
Water	2
Average B-factors (Å^2)	
Protein	133.7
Water	68.3
Zn^{2+}	171.0
Inhibitor	156.7
R.m.s. deviations	
Bond lengths (Å)	0.011
Bond angles (°)	1.82
Ramachandran plot (%)	
Favored	79.55
Disallowed	6.87

[a]Values in parentheses are for the highest-resolution shell.

[b]R_{pim} is a redundancy-independent measure of the quality of intensity measurements.
$R_{pim} = \sum_{hkl} (1/(n-1))^{1/2} \sum_i |I_{hkl,i} - \langle I_{hkl} \rangle| / \sum_{hkl} \sum_i I_{hkl,i}$, where $I_{hkl,I}$ is the scaled intensity of the i^{th} measurement of reflection, h, k, l, $\langle I_{hkl} \rangle$ is the average intensity for that reflection, and n is the redundancy.

[c]$R = \sum ||F_o| - |F_c|| / \sum |F_o|$, where F_o and F_c are the observed and calculated structure factors amplitudes. R_{free} is calculated using 5.1% of reflections omitted from the refinement.

Figure 3.3. Data Collection and Refinement Statistics.

The electron density for the moiramide B ligand is shown in Figure 3.4. While the resolution is 3.5 Å, density was clearly observed for the pyrrolidinedione head group (domain 4). The electron density extends down the backbone of the β-ketoamide group (domain 3) as well as into the β-phenylalanine moiety (domain 2), indicating binding interactions are taking place with these portions of the natural product. However, the resolution is not sufficient to pinpoint the structural features required for binding. No density was observed for the unsaturated fatty acid chain (domain 1) indicating it is very flexible when bound to the enzyme.

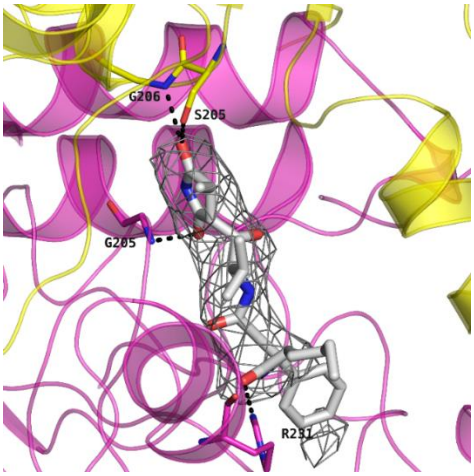

Figure 3.4. Structure of moiramide B in the active site of *E. coli* carboxyltransferase. The F_o-F_c electron density map is contoured at 2.5σ. Hydrogen bonds are indicated by dashes.

Carboxyltransferase is a heterotetramer with two active sites that lie at the interface between the α– and β–subunits.[14] A space-filling model of a heterodimer of carboxyltransferase with moiramide B bound in the active site is shown in Figure 3.5. A closer view of moiramide B bound in the active site shows that the major interactions are with the carbonyl oxygens of the pyrrolidinedione moiety (Figure 3.6). One carbonyl group forms two hydrogen bonds with residues from the α–subunit (Gly206 and Ser205),

while the other carbonyl group forms two hydrogen bonds with residues from the β–subunit (Gly205 and Ala165). This contradicts an earlier report that andrimid, and by inference moiramide B, interact solely with the β–subunit of carboxyltransferase.[11]

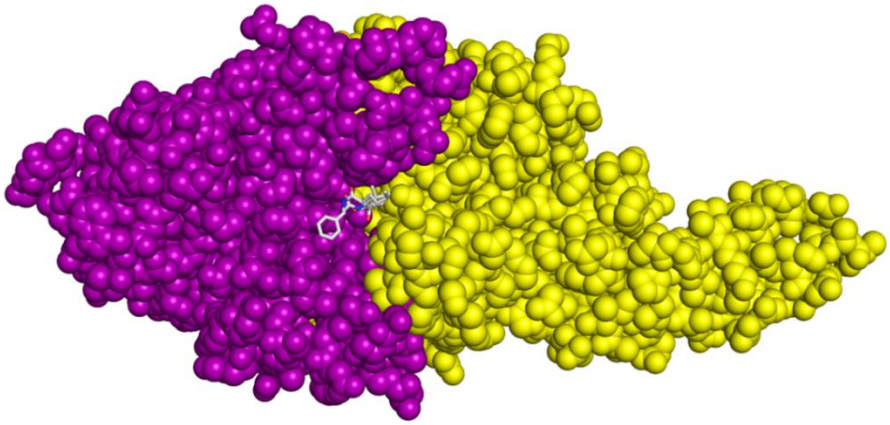

Figure 3.5. Space-filling model of moiramide B bound to carboxyltransferase. The α–subunit of carboxyltransferase is in gold while the β–subunit is in purple. Moiramide B is represented in gray sticks.

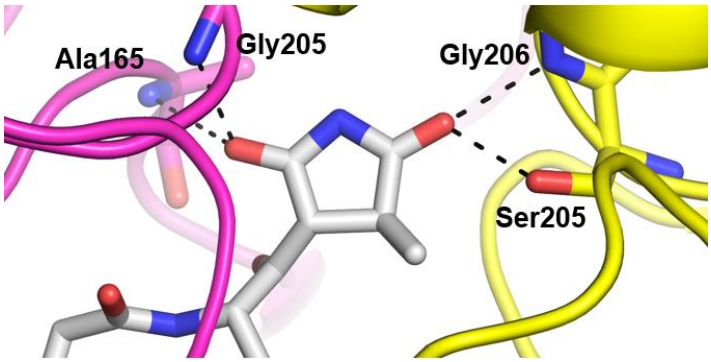

Figure 3.6. Close-up view of the interactions of the pyrrolidinedione moiety of moiramide B with the active site residues of carboxyltransferase.

In carboxyltransferase, oxyanion holes are needed to stabilize the enolates that form in each substrate during catalysis. As shown in Figure 3.7, (A), the peptidic groups from adjacent glycine residues (Gly206 and Gly207 in the α-subunit and Gly204 and Gly205 in the β-subunit) form the oxyanion holes that stabilize the enolate and imidate anions in acetyl-CoA and biotin, respectively.[14] One residue from each subunit that is used

to form the oxyanion hole hydrogen bonds to each pyrrolidinedione carbonyl (Gly206 in the α–subunit and Gly205 in the β–subunit), Figure 3.7, (B).

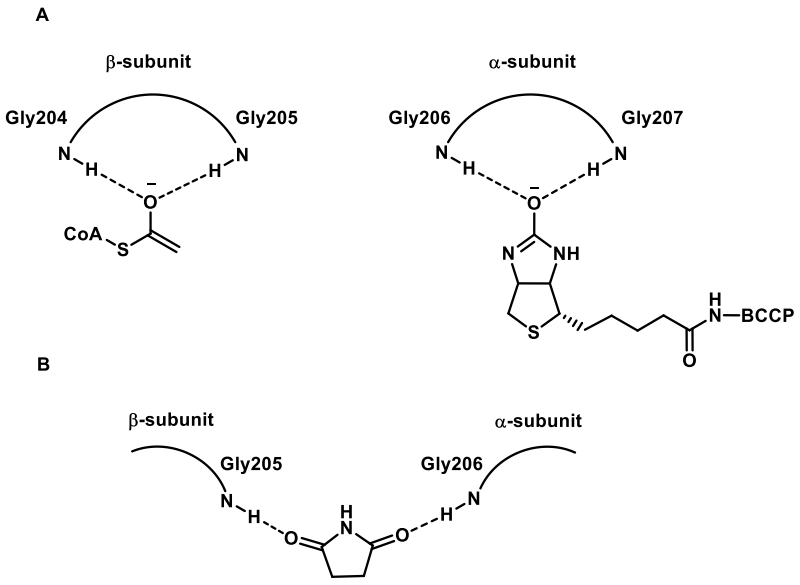

Figure 3.7. (A) The oxyanion holes in the α– and β–subunits of carboxyltransferase that stabilize the enolate of acetyl-CoA in the β-subunit and the imidate of biotin in the α-subunit. (B) The pyrrolidinedione carbonyls interact with oxyanion hole residues, Gly205 from the β-subunit and Gly206 from the α-subunit.

The structure of moiramide B bound to carboxyltransferase shows how nature took advantage of the structural and mechanistic features (i.e. the oxyanion holes) of the enzyme to create a molecule that inhibits activity and is also bactericidal. The structure also explains why nature incorporated a pyrrolidinedione instead of 1,3-cyclopentanedione into moiramide B; delocalization of the electrons from the nitrogen atom into the adjacent carbonyls makes the oxygen atoms have more oxyanion-like character. Furthermore, Pohlmann *et al.* synthesized six-membered piperidinedione derivatives of moiramide B which did not exhibit any antibacterial activity.[13] Therefore, if 2,6-piperidinedione was used in place of pyrrolidinedione, the carbonyls would not have the appropriate geometry to interact with the oxyanion holes. In fact, Pohlmann *et al.* found that as more bulky and

hydrophobic groups were attached to the pyrrolidinedione nitrogen atom, there was a progressive decrease in both IC_{50} and MIC values[13] indicating that the size of this moiety was critical for enzyme inhibition and, thus, antibacterial activity. The structure-activity relationship (SAR) studies of Pohlmann *et al.* also indicated that the (4*S*)-methyl group on the pyrrolidinedione moiety was very important for antibacterial activity. The removal of the methyl group or replacement with an ethyl group resulted in a total loss of activity.[13, 15] Therefore, it is tempting to speculate that the methyl group also contributes to the oxyanion character of the carbonyl oxygen via an inductive effect.

The lack of electron density for the tail (domain 1) of moiramide B bound to carboxyltransferase indicates that it is very flexible and, therefore, unlikely to have any significant interactions with carboxyltransferase. This result is consistent with the findings of Pohlmann *et al.* who found that a wide range of functional groups were tolerated at the tail (domain 1) of moiramide B with respect to the inhibition of carboxyltransferase and the antibacterial activity of the derivatives.[13] This leads to the assumption that the unsaturated nature of the tail end is strictly a necessary component for entry into the bacterial cell.

The structure of moiramide B bound to carboxyltransferase also provides insight into a naturally occurring resistance mutation. The bacterium (*Pantoea agglomerans*) that produces the moiramide B analog, andrimid, is resistant to the effects of the molecule because of a mutation in the β−subunit (M203L in *E. coli* carboxyltransferase).[16] A study by Liu *et al*. revealed the M203L mutation in *E. coli* made the bacteria more resistant to andrimid.[16] The Met203 residue is very close to one of the residues in the β−subunit (Gly205) that interacts with one of the carbonyl oxygens of the pyrrolidinedione; therefore,

the M203L mutation could cause a local conformational change that decreases or eliminates the binding of andrimid (and by inference moiramide B) to the enzyme. Another intriguing possible mechanism for how the M203L mutation leads to resistance against andrimid is the β-phenylalanine moiety of moiramide B is within 5 Å from the sulfur atom of Met203 (Figure 3.8). A report by Valley *et al.* suggested that the sulfur of a methionine side chain can form a stable interaction with aromatic residues within ~5 Å.[17] Thus, the incorporation of the unnatural β-amino acid of phenylalanine into andrimid and moiramide B may be to allow this strong interaction with the enzyme to occur and contributing to the nanomolar affinity of the ligand for the enzyme.

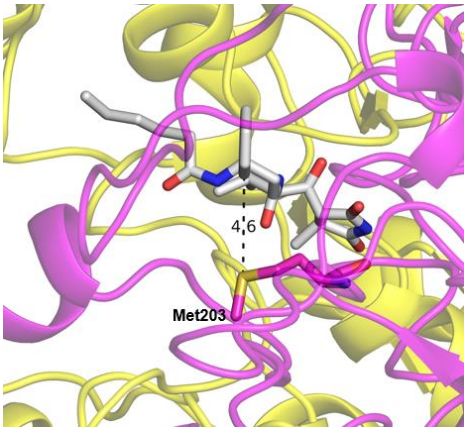

Figure 3.8. The β-phenylalanine moiety of moiramide B shown within 5 Å of the methionine sulfur atom of the Met203 side chain on the β-subunit of carboxyltransferase.

3.2.2 Structure-Activity Relationships of Moiramide B

Since the moiramide B used in the structural studies was synthetic in origin, this afforded the ability to distinguish the structural characteristics of the molecule required for enzyme inhibition versus the structural features needed for antibacterial activity. The structural fragments of moiramide B tested for enzyme inhibition and antibacterial activity are shown in Figure 3.9. Since the synthesis of moiramide B progresses in a head-to-tail

fashion, the starting pyrrolidinedione fragment came in the form of the commercially available product, succinimide (compound **1**). Compounds **2-4** were intermediates in the synthesis of moiramide B (compound **5**), while compound **6**, the tail fragment, was synthesized for this analysis.

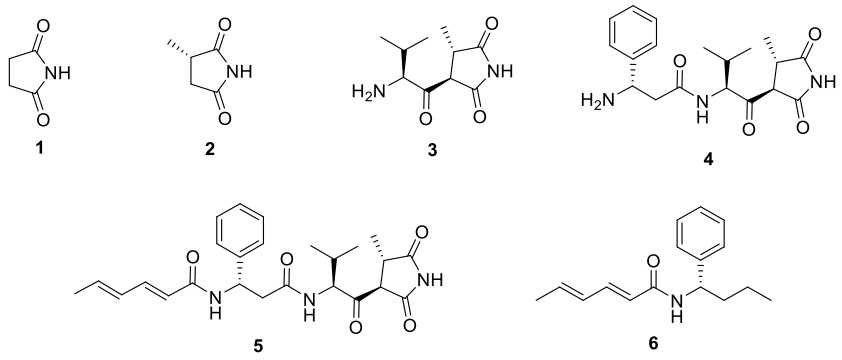

Figure 3.9. Structures of moiramide B intermediates: succinimide (**1**), (4*S*)-methyl-2,5-pyrrolidinedione (**2**), (3*S*)-L-valine-(4*S*)-methyl-2,5-pyrrolidinedione (**3**), (3*S*)-β-phenylalanine-L-valine-(4*S*)-methyl-2,5-pyrrolidinedione (**4**), as well as moiramide B (**5**) and the tail fragment (**6**).

The initial velocity of carboxyltransferase was measured in the presence of 50 nM of each of the compounds, while the substrates malonyl-CoA and biocytin were held constant at a subsaturating level. The results are shown in Figure 3.10, (A). Succinimide (compound **1**) was, within error, not an inhibitor of carboxyltransferase. However, addition of the (4*S*)-methyl substituent to succinimide (compound **2**) resulted in a dramatic decrease in carboxyltransferase activity. The inhibition of carboxyltransferase was stronger with the attachment of the L-valine group. Another significant decrease in activity occurred with the addition of the β-phenylalanine moiety (compound **4**), which corroborates the potential interaction between the aromatic group of the phenylalanine and the methionine sulfur atom to increase the binding affinity of moiramide B. Moiramide B (compound **5**) showed a similar level of activity to compound **4** indicating the addition of the fatty acyl

tail has no further impact on inhibition. The tail end alone (compound **6**) of moiramide exhibited no inhibition of carboxyltransferase.

The absence of any inhibitory activity for the tail end (compound **6**) of moiramide B (compound **5**) is consistent with the hypothesis that the (4*S*)-methyl pyrrolidinedione group is required for inhibiting carboxyltransferase, while the fatty acyl tail must only be needed for gaining entry into the bacterial cell. To test this hypothesis, the enzyme inhibition data for each of the compounds in Figure 3.10, (A) was compared to their antibacterial activity. A final concentration of 50 μM for each compound was added to culture media inoculated with *E. coli* and incubated for 4 hrs. As shown in Figure 3.10, (B), all of the compounds, except for moiramide B (compound **5**), did not exhibit any antibacterial activity.

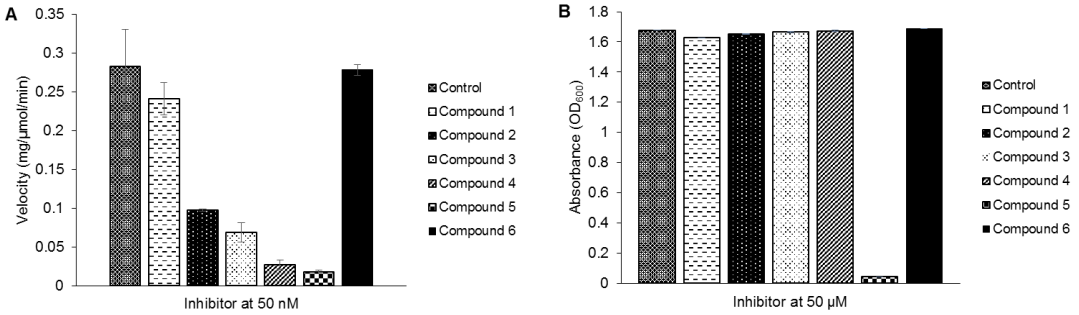

Figure 3.10. (A) Inhibitory activity of compounds **1-6**. Initial velocities of carboxyltransferase were measured in the presence of 50 nM of each compound while holding the substrates (malonyl-CoA and biocytin) at subsaturating levels. (B) Antibacterial activity of compounds **1-6**. Final concentrations of 50 μM for each compound were inoculated with *E. coli* and incubated at 37 °C. After a 4 hour incubation, the absorbance at 600 nm was measured.

Even though compounds **2**, **3**, and **4** all inhibited carboxyltransferase significantly, they did not exhibit any antibacterial activity at a concentration of 50 μM. The only difference between compound **4** and moiramide B (compound **5**) is the absence of the fatty

acyl tail. Therefore, the role of the fatty acyl tail in the mechanism of action of moiramide B appears to be transport of the molecule into the bacterial cell.

3.3 CONCLUSIONS

These studies reveal how nature expropriated the oxyanion holes in carboxyltransferase to design a molecule that is not only a potent enzyme inhibitor, but also a potent antibacterial agent. In nature's version of structure-based drug design, a methyl pyrrolidinedione functionality evolved to inhibit carboxyltransferase by binding in the oxyanion holes found in both the α– and β–subunits. Subsequent additions of L-valine and β-phenylalanine increased the affinity of the molecule for carboxyltransferase, however, none of these additions produced a molecule with strong antibacterial activity. As a result, nature attached an unsaturated fatty acyl tail to the molecule that allowed it to enter the bacterium.

The results described in this report also provide intriguing scaffolds from which to build new antibacterial agents against a novel target molecule, acetyl-CoA carboxylase. For instance, structure-activity studies on the methyl group of pyrrolidinedione can be done to increase the affinity for carboxyltransferase and improve the potency of moiramide B. Lastly, it will be interesting to see if these scaffolds can also be used in the design of inhibitors of human acetyl-CoA carboxylase II, which has a similar mechanism to the bacterial enzyme (i.e. it also utilizes two oxyanion holes for catalysis). The mitochondrial isoform (or acetyl-CoA carboxylase II) is involved in regulating fatty acid oxidation and is a target for anti-obesity agents.[18]

3.4 EXPERIMENTAL SECTION

3.4.1 Materials and Methods

All chemicals and reagents were purchased from Sigma-Aldrich, Fisher, Acros, NovaBiochem, and Fluka and used without further purification. Diisopropylethylamine and triethylamine were dried and distilled from CaH_2 and stored over KOH pellets. Dry methanol was distilled from Mg turnings and stored over 3Å molecular sieves. All reactions were performed under a dry nitrogen atmosphere unless otherwise noted. Flash chromatography was performed using 230-400 mesh silica gel (40-63 μm) from Fluka. Thin layer chromatography was performed on aluminum-backed 60 F_{254} silica plates from EMD Chemicals, Inc. Optical rotations were recorded on a Jasco P-2000 digital polarimeter. ^{1}H and ^{13}C NMR spectra were collected at room temperature on a Bruker AV-400 spectrometer. All NMR experiments were performed in deuterated solvents and the chemical shifts are reported in standard δ notation as parts per million, using tetramethylsilane (TMS) and $CDCl_3$ as an internal standard with coupling constants (*J*) reported in Hertz (Hz). High resolution mass spectrometry (HRMS) was carried out using an Agilent 6210 electrospray ionization-time-of-flight (ESI-TOF) mass spectrometer.

Synthesis of (4*S*)-methyl-pyrrolidine-2,5-dione (**2**). A catalytic amount of 5% Pd/C (100 mg, 20% w/w) was added to a solution of (4*S*)-methyl-*N*-*O*-benzyl-pyrrolidine-2,5-dione (500 mg, 2.28 mmol, 1.00 equiv.) in dry methanol (25 mL) and the mixture stirred under H_2 for 1 h. The reaction mixture was filtered through a pad of Celite®, washed with methanol, and concentrated. The residue was dissolved in acetonitrile (5 mL) and added dropwise to a stirred solution of 2-bromoacetophenone (454 mg, 2.28 mmol, 1.00 equiv.) in acetonitrile (5 mL) at rt. A solution of triethylamine (477 μL, 346 mg, 3.42 mmol, 1.50

equiv.) in acetonitrile (2 mL) was added dropwise over 2 h and the reaction mixture was stirred at rt overnight. The mixture was concentrated and then partitioned between CH_2Cl_2 (20 mL) and 5% hydrochloric acid (2 x 20 mL). The organic layer was washed with brine (20 mL), dried over $MgSO_4$, filtered, concentrated, and purified by flash chromatography on silica gel eluting with 5:1 CH_2Cl_2:EtOAc to give **2** as a clear oil (25 mg, 10%). R_f 0.56 (4:1 EtOAc:CH_2Cl_2). $[\alpha]_D^{20}$ -16.3 (*c* 0.13, MeOH). ^{1}H NMR ($CDCl_3$, 400 MHz) δ 1.37 (d, *J* = 7.2 Hz, 3H), 2.39 (dd, *J* = 16.1, 2.9 Hz, 1H), 2.81-3.07 (m, 2H), 8.22 (s, 1H); ^{13}C NMR ($CDCl_3$, 100 MHz) δ 16.5, 36.2, 37.6, 176.4, 180.7. HRMS (ESI-TOF) calcd for $C_5H_8NO_2$ $(M+H)^+$: 114.0550, obsd: 114.0548.

Synthesis of (2*E*,4*E*)-*N*-[(*S*)-1-phenylbutyl]hexa-2,4-dienamide (**6**). Sorbic acid (50 mg, 0.45 mmol, 1.20 equiv.) was added to a solution of (*S*)-1-phenylbutylamine (55 mg, 0.37 mmol, 1.00 equiv.) and TBTU (155 mg, 0.48 mmol, 1.30 equiv.) in DMF (5 mL) followed by addition of *N*,*N*-diisopropylethylamine (162 µL, 120 mg, 0.93 mmol, 2.50 equiv.) and the mixture was stirred under N_2 for 20 h. The solvent was removed *in vacuo* and the resulting residue was purified by flash chromatography on silica gel eluting with 1:1 Hex:EtOAc to give **6** as a light yellow solid (66 mg, 73%). R_f 0.56 (1:1 Hex:EtOAc). $[\alpha]_D^{24}$ -136.2 (*c* 1.00, $CHCl_3$). ^{1}H NMR ($CDCl_3$, 400 MHz) δ 0.90 (t, *J* = 7.3 Hz, 3H), 1.18-1.42 (m, 2H), 1.70-1.87 (m, 5H), 5.05 (q, *J* = 7.7 Hz, 1H), 5.79 (d, *J* = 15.0 Hz, 1H), 5.95-6.23 (m, 3H), 7.10-7.38 (m, 6H); ^{13}C NMR ($CDCl_3$, 100 MHz) δ 14.5, 17.9, 19.5, 38.4, 52.5, 122.5, 125.9, 127.5, 127.7, 129.3, 130.5, 136.8, 140.6, 142.7, 165.7. HRMS (ESI-TOF) calcd for $C_{16}H_{22}NO$ $(M+H)^+$: 244.1696, obsd: 244.1704.

3.4.2 Enzyme Purification

Carboxyltransferase from *E. coli* was purified as previously described.[10] Briefly, the genes coding for the α- and β-subunits of carboxyltransferase were placed in a minioperon on the plasmid pET14b such that the N-terminus of the α-subunit contained a His-tag. The genes were overexpressed and the protein was purified using nickel affinity chromatography followed by gel-filtration chromatography.

3.4.3 Crystallization and Data Collection

Crystals were obtained by sitting drop vapor diffusion at 22 °C using a solution of 10 mg/mL carboxyltransferase and 300 μM moiramide B. The crystallization condition contained a reservoir solution of 0.1 M MES (pH 6.5), 0.1 M malonate, and 20% w/v polyacrylic acid 2100. The sitting drop contained a well to protein ratio of 2:2 μL. Crystals appeared after 1-2 weeks and were cryoprotected with a 20% v/v ethylene glycol/reservoir solution and then mixing that solution with crystal mother liquor in a 1:1 ratio. The crystal was submerged in the cryoprotectant and then immediately flash-cooled in liquid nitrogen. X-ray diffraction data were collected to 3.53 Å at the Advanced Photon Source beamline NE-CAT 24-ID-E equipped with the ADSC Q315r detector. The data was processed and scaled using XDS.[19] Data collection and refinement statistics are in Figure 3.3.

3.4.4 Crystal Structure Determination

The crystal structure was solved by Dr. Svetlana Pakhomova (LSU) by molecular replacement. The molecular replacement procedure was applied to locate a solution using the program MOLREP.[20] A carboxyltransferase subunit of ACC from *E. coli* (PDB accession code 2F9Y) was used as a search model. The positioned MR model was refined against 3.52 Å using the "jelly" body and the maximum likelihood refinement in

REFMAC.[21] A difference Fourier map unambiguously revealed the presence of the inhibitor between the alpha and beta chains (Figure 3.4). The final model consists of residues 1-319 for the alpha chain, residues 23-287 for the beta chain, one Zn^{2+} cation, one inhibitor molecule and two water molecules. The program Coot[20] was used for model building throughout the refinement.

3.4.5 Kinetic Assays

Carboxyltransferase activity was measured in the reverse, non-physiological direction and was determined spectrophotometrically by measuring the production of acetyl-CoA using citrate synthase and malate dehydrogenase and following the reduction of NAD^+ at 340 nm. Each reaction mixture contained 0.12 mg/mL of malate dehydrogenase, 0.05 mg/mL of citrate synthase, 0.5 mM NAD^+, 0.01 mM malic acid, 0.6 mg/mL bovine serum albumin (BSA), and 100 mM Tris (pH 8.0). All reactions held the substrates malonyl-CoA and biocytin (a biotin analog) constant at 150 μM and 6 mM, respectively. A final concentration of 50 nM of compounds **1-6** was added to measure the effect on activity. All reactions were conducted in a total of 0.5 mL in a 1 cm pathlength quartz cuvette and all reactions were initiated by the addition of enzyme and were measured in triplicate. Spectrophotometric data were collected using an Agilent Cary 60 UV-Vis spectrophotometer interfaced with a personal computer with a data acquisition program.

3.4.6 Whole-cell Growth Assays

A culture of *E. coli* strain JM109 was grown overnight in Luria broth (LB) at 37 °C. Culture tubes containing 2 mL of fresh LB media were inoculated with 10 μL of the saturated *E. coli* culture. Compounds **1-6** were dissolved in 100% DMSO to achieve a 5

mM stock solution and inoculated into tubes to generate final concentrations of 50 μM. After inoculation, the culture tubes were incubated for 4 hours at 37 °C. Optical density (OD) readings were measured at 600 nm in 1 mL plastic cuvettes. Spectrophotometric data were collected using an Agilent Cary 60 UV-Vis spectrophotometer.

3.5 REFERENCES

(1) Campbell, J. W.; Cronan, J. E., Jr., Bacterial fatty acid biosynthesis: targets for antibacterial drug discovery. *Annu. Rev. Microbiol.* **2001,** *55*, 305-332.

(2) Davis, M. S.; Solbiati, J.; Cronan, J. E., Jr., Overproduction of acetyl-CoA carboxylase activity increases the rate of fatty acid biosynthesis in *Escherichia coli*. *J. Biol. Chem.* **2000,** *275*, 28593-28598.

(3) Cronan, J. E., Jr.; Waldrop, G. L., Multi-subunit acetyl-CoA carboxylases. *Prog. Lipid Res.* **2002,** *41*, 407-435.

(4) Knowles, J. R., The mechanism of biotin-dependent enzymes. *Annu. Rev. Biochem.* **1989,** *58*, 195-221.

(5) Miller, J. R.; Dunham, S.; Mochalkin, I.; Banotai, C.; Bowman, M.; Buist, S.; Dunkle, B.; Hanna, D.; Harwood, H. J.; Huband, M. D.; Karnovsky, A.; Kuhn, M.; Limberakis, C.; Liu, J. Y.; Mehrens, S.; Mueller, W. T.; Narasimhan, L.; Ogden, A.; Ohren, J.; Prasad, J. V.; Shelly, J. A.; Skerlos, L.; Sulavik, M.; Thomas, V. H.; VanderRoest, S.; Wang, L.; Wang, Z.; Whitton, A.; Zhu, T.; Stover, C. K., A class of selective antibacterials derived from a protein kinase inhibitor pharmacophore. *Proc. Natl. Acad. Sci. USA* **2009,** *106*, 1737-1742.

(6) Mochalkin, I.; Miller, J. R.; Narasimhan, L.; Thanabal, V.; Erdman, P.; Cox, P. B.; Prasad, J. V.; Lightle, S.; Huband, M. D.; Stover, C. K., Discovery of antibacterial biotin carboxylase inhibitors by virtual screening and fragment-based approaches. *ACS Chem. Biol.* **2009,** *4*, 473-483.

(7) Cheng, C. C.; Shipps, G. W., Jr.; Yang, Z.; Sun, B.; Kawahata, N.; Soucy, K. A.; Soriano, A.; Orth, P.; Xiao, L.; Mann, P.; Black, T., Discovery and optimization of antibacterial AccC inhibitors. *Bioorg. Med. Chem. Lett.* **2009,** *19*, 6507-6514.

(8) Needham, J.; Kelly, M. T.; Ishige, M.; Andersen, R. J., Andrimid and moiramides A-C, metabolites produced in culture by a marine isolate of the bacterium *Pseudomonas fluorescens*: Structure elucidation and biosynthesis. *J. Org. Chem.* **1994,** *59*, 2058-2063.

(9) Freiberg, C.; Brunner, N. A.; Schiffer, G.; Lampe, T.; Pohlmann, J.; Brands, M.; Raabe, M.; Habich, D.; Ziegelbauer, K., Identification and characterization of the

first class of potent bacterial acetyl-CoA carboxylase inhibitors with antibacterial activity. *J. Biol. Chem.* **2004,** *279*, 26066-26073.

(10) Blanchard, C. Z.; Waldrop, G. L., Overexpression and kinetic characterization of the carboxyltransferase component of acetyl-CoA carboxylase. *J. Biol. Chem.* **1998,** *273*, 19140-19145.

(11) Jin, M.; Fischbach, M. A.; Clardy, J., A biosynthetic gene cluster for the acetyl-CoA carboxylase inhibitor andrimid. *J. Am. Chem. Soc.* **2006,** *128*, 10660-10661.

(12) Davies, S. G.; Dixon, D. J., Asymmetric syntheses of moiramide B and andrimid. *J. Chem. Soc., Perkin Trans. 1* **1998**, 2635-2643.

(13) Pohlmann, J.; Lampe, T.; Shimada, M.; Nell, P. G.; Pernerstorfer, J.; Svenstrup, N.; Brunner, N. A.; Schiffer, G.; Freiberg, C., Pyrrolidinedione derivatives as antibacterial agents with a novel mode of action. *Bioorg. Med. Chem. Lett.* **2005,** *15*, 1189-1192.

(14) Bilder, P.; Lightle, S.; Bainbridge, G.; Ohren, J.; Finzel, B.; Sun, F.; Holley, S.; Al-Kassim, L.; Spessard, C.; Melnick, M.; Newcomer, M.; Waldrop, G. L., The structure of the carboxyltransferase component of acetyl-coA carboxylase reveals a zinc-binding motif unique to the bacterial enzyme. *Biochemistry* **2006,** *45*, 1712-1722.

(15) McWhorter, W.; Fredenhagen, A.; Nakanishi, K.; Komura, H., Stereocontrolled synthesis of andrimid and a structural requirement for the activity. *J. Chem. Soc., Chem. Commun.* **1989**, 299-301.

(16) Liu, X.; Fortin, P. D.; Walsh, C. T., Andrimid producers encode an acetyl-CoA carboxyltransferase subunit resistant to the action of the antibiotic. *Proc. Natl. Acad. Sci. USA* **2008,** *105*, 13321-13326.

(17) Valley, C. C.; Cembran, A.; Perlmutter, J. D.; Lewis, A. K.; Labello, N. P.; Gao, J.; Sachs, J. N., The methionine-aromatic motif plays a unique role in stabilizing protein structure. *J. Biol. Chem.* **2012,** *287*, 34979-34991.

(18) Wakil, S. J.; Abu-Elheiga, L. A., Fatty acid metabolism: target for metabolic syndrome. *J. Lipid Res.* **2009,** *50 Suppl*, S138-143.

(19) Kabsch, W., XDS. *Acta Crystallogr. D Biol. Crystallogr.* **2010,** *66*, 125-132.

(20) Bailey, S., The CCP4 suite: programs for protein crystallography. *Acta Crystallogr. D. Biol. Crystallogr.* **1994,** *50*, 760-763.

(21) Bailey, S., The Ccp4 Suite - Programs for Protein Crystallography. *Acta Crystallogr D-Biological Crystallography* **1994,** *50*, 760-763.

3.6 SPECTRA

^{1}H NMR of Compound **2**

(4S)–Methyl–pyrrolidine–2,5–dione in CDCl3 at 400 MHz

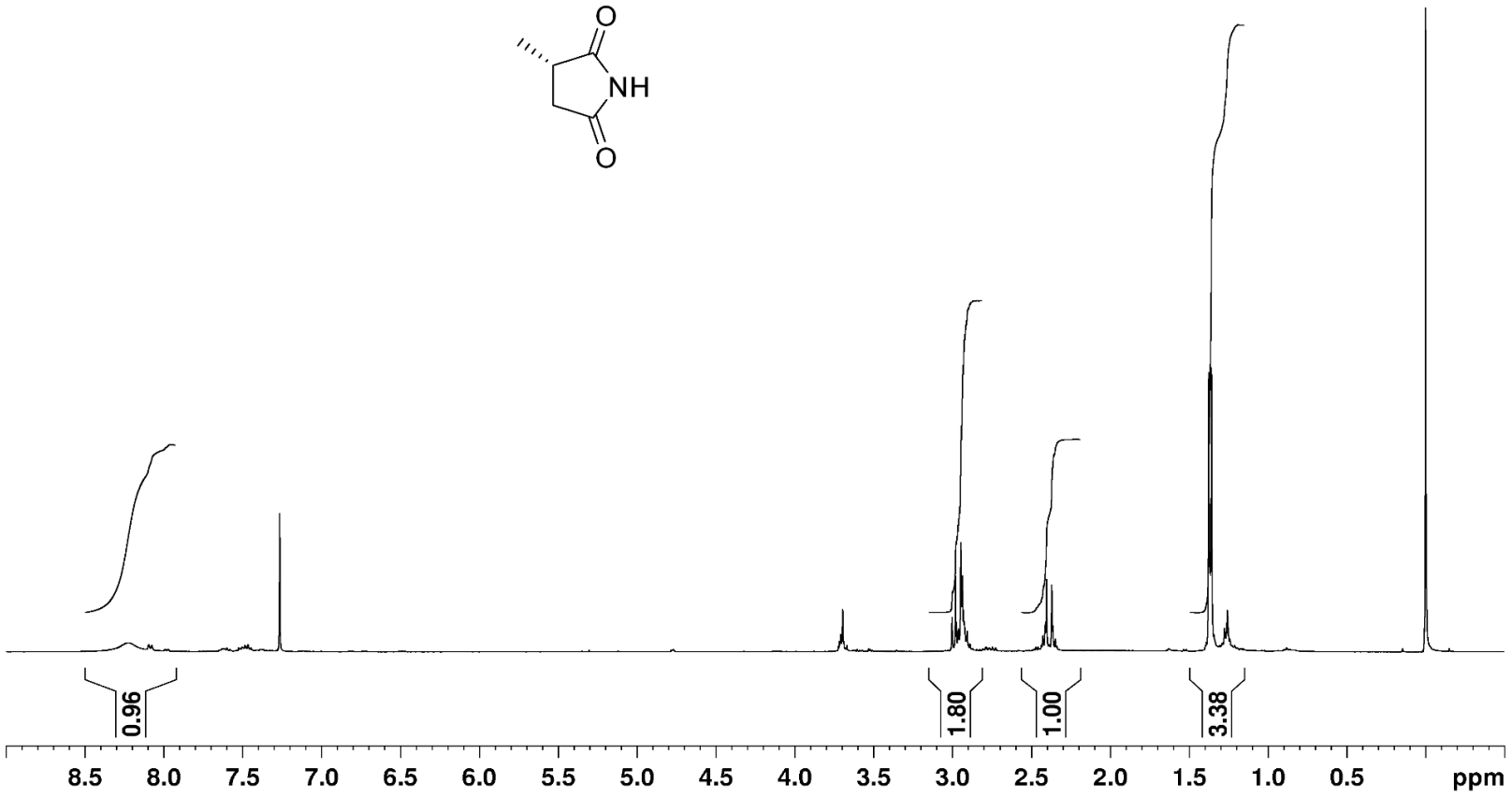

^{13}C NMR of Compound **2**

(4S)–Methyl–pyrrolidine–2,5–dione in CDCl3 at 100 MHz

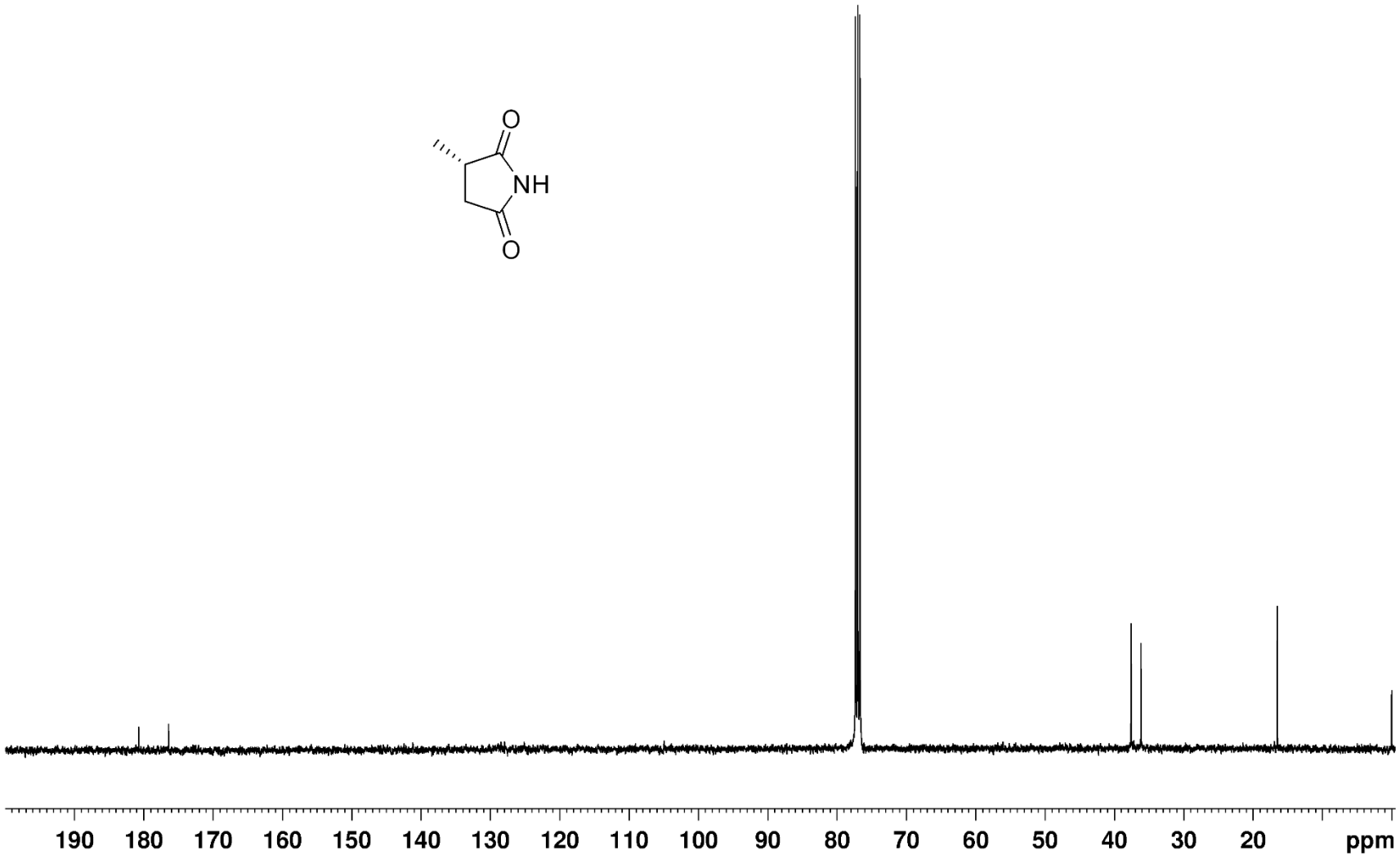

^{1}H NMR of Compound **6**

(2E,4E)–N–[(S)–1–phenylbutyl]hexa–2,4–dienamide in CDCl3 at 400 MHz

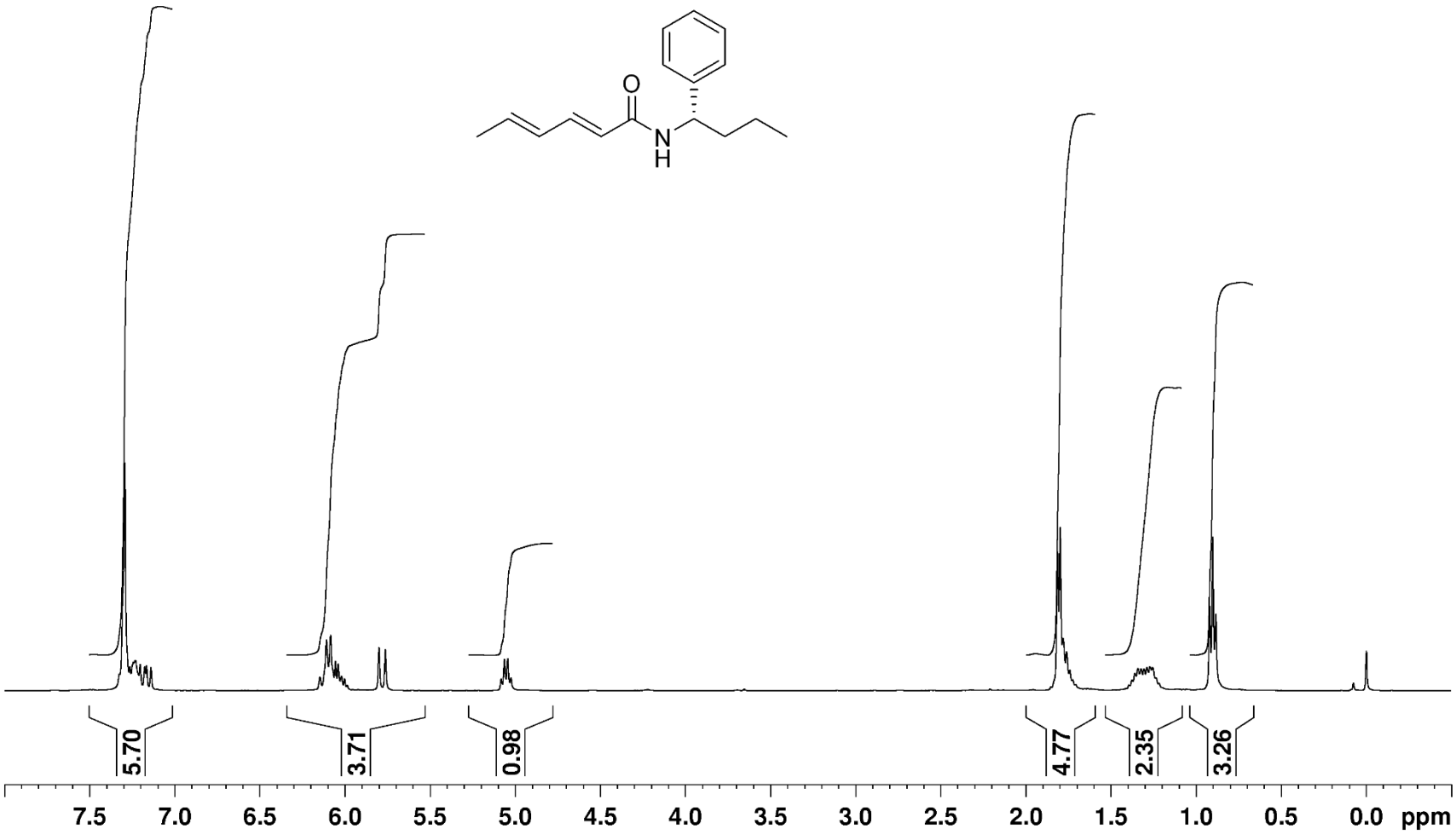

^{13}C NMR of Compound **6**

(2E,4E)–N–[(S)–1–phenylbutyl]hexa–2,4–dienamide in CDCl3 at 100 MHz

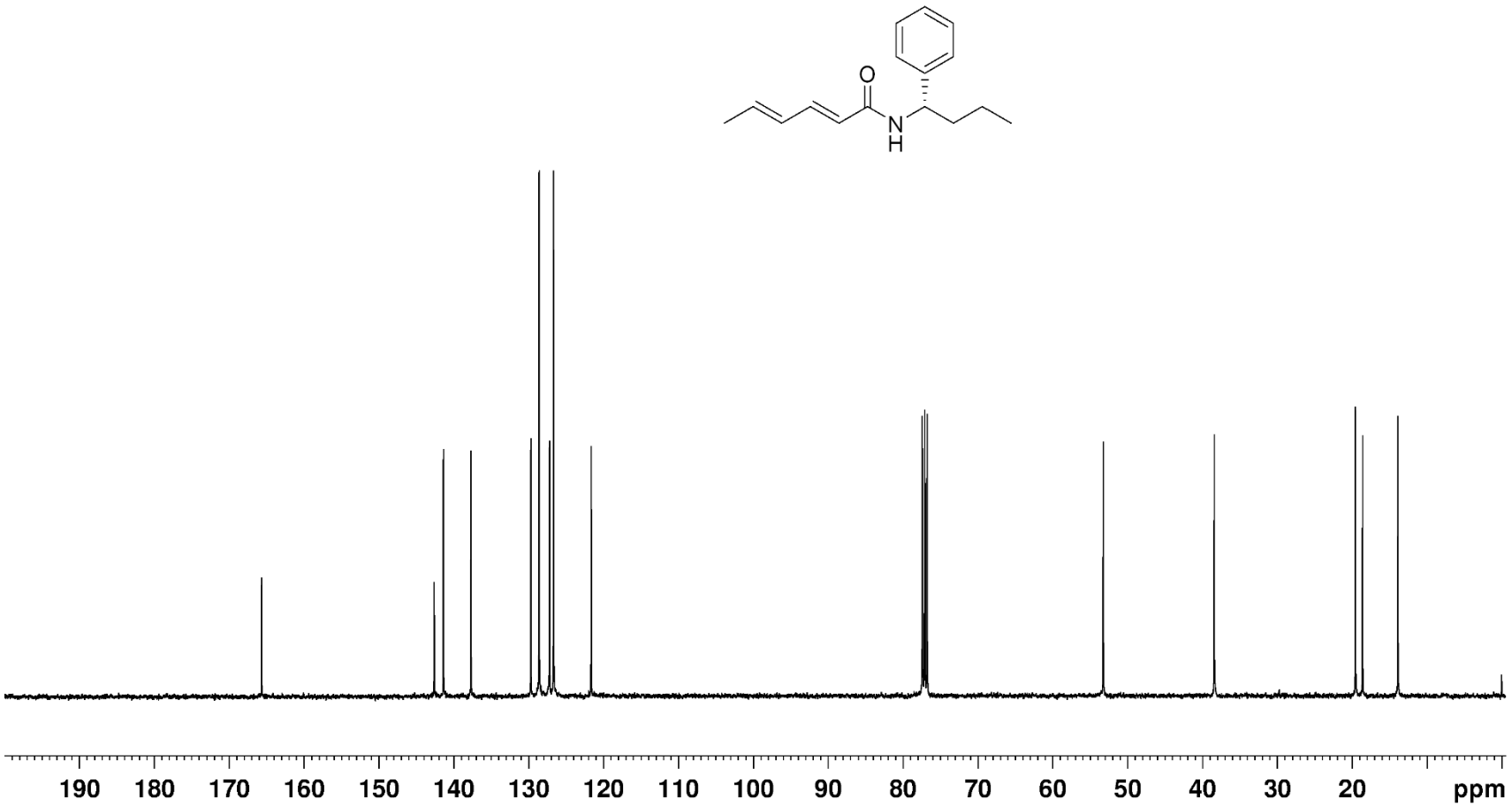

CHAPTER 4: CONCLUSIONS AND OUTLOOK

4.1 SUMMARY

The overall goal of this research was the development of dual-ligand inhibitors against the novel target acetyl-CoA carboxylase that could act as antibacterial agents. The identification of antibacterial agents for both enzymes of the acetyl-CoA carboxylase (ACC) reaction, biotin carboxylase (BC) and carboxyltransferase (CT), allowed for the covalent attachment of these inhibitors via saturated hydrocarbon linkers (15 carbons and 7 carbons) into multitarget agents. Although a multitarget approach will not solve the resistance problem permanently, it can delay the onset of resistance that is being observed with single agent antibiotics. For example, spontaneous resistance mutations of single targets occur between 10^{-6} and 10^{-9}; therefore, a multitarget approach should result in a much lower frequency of resistance because bacteria would have to develop viable resistance mutations on more than one target.[1]

Once the dual-ligand inhibitors were generated, the inhibitory and antibacterial properties were determined. Enzyme kinetic studies on acetyl-CoA carboxylase yielded an unexpected result. The aminooxazole inhibitor exhibits competitive inhibition against the isolated BC subunit, but for the studies with the ACC complex, it displayed a noncompetitive inhibition pattern. Due to the high intracellular concentration of ATP, ACC is likely saturated with ATP *in vivo*. Therefore, the noncompetitive inhibition pattern indicates the aminooxazole compound can still inhibit BC even in the presence of saturating levels of ATP. These results show that it is crucial that any potential antibacterial agents targeting the BC subunit of ACC must be characterized with the ACC complex and not just the isolated subunit in order to determine how BC inhibitors will act *in vivo*.

The antibacterial properties of the parent compounds and the dual-ligands were tested against a variety of both Gram-negative and Gram-positive bacteria. The 15-carbon dual-ligand did not display any antibacterial activity to any of the tested strains, while the 7-carbon dual-ligand exhibited activity against not only membrane-compromised *E. coli*, but also several Gram-positive strains. The frequency of resistance studies using the 7-carbon dual-ligand showed a restriction for the selection of resistance with a frequency of $<2.5 \times 10^{-10}$, which was a much lower frequency than expected with single agents. Studies inoculating the 15-carbon dual-ligand with the antibiotic polymyxin B nonapeptide revealed the longer linker was impeding the ability for this dual-ligand to diffuse across the bacterial membrane. The dual-ligand studies provide a proof-of-concept for the use of multitargeted therapies against bacterial ACC, and also revealed the selection of the linking component between multiple agents is of vital importance for inhibitory and antibacterial activity.

Since the moiramide B used for the dual-ligand studies was synthesized, this allowed for the determination of the structural features of moiramide B that contribute to its mechanism of action. Previous studies have shown the (4*S*)-methyl group on the pyrrolidinedione moiety was very important for antibacterial activity, but the exact mechanism was never determined.[2-3] The elucidation of our three-dimensional structure shows the five-membered ring geometry of the pyrrolidinedione allows the carbonyls to bind directly in the oxyanion holes of carboxyltransferase. The incorporation of the central nitrogen atom instead of a carbon atom also was strategic to increase binding affinity by causing delocalization of electrons to make the carbonyls have more 'oxyanion-like' character. Essentially, nature designed moiramide B to explicitly take advantage of the

mechanistic features of carboxyltransferase by binding in the oxyanion holes that are needed for catalysis. Furthermore, the enzymatic assays confirmed the unsaturated fatty acyl tail has no impact on the inhibitory activity, and additional whole-cell growth studies led us to conclude the unsaturated tail was strictly implemented to allow for moiramide B to enter the bacterium.

4.2 FUTURE DIRECTIONS

The ACC dual-ligand inhibitors have created new avenues for exploring multiligand therapeutics against this novel target. The incorporation of a more potent, and ideally, broad-spectrum BC inhibitor, in conjugation with moiramide B, could lead to more potent dual-ligand inhibitors for bacterial ACC. An additional design modification to the dual-ligand design would be implementing various linking components. Based on our results, altering the length, and possibly other physiochemical properties (e.g., hydrophobicity, degree of unsaturation), can effect both the inhibitory and antibacterial activities of dual-ligand inhibitors. The information gained during these dual-ligand studies cannot only be utilized in the generation of new dual-ligand inhibitors for ACC, but also can be applied towards multiligand inhibitors against other known enzyme complexes.

The three-dimensional structure of moiramide B bound to carboxyltransferase provided valuable information on the essential binding features. A structure with a higher resolution could more accurately pinpoint the position of the pseudopeptide moieties on the moiramide B backbone. The orientation of these domains in relation to the side chain residues of the CT subunits would provide more insight into how to design inhibitors that would interact with these residues to increase the potency of moiramide B or moiramide B analogs.

A particularly interesting residue is the Met203 residue found on the β−subunit of CT. The bacterium that produces a moiramide B analog (andrimid) is resistant to this compound due to the mutation of the methionine to a leucine, indicating the leucine causes a disruption in binding affinity. The sulfur atom of the Met203 residue (*E. coli* numbering) is within 5 Å from the unnatural β-amino acid of phenylalanine found in moiramide B. A report by Valley *et al.* suggests the interaction between the methionine sulfur atom and an aromatic residue can form a stable interaction.[4] Mutagenic analysis of Met203 and subsequent measurement of the inhibitory activity would assist in the confirmation of this residue being involved with the recognition and binding of moiramide B. Mutagenesis studies, as well as obtaining a crystal structure that diffracts to a higher resolution, could greatly benefit the development of novel antibiotics that can target the carboxyltransferase enzyme of ACC.

The precedent set by the dual-ligand inhibitor studies in this dissertation provide a strong foundation for the development of subsequent multitarget agents against bacterial acetyl-CoA carboxylase and other antibacterial targets. The structural studies of moiramide B provide a framework from which to design new antibacterial agents against the CT component of ACC as well as lay the groundwork for potential virtual screening studies to identify potent inhibitors of carboxyltransferase.

4.3 REFERENCES

(1) East, S. P.; Silver, L. L., Multitarget ligands in antibacterial research: progress and opportunities. *Expert Opin. Drug Discov.* **2013,** *8,* 143-156.

(2) McWhorter, W.; Fredenhagen, A.; Nakanishi, K.; Komura, H., Stereocontrolled synthesis of andrimid and a structural requirement for the activity. *J. Chem. Soc., Chem. Commun.* **1989**, 299-301.

(3) Pohlmann, J.; Lampe, T.; Shimada, M.; Nell, P. G.; Pernerstorfer, J.; Svenstrup, N.; Brunner, N. A.; Schiffer, G.; Freiberg, C., Pyrrolidinedione derivatives as antibacterial agents with a novel mode of action. *Bioorg. Med. Chem. Lett.* **2005,** *15*, 1189-1192.

(4) Valley, C. C.; Cembran, A.; Perlmutter, J. D.; Lewis, A. K.; Labello, N. P.; Gao, J.; Sachs, J. N., The methionine-aromatic motif plays a unique role in stabilizing protein structure. *J. Biol. Chem.* **2012,** *287*, 34979-34991.

VITA

Molly Silvers was born in Cincinnati, Ohio in the summer of 1987. After moving to Spartanburg, South Carolina in 1996, Molly moved to Fort Mill, South Carolina in 2001 and graduated from Fort Mill High School in 2005. After high school, Molly and her family moved to Baton Rouge, Louisiana where she enrolled at Louisiana State University to pursue a Bachelor of Science degree in Biological Sciences. She completed her degree in December 2009 and started graduate school in January 2010. She joined Dr. Grover Waldrop's lab in May 2010 and expects to receive her Doctor of Philosophy degree in Biochemistry at the Fall 2014 Commencement ceremony.